

สารออกฤทธิ์ชีวภาพที่มีฤทธิ์ด้านการเปลี่ยนสภาพของเซลล์สลายกระดูกและกลไกการออกฤทธิ์



นางสาวสุพัตรา ชวลิตพงษ์

บทคัดย่อและแฟ้มข้อมูลฉบับเต็มของวิทยานิพนธ์ตั้งแต่ปีการศึกษา 2554 ที่ให้บริการในคลังปัญญาจุฬาฯ (CUIR)  
เป็นแฟ้มข้อมูลของนิสิตเจ้าของวิทยานิพนธ์ ที่ส่งผ่านทางบัณฑิตวิทยาลัย

The abstract and full text of theses from the academic year 2011 in Chulalongkorn University Intellectual Repository (CUIR)  
are the thesis authors' files submitted through the University Graduate School.

วิทยานิพนธ์นี้เป็นส่วนหนึ่งของการศึกษาตามหลักสูตรปริญญาวิทยาศาสตรดุษฎีบัณฑิต

สาขาวิชาเทคโนโลยีชีวภาพ

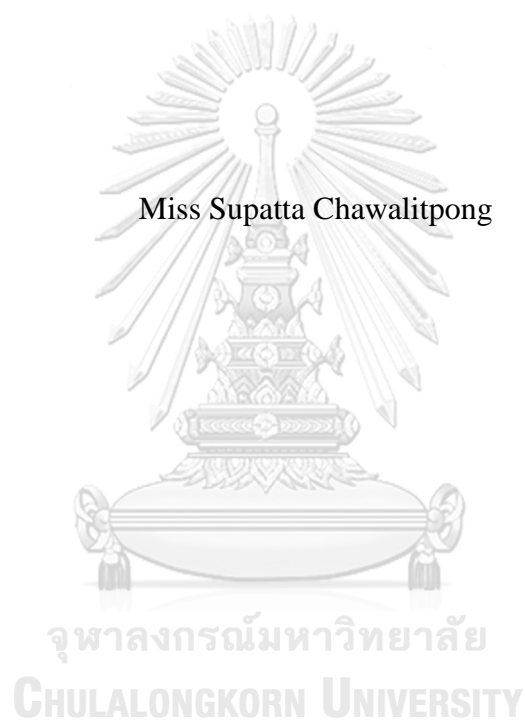
คณะวิทยาศาสตร์ จุฬาลงกรณ์มหาวิทยาลัย

ปีการศึกษา 2560

ลิขสิทธิ์ของจุฬาลงกรณ์มหาวิทยาลัย

BIOACTIVE COMPOUNDS WITH AN INHIBITORY ACTIVITY AGAINST  
OSTEOCLAST DIFFERENTIATION AND MECHANISMS

Miss Supatta Chawalitpong



A Dissertation Submitted in Partial Fulfillment of the Requirements  
for the Degree of Doctor of Philosophy Program in Biotechnology  
Faculty of Science  
Chulalongkorn University  
Academic Year 2017  
Copyright of Chulalongkorn University



สุพัตรา ชาลิตพงษ์ : สารออกฤทธิ์ชีวภาพที่มีฤทธิ์ต้านการเปลี่ยนสภาพของเซลล์สลายกระดูกและกลไกการออกฤทธิ์ (BIOACTIVE COMPOUNDS WITH AN INHIBITORY ACTIVITY AGAINST OSTEOCLAST DIFFERENTIATION AND MECHANISMS) อ.ที่ปรึกษาวิทยานิพนธ์หลัก: รศ. ดร. ธนาภัทร ปาลกะ, อ.ที่ปรึกษาวิทยานิพนธ์ร่วม: ศ. ดร. อภิชาติ สุขสำราญ, หน้า.

โรคกระดูกพรุนเป็นปัญหาสุขภาพที่สำคัญอย่างหนึ่งของสังคมผู้สูงอายุ สาเหตุหลักของภาวะดังกล่าวเกิดจากความไม่สมดุลของเซลล์ที่ทำหน้าที่สร้างกระดูก (osteoblast) และเซลล์ที่ทำหน้าที่สลายกระดูก (osteoclast) การลดลงของมวลกระดูกในผู้สูงอายุนำมาซึ่งความเสี่ยงในการแตกหักของกระดูก จุดประสงค์ของการศึกษานี้ คือ การคัดกรองสารออกฤทธิ์ทางชีวภาพที่มีฤทธิ์ในการต้านการเปลี่ยนสภาพของเซลล์สลายกระดูกและกลไกการออกฤทธิ์ของสารนั้นๆ ในกลุ่มสารทดสอบอนุพันธ์สาร (3S)-1-(3,4-dihydroxyphenyl)-3-hydroxy-7-phenyl-(6E)-6-heptene (DHPH) และ กรดไซเปอร์เรโนอิก (Cyperenoic acid) ซึ่งสกัดได้จากส่วนเหง้า *Curcuma comosa* Rox. และราก *Croton crassifolius* Geiseler. ตามลำดับ มีฤทธิ์แรงในการต้านการเกิดเซลล์สลายกระดูกในระดับ *in vitro* ใช้เซลล์จากไขกระดูกที่ถูกกระตุ้นด้วย receptor activator of nuclear factor- $\kappa$ B ligand (RANKL) DHPH มีฤทธิ์ในการยับยั้งการเปลี่ยนสภาพไปเป็นเซลล์สลายกระดูก โดยยับยั้งการเกิด TRAP-positive multinucleated cells (TRAP<sup>+</sup> MNCs) ที่ระดับความเข้มข้นยับยั้งกึ่งหนึ่ง (IC<sub>50</sub>) 325±1.37 นาโนโมลาร์ การยับยั้งดังกล่าวสอดคล้องกับการลดลงของสัญญาณภายใต้การกระตุ้นของ RANKL โดยรวมถึงวิถี Mitogen-activated protein kinases (MAPKs) เช่น ERK (p44/42) และ p38 แต่ไม่มีผลต่อวิถี NF- $\kappa$ B โดยผลของสารดังกล่าวยังส่งผลกระทบต่อระดับของ transcription factor เช่น nuclear factor of activation T cells (NFATc1) และ c-Fos ซึ่งมีความสำคัญมากในการเปลี่ยนสภาพเป็นเซลล์สลายกระดูก DHPH ลดการกักร่อนกระดูก (bone resorption) บนแผ่นกระดูก (bone slices) นอกจากนี้สาร DHPH ยังสามารถเพิ่มกิจกรรมของเอนไซม์ alkaline phosphatase (ALP) ที่เกี่ยวข้องกับการเปลี่ยนสภาพของเซลล์สร้างกระดูกในเซลล์ชนิด MC3T3-E1 ในกรณีของกรดไซเปอร์เรโนอิกนั้น พบว่าสามารถลดการเกิด TRAP<sup>+</sup> MNCs ที่ระดับความเข้มข้น IC<sub>50</sub> ที่ 36.69±1.02 ไมโครโมลาร์ โดยกรดไซเปอร์เรโนอิกนั้นไม่ส่งผลกระทบต่อวิถีสัญญาณ MAPKs และ canonical NF- $\kappa$ B ซึ่งเป็นสัญญาณภายใต้การกระตุ้นโดย RANKL แต่กรดไซเปอร์เรโนอิกมีผลต่อวิถีสัญญาณ non-canonical NF- $\kappa$ B โดยส่งผลกระทบต่อโปรตีนของ p100/p52 และ TRAF3 และกรดไซเปอร์เรโนอิกมีฤทธิ์ในการลดการแสดงออกของ NFATc1 และ c-Fos และยังส่งผลถึงยีนที่เกี่ยวข้องกับเซลล์สลายกระดูก อาทิ เช่น *nfatc1*, *ctsk* และ *irf8* อีกด้วย ผลการยับยั้งดังกล่าวมีความสอดคล้องกับการลดลงของปริมาณการกักร่อนกระดูกในแผ่นเนื้อฟัน (Dentin slices) ในการศึกษาฤทธิ์ของสารในระดับ *in vivo* โดยใช้หนูทดลองสายพันธุ์ Senescence-accelerated mouse prone 6 (SAMP6) พบว่ากรดไซเปอร์เรโนอิกส่งผลต่อการเพิ่มพื้นที่ของเนื้อกระดูก (bone area) และพื้นที่ของกระดูกชนิด trabecular (trabecular area) ในหนูทดลองสายพันธุ์ SAMP6 โดยพบว่าสารดังกล่าวเพิ่มการแสดงออกของยีน *ibsp* ซึ่งเป็นยีนที่ประมวลรหัสโปรตีน bone sialoprotein ในขณะที่สารดังกล่าวไม่มีผลต่อยีนที่เกี่ยวข้องกับกระบวนการอักเสบ สารออกฤทธิ์ทางชีวภาพที่ได้จากพืชทั้ง DHPH และกรดไซเปอร์เรโนอิก สารทั้งสองชนิดมีผลในการยับยั้งการเกิดและการทำงานของเซลล์สลายกระดูก ดังนั้นสารทั้งสองชนิดมีศักยภาพที่สามารถพัฒนาเป็นสารประกอบมุ่งหวังในการรักษาโรคกระดูกพรุน

สาขาวิชา เทคโนโลยีชีวภาพ

ปีการศึกษา 2560

ลายมือชื่อ นิสิต .....

ลายมือชื่อ อ.ที่ปรึกษาหลัก .....

ลายมือชื่อ อ.ที่ปรึกษาร่วม .....

# # 5672876223 : MAJOR BIOTECHNOLOGY

KEYWORDS: OSTEOPOROSIS / OSTEOCLAST / DIARYLHEPTANOID / CYPERENOIC ACID / MAPK / NF- $\kappa$ B / SAMP6

SUPATTA CHAWALITPONG: BIOACTIVE COMPOUNDS WITH AN INHIBITORY ACTIVITY AGAINST OSTEOCLAST DIFFERENTIATION AND MECHANISMS. ADVISOR: ASSOC. PROF. TANAPAT PALAGA, Ph.D., CO-ADVISOR: PROF. APICHART SUKSAMRARN, Ph.D., pp.

Osteoporosis is one of the major health concerns for aging societies. The major cause of this condition is an imbalance in cellular function between bone forming cells, osteoblasts, and bone resorbing cells, osteoclasts. The progressive decrease in bone mass especially in aging individuals leads to increased susceptibility to fracture. This study aimed to screen and identify bioactive compounds from plants with activity against osteoclast differentiation and to elucidate its mode of action. Among these compounds, (3*S*)-1-(3,4-dihydroxyphenyl)-3-hydroxy-7-phenyl-(6*E*)-6-heptene (DHPH) and cyperenoic acid isolated from the rhizomes of *Curcuma comosa* Rox and the roots of *Croton crassifolius* Geiseler, respectively, showed strong anti-osteoclastogenesis activity in receptor activator of nuclear factor- $\kappa$ B (RANK) ligand-induced bone marrow-derived osteoclast *in vitro* system. DHPH significantly inhibited RANKL-induced osteoclast differentiation by inhibiting the formation of tartrate resistance acid phosphatase (TRAP)-positive multinucleated cells (MNCs) with the half maximum inhibitory concentration (IC<sub>50</sub>) at 325±1.37 nM. The inhibitory effect of DHPH is associated with impaired activation of multiple signaling pathways downstream of RANKL/RANK, mainly mitogen-activated protein kinases (MAPKs), including ERK (p44/42) and p38, but not NF- $\kappa$ B pathway. Treatment with DHPH effectively suppressed two transcriptional factors, nuclear factor of activated T cells (NFATc1) and c-Fos, both of which are critical for osteoclast differentiation. DHPH treatment also decreased bone resorption on bone slices. In addition, DHPH clearly enhanced alkaline phosphatase activity (ALP) in osteoblast precursor cell line MC3T3-E1. Cyperenoic acid dramatically suppressed TRAP<sup>+</sup>MNCs with an IC<sub>50</sub> of 36.69±1.02 mM. Both MAPK and canonical NF- $\kappa$ B pathway, downstream of RANKL/RANK were not affected by cyperenoic acid treatment. Interestingly, non-canonical NF- $\kappa$ B pathway ((p100/p52) and TRAF3), was found to be affected by cyperenoic acid. Cyperenoic acid significantly reduced the expression of NFATc1 and c-Fos. Osteoclast-related genes i.e. *nfatc1*, *ctsk* and *irf8*, were all affected. The inhibitory effect of cyperenoic acid is associated with a diminution of bone resorption on the dentin slices. *In vivo* study using senescence-accelerated mouse prone 6 (SAMP6) mice strain revealed that cyperenoic acid significantly increased both bone area and the trabecular area in SAMP6 mice. Expression of *ibsp*, encoding bone sialoprotein, increased while the mRNA level of inflammatory-related genes was not affected. Taken together, plant-derived compounds, both DHPH and cyperenoic acid, were effective in inhibiting osteoclast differentiation and function. Therefore, they have potential to be lead compounds for osteoporosis treatment.

Field of Study: Biotechnology

Academic Year: 2017

Student's Signature .....

Advisor's Signature .....

Co-Advisor's Signature .....

## ACKNOWLEDGEMENTS

Firstly, I would like to express my sincere gratitude to my advisor, Associate Professor Dr. Tanapat Palaga, Department of Microbiology, Chulalongkorn University, for his valuable suggestion and encouragement through the learning process of my Ph.D. study and related research. I would like to express my deeply grateful to my co-advisor Professor Dr. Apichart Suksamrarn, Department of Chemistry and Center of Excellence for Innovation in Chemistry, Ramkhamhaeng University, for the kindness and supporting on my research, as well. Besides my advisor, I would like to thank the rest of my thesis committee: Assistant Professor Dr. Chulee Yompakdee, Associate Professor Dr. Chanpen Chanchao, Associate Professor Dr. Aphichart Karnchanatat, and Professor Dr. Narattaphol Charoenphandhu

Furthermore, I would like to express my appreciation to Professor Dr. Soichiro Nakamura, Associate Professor Dr. Shigeru Katayama, and Assistant Professor Dr. Takakazu Mitani, Interdisciplinary Graduate School of Science and Technology, Shinshu University who gave me a golden opportunity to do this research in Japan.

A very special gratitude for the Science Achievement Scholarship of Thailand and Overseas Research Experience Scholarship for Graduated student from Graduate School and Faculty of Science, Chulalongkorn University for helping and providing the funding for this research.

Thankfulness would be given to all TP's laboratory members especially, Dr. Wipawee Wongchana and Miss Preeyapan Sriploy, Graduate Program in Biotechnology and Microbiology, Chulalongkorn University, respectively for counseling and encouragement. Further, gratefulness would be given to Henry M. Corpuz, Ahmad Al Athamneh, Misa Arimura and other friends who have supported me along the way in Shinshu University, Japan.

Finally, I would like to thank my family for supporting me spiritually throughout working on this thesis and my life in general.

## CONTENTS

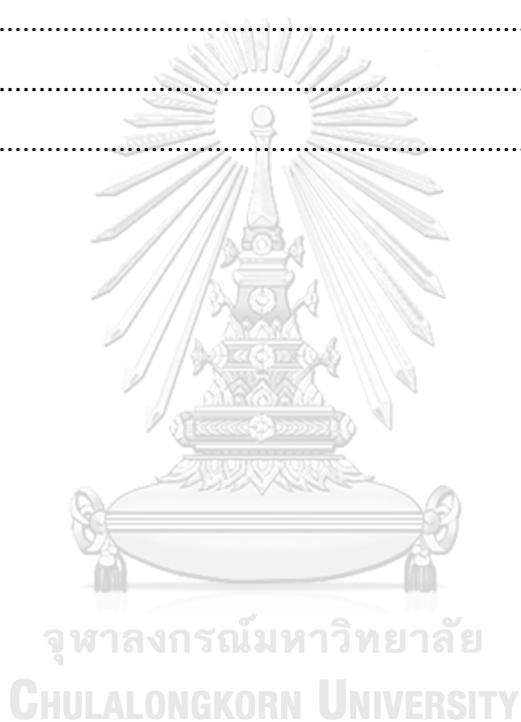
|   | Page |
|---|------|
| THAI ABSTRACT .....   | iv   |
| ENGLISH ABSTRACT.....   | v    |
| ACKNOWLEDGEMENTS.....   | vi   |
| CONTENTS.....   | vii  |
| LIST OF FIGURES .....   | xi   |
| LIST OF TABLES .....  | xiii |
| LIST OF ABBREVIATIONS.....  | xiv  |
| CHAPTER I INTRODUCTION.....   | 1    |
| CHAPTER II LITERATURE REVIEW .....  | 3    |
| 2.1 Bone.....   | 3    |
| 2.1.1 Cell involved in bone formation.....  | 3    |
| 2.1.1.1 Osteoblast .....  | 3    |
| 2.1.1.2 Osteoclast .....  | 4    |
| 2.2 Bone remodeling process.....  | 6    |
| 2.2.1 Regulation of bone remodeling .....   | 6    |
| 2.2.1.1 Systemic regulators .....   | 6    |
| 2.2.1.2 Local regulators .....  | 7    |
| 2.3 Regulation of osteoclast differentiation and the associated signaling pathways..... | 8    |
| 2.3.1 Cytokines involved in osteoclast differentiation .....                            | 8    |
| 2.3.2 RANK/RANKL associated signaling pathways.....                                     | 10   |
| 2.3.2.1 MAPKs pathway .....   | 10   |
| 2.3.2.2 NF- $\kappa$ B pathways.....  | 10   |
| 2.3.3 Transcription factors regulating osteoclast differentiation.....                  | 12   |
| 2.4 Bone turnover marker (BTMs) .....   | 13   |
| 2.4.1 Bone resorption markers .....   | 13   |
| 2.4.2 Bone formation markers .....  | 13   |
| 2.5 Senile osteoporosis mouse models .....  | 14   |

|  | Page |
|--|------|
| 2.6 Effects of Thai medicinal plants and their bioactive compounds on osteoclast differentiation .....       | 15   |
| 2.7 Currently available agents to target bone loss and osteoporosis .....                                    | 19   |
| CHAPTER III MATERIAL AND METHODS .....   | 21   |
| 3.1 Bioactive compounds .....  | 21   |
| 3.2 Cell cultures.....   | 25   |
| 3.2.1 RAW264.7 cell line.....  | 25   |
| 3.2.2 Bone marrow derived macrophage (BMMs).....   | 25   |
| 3.2.3 Pre-osteoblast cell line (MC3T3-E1) .....  | 25   |
| 3.3 Cell viability assay .....   | 25   |
| 3.3.1 Thiazolyl blue tetrazolium bromide (MTT) assay .....   | 25   |
| 3.3.2 Methyl tetrazolium salt (MTS) assay .....  | 26   |
| 3.4 Anti-inflammatory activity assay .....   | 26   |
| 3.5 Anti-osteoclastogenesis activity screening assay .....   | 26   |
| 3.6 Qualitative reverse transcription polymerase chain reaction (RT-qPCR).....                               | 27   |
| 3.6.1 RNA extraction.....  | 27   |
| 3.6.2 Reverse transcription and quantitative polymerase chain reaction (qPCR).....                           | 27   |
| 3.7 Western blot.....  | 28   |
| 3.7.1 Cell lysate preparation and sodium dodecyl sulfate-polyacrylamide gel electrophoresis (SDS-PAGE) ..... | 28   |
| 3.8 Immunofluorescence staining.....   | 29   |
| 3.9 Bone resorption assay.....   | 31   |
| 3.10 Alkaline phosphatase activity assay (ALP) for osteoblast differentiation.....                           | 31   |
| 3.11 <i>In vivo</i> study using Senescence Accelerated Mouse Prone 6 (SAMP6) mice .31                        |      |
| 3.11.1 Standard diet food AIN-93M.....   | 31   |
| 3.11.2 Animal treatment .....  | 32   |
| 3.11.3 Bone histomorphometry .....   | 32   |
| 3.11.4 ELISA for serum bone sialoprotein.....  | 33   |



|   | Page |
|---|------|
| 3.12 Statistical analyses .....   | 33   |
| CHAPTER IV RESULTS.....   | 34   |
| 4.1 Screening compounds from Thai medicinal plants with anti-osteoclastogenic activity.....   | 34   |
| 4.1.1 The effect of pure compounds from Thai medicinal plants on cell viability in RAW264.7 cells.....  | 34   |
| 4.1.2 Effect of pure compounds on nitric oxide production in LPS and IFN- $\gamma$ stimulated RAW264.7 cells .....                                | 34   |
| 4.1.3 Effect of pure compounds on RANKL-stimulated osteoclast formation .....   | 39   |
| 4.2 The molecular mechanism of diarylheptanoid (DHPH, ASTP019) from <i>C. comosa</i> Roxb. on RANKL-stimulated osteoclast differentiation.....    | 40   |
| 4.2.1 Effect of DHPH on RANKL-stimulated osteoclast formation.....  | 40   |
| 4.2.2 Effect of DHPH on the expression of osteoclast-related genes in RANKL-stimulated BMMs .....   | 40   |
| 4.2.3 Effect of DHPH on expression of NFATc1 and c-Fos in RANKL-stimulated BMMs .....   | 43   |
| 4.2.4 Effect of DHPH on NFATc1 nuclear translocation in RANKL-stimulated BMMs .....   | 43   |
| 4.2.5 Effect of DHPH on downstream signaling of the RANKL/RANK .....  | 46   |
| 4.2.6 Effect of DHPH on bone resorption activity or osteoclast activation .....   | 48   |
| 4.2.7 Effect of DHPH on osteoblast differentiation .....  | 49   |
| 4.3 The molecular mechanism of cyperenoic acid (ASTP053) from <i>C. crassifolius</i> Geiseler on RANKL-stimulated osteoclast differentiation..... | 51   |
| 4.3.1 Effect of cyperenoic acid, cyperenol and CATC on RANKL-stimulated osteoclast formation.....   | 51   |
| 4.3.2 Effect of cyperenoic acid on expression of osteoclast related genes in RANKL-stimulated BMMs .....  | 51   |
| 4.3.3 Effect of cyperenoic acid on NFATc1 and c-Fos in RANKL-stimulated BMMs. ....  | 54   |
| 4.3.4 Effect of cyperenoic acid on signaling downstream of RANKL/RANK in RANKL-stimulated BMMs.....   | 55   |

|   | Page |
|---|------|
| 4.3.5 Effect of cyperenoic acid on bone resorption activation in RANKL-stimulated osteoclasts ..... | 58   |
| 4.3.6 Effect of cyperenoic acid on ALP activity in osteoblasts .....                                | 59   |
| 4.3.7 Effect of cyperenoic acid on SAMP6 mice as a senile osteoporosis model.....                   | 60   |
| CHAPTER V DISCUSSION .....  | 66   |
| CHAPTER VI CONCLUSION .....   | 73   |
| REFERENCES .....  | 74   |
| APPENDIX.....   | 86   |
| VITA.....   | 96   |



## LIST OF FIGURES

|   |    |
|---|----|
| Figure 1. Differentiation and function of osteoblasts and osteoclasts during bone formation.....              | 5  |
| Figure 2. The bone remodeling process.....  | 9  |
| Figure 3. Major signaling pathways governing osteoclast formation and activation. .                           | 11 |
| Figure 4. Anti-inflammation activity in stimulated RAW264.7 cells.....  | 38 |
| Figure 5. Effect of plant-derived pure compounds on RANKL-stimulated osteoclast formation.....                | 39 |
| Figure 6. Effect of DHPH on RANKL-stimulated osteoclast formation.....  | 41 |
| Figure 7. Effect of DHPH on mRNA expression of osteoclast-related genes in RANKL-stimulated BMMs. ....        | 42 |
| Figure 8. Effect of DHPH on NFATc1 and c-Fos in RANKL-stimulated BMMs. ....                                   | 44 |
| Figure 9. Effect of DHPH on nuclear translocation of NFATc1 in RANKL stimulated BMMs.....                     | 45 |
| Figure 10. Effect of DHPH on downstream signaling of the RANKL/RANK. ....                                     | 47 |
| Figure 11. Effect of DHPH on bone resorption in RANKL-stimulated osteoclasts....                              | 48 |
| Figure 12. Effect of DHPH on cell viability and cell differentiation of pre-osteoblast MC3T3-E1 cells.....    | 50 |
| Figure 13. Effect of cyperenoic acid and other compounds on RANKL-stimulated osteoclast formation.....        | 52 |
| Figure 14. Effect of cyperenoic acid on expression of osteoclast-related genes in RANKL-stimulated BMMs. .... | 53 |
| Figure 15. Effect cyperenoic acid on transcription factor in RANKL-stimulated BMMs.....                       | 54 |
| Figure 16. Effect of cyperenoic acid on MAPK and canonical NF-κB pathway in RANKL-stimulated BMMs. ....       | 56 |

|   |    |
|---|----|
| Figure 17. Effect of cyperenoic acid on non-canonical NF- $\kappa$ B pathway in RANKL-stimulated BMMs. ....   | 57 |
| Figure 18. Effect of cyperenoic acid on bone resorption in RANKL-stimulated osteoclasts. ....   | 58 |
| Figure 19. Effect of cyperenoic acid on cell viability and osteoblast differentiation in MC3T3-E1 cells.....  | 59 |
| Figure 20. The body weight, diet consumption and pathology of liver and kidney in SAMP6 mice.....   | 62 |
| Figure 21. Effect of cyperenoic acid on bone histomorphometry at distal femur. ....   | 63 |
| Figure 22. Effect of cyperenoic acid on expression of bone formation-related genes, bone resorption-related genes and pro-inflammatory cytokine genes in BMMs of SAMP6 mice. .... | 64 |
| Figure 23. Effect of cyperenoic acid on bone resorption marker in SAMP6 mice serum.....   | 65 |
| Figure 24. Proposed model of anti-osteoclastogenic activity of DHPH or cyperenoic acid .....  | 72 |

**LIST OF TABLES**

|   |    |
|---|----|
| Table 1. Anti-osteoclastogenic compounds isolated from medical plants.....                | 17 |
| Table 2. Bioactive compounds used in this study.....                                      | 22 |
| Table 3. List of primers used in this study.....  | 29 |
| Table 4. List of primary antibodies used in this study.....                               | 30 |
| Table 5. IC <sub>50</sub> and IC <sub>20</sub> for cell viability in RAW264.7 cells ..... | 35 |



## LIST OF ABBREVIATIONS

|                 |  |
|-----------------|--|
| %               | Percentage   |
| μg              | Microgram  |
| μM              | Micromolar   |
| /               | Per  |
| :               | Ratio  |
| Ab              | Antibody   |
| ALP             | Alkaline phosphatase   |
| avb3            | Alpha-v beta-3   |
| BMD             | Bone mineral density   |
| BMMs            | Bone marrow derived macrophage precursors  |
| bp              | Base pair  |
| BSA             | Bovine serum albumin   |
| BSAP            | Bone-specific alkaline phosphatase   |
| BSP             | Bone sialoprotein  |
| cDNA            | Complementary DNA  |
| cFMS            | M-CSF receptor   |
| cIAP            | Cellular inhibitor of apoptosis  |
| CO <sub>2</sub> | Carbon dioxide   |
| DHPH            | Diarylheptanoid (3 <i>S</i> )-1-(3,4-dihydroxyphenyl)-3-hydroxy-7-phenyl-(6 <i>E</i> )-6-heptene |
| DMAb            | Denosumab  |
| DNA             | Deoxyribonucleic acid  |
| dNTP            | dATP, dCTP, dGTP and dTTP  |
| ER              | Estrogen receptor  |
| FBS             | Fetal bovine serum   |
| g               | Gravity (Centrifuge speed)   |
| hr              | Hour   |
| HSCs            | Hematopoietic stem cells   |

|                  |  |
|------------------|--|
| IC <sub>20</sub> | 20 % of inhibitory concentration   |
| IC <sub>50</sub> | 50 % of inhibitory concentration   |
| IFN- $\gamma$    | Interferon gamma   |
| IgG              | Immunoglobulin G   |
| IL               | Interleukin  |
| kDa              | Kilo Dalton  |
| LPS              | Lipopolysaccharide   |
| MAPK             | Mitogen-activated protein kinase   |
| M-CSF            | Macrophage colony-stimulating factor   |
| mg               | Milligram  |
| min              | Minute   |
| ml               | Milliliter   |
| mM               | Millimolar   |
| MMP9             | Matrix metalloprotein-9  |
| mRNA             | Messenger RNA  |
| MSCs             | Mesenchymal stromal cells  |
| MTS              | 3-(4,5-dimethyl-2-yl)-5-(3-carboxymethoxyphenyl)-2-(4-sulfophenyl)-2H-tetrazolium, inner salt<br>3-(4,5-dimethylthiazol-2-yl)-2,5- diphenyltetrazolium |
| MTT              | brominde   |
| N                | Normality (Concentration)  |
| NED              | N-(1-naphthyl-ethylenediamine dihydrochloride)   |
| NF- $\kappa$ B   | Nuclear factor - kappa B   |
| NFATc1           | Activate nuclear factor of activated T cells   |
| ng               | Nanogram   |
| NIK              | NF- $\kappa$ B-inducing kinase   |
| nM               | Nanomolar  |
| NO               | Nitric oxide   |
| OC               | Osteocalcin  |
| °C               | Degree Celsius   |
| OD               | Optical density  |

|           |   |
|-----------|---|
| ODN       | Odanacatib  |
| OPG       | Osteoprotegerin   |
| PAGE      | Polyacrylamide gel electrophoresis                          |
| PBS       | Phosphate buffer saline                                     |
| PBST      | Phosphate buffer saline - Tween 20                          |
| PCR       | Polymerase chain reaction                                   |
| pNPP      | p-nitrophenyl phosphate                                     |
| PTH       | Parathyroid hormone   |
| PVDF      | Polyvinylidene fluoride                                     |
| qPCR      | Quantitative polymerase chain reaction                      |
| RANKL     | Receptor activator of NF- $\kappa$ B ligand                 |
| RNA       | Ribonucleic acid  |
| rpm       | Round per minute  |
| RT        | Reverse transcription                                       |
| RT-qPCR   | Qualitative Reverse transcription polymerase chain reaction |
| SAMP6     | Senescence accelerated mouse prone                          |
| SDS       | Sodium dodecyl sulfate                                      |
| sec       | Second  |
| TNF       | Tumor necrosis factor                                       |
| TRAF6     | TNF receptor-associated factor 6                            |
| TRAP      | Tartrate-resistant acid phosphatase                         |
| TRAP+MNCs | TRAP positive cells multinucleated giant cells              |
| U         | Unit  |
| v         | Volume  |
| Vitamin D | 1,25-Dihydroxyvitamin D                                     |
| w         | Weight  |



## CHAPTER I

### INTRODUCTION

Osteoporosis is a major health concern for aging communities. The progressive decreasing in bone mass leads to an increased susceptibility to fracture. The major cause of this condition is an imbalance between bone forming cells, osteoblasts, and bone resorbing cells, osteoclasts. Osteoblasts derived from mesenchymal stem cell are responsible for bone formation. Osteoclasts develop from hematopoietic stem cells through the fusion of mononuclear myeloid precursors and mature to become multinucleated giant cells. Mature osteoclasts play a role in bone resorption. The functions of these two cell types are under tight regulation during bone remodeling by systemic or local regulators. Although currently there are therapeutic drugs to treat osteoporosis the cost and the side effects of the drugs warrant the search for new therapeutic drugs. Therefore, new prevention and therapeutic measures to treat this condition is urgently needed.

During osteoclastogenesis, bone marrow derived macrophage precursors (BMMs) differentiate into tartrate-resistant acid phosphatase (TRAP)-positive cells, which fuse with each other to form mature osteoclasts. Mature osteoclasts have highly specialized functions. They have an ability to digest both the organic bone matrix and the inorganic minerals by secretion of acid and proteolytic enzymes such as TRAP, cathepsin K and matrix metalloproteinase 9 (MMP9).

In particular, two cytokines macrophage-colony stimulating factor (M-CSF) and receptor activator of nuclear factor- $\kappa$  ligand (RANKL) provide necessary signals for osteoclast differentiation. These two cytokines signal through MAPKs (p38, SAPK/JNK and p44/42), canonical NF- $\kappa$ B (IKKs, I $\kappa$ B $\alpha$  and RelA/p50), non-canonical NF- $\kappa$ B (IKK $\alpha$ , NIK and RelB/p52) and costimulatory signal (PLC $\gamma$ -Ca<sup>2+</sup>) pathway. These signals result in activation of key transcription factors in osteoclastogenesis including c-Fos, AP-1 and NFATc1.

Senescence Accelerated Mouse Prone 6 (SAMP6) is a senile osteoporosis model characterized by a low peak in bone mass after 16 weeks old. The decreasing in

bone formation and the increasing in bone resorption in SAMP6 mice owing to a deficiency of osteoblast progenitor cell and increasing maturation of osteoclast, respectively. The symptoms of mice are similar to aging human. Therefore, SAMP6 mice are useful model for study in term of senile osteoporosis.

Many natural products from medicinal plants have been invaluable sources in the discovery of new lead compounds for therapies, including therapeutic agents for bone loss.

In this study, osteoclasts derived from murine BMMs were induced by RANKL and M-CSF and used for screening of plant-derived compounds with an anti-osteoclastogenesis. The positive compounds were further investigated for the molecular mechanism. For an *in vivo* study, SAMP6 mice were used to examine for the effect of identified compound on bone loss.

### **Objective**

- 1) To screen Thai medicinal plant-derived compounds or their derivatives for the anti-osteoclastogenesis activity
- 2) To investigate the molecular mechanism of action

## CHAPTER II

### LITERATURE REVIEW

#### 2.1 Bone

Bone is rigid dynamic organ with porous mineralized structure. The main functions of bone consist of structural function, metabolic function, and hematopoietic function. There are two major types of bone, trabecular bone, and cortical bone. Further, the structural components of bone consist of an extracellular matrix, collagen, and cells (1).

##### 2.1.1 Cell involved in bone formation

###### 2.1.1.1 Osteoblast

Osteoblast is responsible for bone formation. Osteoblasts originated from mesenchymal stem cells like adipocytes, chondrocytes, myoblasts, and fibroblasts (2). They also produce extracellular protein, collagen type I, osteocalcin and alkaline phosphatase which are used as bone formation markers (3). Bone formation process consists of three steps:

- a) Production of osteoid which is extracellular organic matrix, by osteoblast and deposition a collagen to bone matrix
- b) Maturation of osteoid through increasing the mineralization rate in osteoid.
- c) Matrix mineralization by fully mineralized osteoid (1, 4).

Furthermore, osteoblasts have the capacity to produce cytokines that are a critical for osteoclast differentiation such as macrophage colony-stimulating factor (M-CSF) and receptor activator of nuclear factor kappa-B ligand (RANKL). These cytokines enhance cell survival, cell proliferation and cell differentiation in osteoclasts while osteoprotegerin (OPG) inhibits osteoclastogenesis by competition with RANK receptor (5) (Fig. 1). In osteoblast deficient mice are also affected osteoclastogenesis (6). The activation of osteoblast is generated by bone remodeling regulators such as endocrines and growth factors (4).

### 2.1.1.2 Osteoclast

Osteoclasts are originated from hematopoietic stem cells, which develop through the fusion of mononuclear myeloid precursors and mature to become mature osteoclasts under the regulation of cytokines and growth factors similar to osteoblasts (4).

Precursor osteoclasts express M-CSF receptor (cFMS) and the RANK receptor on the cell surface. Binding between receptors and these ligands such as cFMS/M-CSF and RANK/RANKL leads to osteoclast maturation (7). During osteoclast differentiation, bone marrow-derived macrophage precursors (BMMs) differentiate into tartrate-resistant acid phosphatase (TRAP) positive cells, which fuse with each other to form multinucleated giant cells (TRAP+MNCs) (8) (Fig. 1).

Osteoclasts are responsible for bone resorption with highly specialized function. They have an ability to digest both the organic bone matrix and the inorganic minerals by secretion enzymes (9). Bone resorption process is initiated by the following step:

- a) Attachment of osteoclasts on bone surface by alpha-v beta-3 (avb3) integrin binding molecule
- b) Cytoskeleton reorganization, avb3 integrin binding on matrix surface leading to activate cytoskeleton processing within osteoclasts and movement of osteoclasts during bone resorption process
- c) Releasing of acidified and proteolytic enzymes to bone matrix such as TRAP, cathepsin K and matrix metalloprotein-9 (MMP9) (10)

Therefore, osteoblast, a bone formation cell, and osteoclast, a bone resorption cell play an important role in bone turnover process.

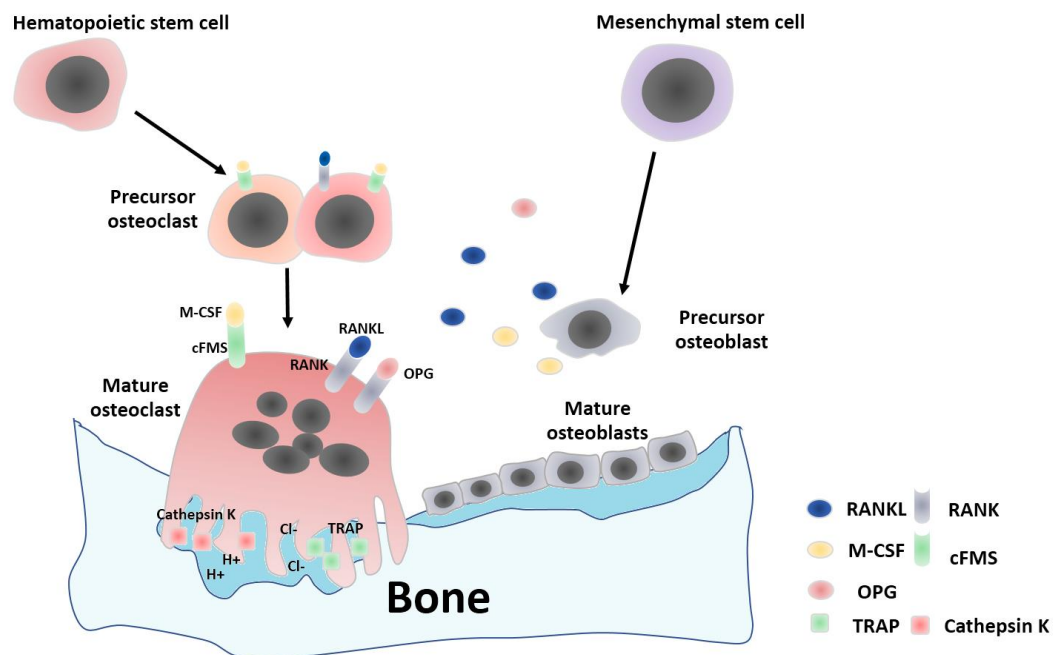


**Figure 1. Differentiation and function of osteoblasts and osteoclasts during bone formation.**

Osteoblasts originated from mesenchymal stem cells become mature osteoblasts via precursor osteoblasts. Precursor osteoblasts produce necessary cytokines, RANKL, M-CSF, and OPG. They play a critical role in osteoclastogenesis. On the other hand, osteoclasts are originated from hematopoietic stem cells through precursor osteoclasts. Precursor osteoclasts express cFMS, a receptor for M-CSF. The binding of M-CSF to its receptor stimulates cell proliferation and cell survival further activates the expression of the RANK receptor on the cell surface of precursor osteoclast. Both M-CSF and RANKL induce maturation of osteoclasts resulting in cell-cell fusion of multinucleated giant cells. Mature osteoclasts produce enzymes such as TRAP, cathepsin K and MMP-9 for bone resorption process. OPG is a negative regulator for osteoclastogenesis by competition for RANK receptor (1, 4, 7) (Modified from Kini and Nandeesh (2001) (4) and Takayanagi (2007) (7)).

## 2.2 Bone remodeling process

The bone remodeling is a continuous process. This process involves the elimination of mineralized bone by mature osteoclasts and formation of bone matrix by osteoblasts. Bone remodeling could be divided into three stages (Fig. 2) (1, 11).

a) Resorption stage

The hematopoietic stem cells (HSCs) recruit to the bone where they differentiate to precursor osteoclasts and become mature osteoclasts. The mature osteoclasts generate the resorption lacunae or resorption pits on bone surface by secreting the acidified and proteolytic enzymes to the bone surface.

b) Reversal stage

The precursor osteoblasts move to bone surface. They prepare the appropriate bone surface for new osteoblasts then provide signals for osteoblast migration and differentiation.

c) Formation stage

The mature osteoblasts move to resorption lacunae and deposit the new bone into the cavity.

In normal bone turnover the processing of bone resorption and bone formation should be balanced. In the case of osteoporosis, the resorbed rate of osteoclasts is higher than the deposited rate of osteoblasts. The major cause of this condition is age-related condition leading to progressive decrease in bone mass and increase in bone fracture (11-13).

### 2.2.1 Regulation of bone remodeling

#### 2.2.1.1 Systemic regulators

The systemic regulator is controlled by several types of hormones or vitamins with stimulatory and/or inhibitory activity in bone cells for example, parathyroid hormone, calcitriol, calcitonin, glucocorticoids, thyroid hormone, estrogen, androgen and vitamin D.

a) Parathyroid hormone (PTH)

PTH is secreted from parathyroid gland. PTH plays a role in calcium homeostasis and stimulates bone resorption for calcium releasing to blood circulation. The effect of PTH is mediated by PTH receptor on osteoblasts. The activated osteoblasts subsequently produce RANKL and M-CSF, lead to resorb on the bone surface (14).

b) 1,25-Dihydroxyvitamin D (Vitamin D)

Vitamin D is responsible for bone mineralization of osteoids. It promotes the activation of gene expression related to osteoblast differentiation and bone mineralization such as osteocalcin, collagen type I and alkaline phosphate. However, vitamin D also plays a role in bone metabolism via RANK/RANKL pathway by inducing the production of RANKL in osteoblast (15).

c) Androgen

Androgen, a steroid hormone, is one of sex hormones secreted from testes. This hormone is necessary for bone formation via androgen receptor in all of bone cell (16).

d) Estrogen

Estrogen is released by corpus luteum and ovary. Estrogen plays an important role in osteoclastogenesis regulator. It suppresses osteoclast activation by pass through estrogen receptor on osteoblast resulting in increasing of OPG and suppressing of RANKL and M-CSF. Moreover, estrogen also supports bone formation and osteoblast proliferation (17).

### 2.2.1.2 Local regulators

The local regulator is controlled by OPG/RANKL/RANK system (Fig. 1) and other cytokines (18). This system plays a critical role both for enhancement and for suppression of osteoclastogenesis (19). RANKL is expressed by precursor osteoblasts and stromal cells. In addition, RANK receptor expresses on precursor osteoclasts and mature osteoclasts. RANK and RANKL binding triggers the downstream signaling. M-CSF binding to cFMS

provides a signal which for cell proliferation and cell survivor in osteoclasts. Thus, both RANKL/M-CSF are essential factors for osteoclast development. On the other hand, OPG secreted by osteoblasts, acts as an inhibitor for osteoclastogenesis with competitive binding to RANK receptor (5, 20).

A number of cytokines are involved in bone metabolism with regulation of osteoclast differentiation. For example, interleukin (IL) 1 (21), IL-6 (22) and tumor-necrosis factor (TNF) (21) induce osteoclast differentiation and activation via inflammatory. Furthermore, IL-10 and interferon (IFN)  $\gamma$  inhibit RANKL signaling in osteoclast differentiation via cellular and humoral immunity, respectively (23).

## **2.3 Regulation of osteoclast differentiation and the associated signaling pathways**

### **2.3.1 Cytokines involved in osteoclast differentiation**

M-CSF and RANKL provide the necessary signals for osteoclast differentiation (24). Interaction between M-CSF and cFMS in osteoclast precursors promotes cell proliferation, survival and differentiation of early precursors osteoclast via the activation of kinases such as Src, PLC- $\gamma$ , PI3-kinase, Akt and ERK (p44/42) (25). In mice, point mutation in *csf1* encoding M-CSF showed an osteopetrosis phenotype similar to osteopetrotic (*op/op*) mutant mice (26).

Binding of RANKL to RANK receptor on the cell surface of BMMs induces the recruitment of TNF receptor associated factor (TRAF) signal transduction molecules including in TRAF2, TRAF5 and TRAF6 to RANK. TRAF6 activates mitogen-activated protein kinases (MAPKs), including ERK, SAPK/JNK and p38 and canonical nuclear factor- $\kappa$ B (NF- $\kappa$ B) pathways, including IKK complex, RelA/p50 (p65/p50) and I $\kappa$ B $\alpha$ . In mice lacking TRAF6 exhibit severe osteopetrosis phenotype and osteoclast malformation (27). In addition, TRAF2 and TRAF3 also activate non-canonical NF- $\kappa$ B pathways which are IKK $\alpha$ , NF- $\kappa$ B-inducing kinase (NIK), RelB/p52. These kinases activate nuclear factor of activated T cells (NFATc1), a master transcription factor responsible for osteoclast differentiation and function (28) (Fig. 3).



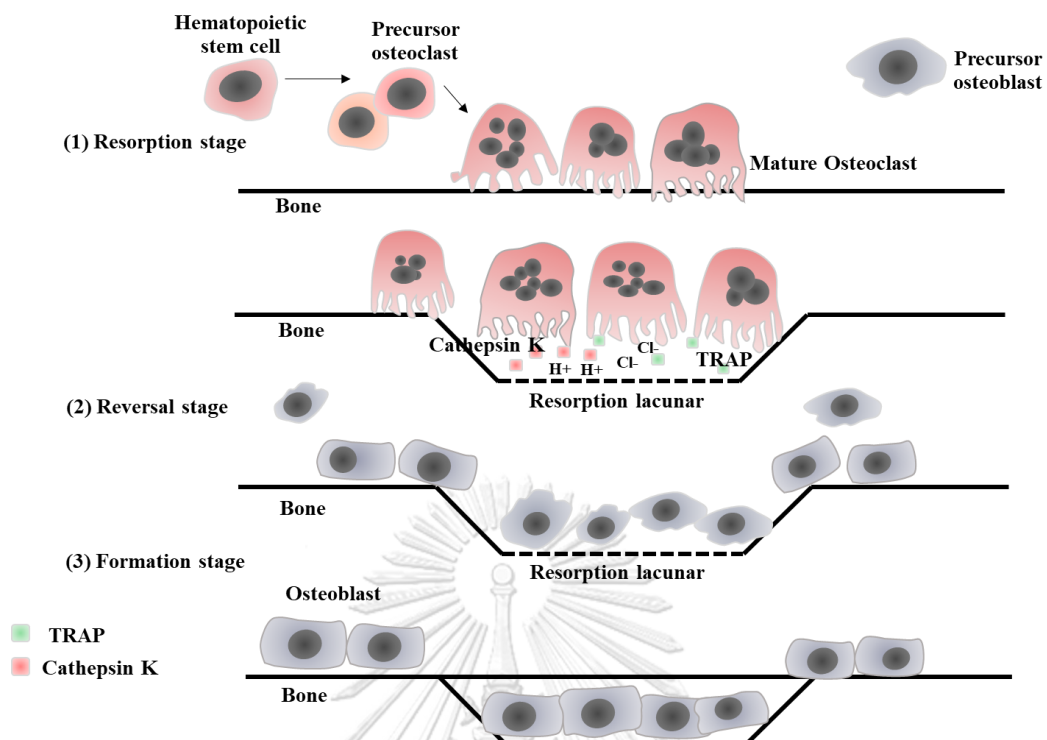


**Figure 2. The bone remodeling process.**

The bone remodeling process consists of three stages i.e. resorption stage, hematopoietic stem cells move to the bone where they become precursor osteoclasts and mature osteoclasts, respectively. The mature osteoclasts generate resorption lacunae (pits) by releasing the proteolytic enzymes and acidified enzymes such as TRAP and cathepsin K to the bone matrix. Reversal stage, the precursor osteoblasts provide signals for osteoblast migration and differentiation. Formation stage, precursor osteoblasts differentiate to mature osteoblasts and deposit the new bone to the cavity belonged to bone formation process (Modified from Teitelbaum and Ross (2003) (11)).

## 2.3.2 RANK/RANKL associated signaling pathways

### 2.3.2.1 MAPKs pathway

MAPKs family consist of p38 (p38 $\alpha$ ,  $\beta$ ,  $\gamma$  and  $\sigma$ ), c-Jun-N-terminal kinase (JNK1, 2 and 3) and extracellular signal-regulated kinase (ERK1 and ERK2) (29). MAPKs play a critical role in osteoclast differentiation. p38 $\alpha$ -deficient monocytes failed to differentiate to osteoclasts (30). These MAPKs regulate activation of various transcription factors through either direct phosphorylation or indirect activation. Using, p38 inhibitor (SB203580), it was found to completely block the expression of c-Fos and NFATc1 in BMMs (31). Furthermore, active MAPKs (p38, ERK and JNK) could directly phosphorylate c-Fos and AP-1 and activate NFATc1 (Fig. 3) (32).

### 2.3.2.2 NF- $\kappa$ B pathways

NF- $\kappa$ B pathway is a family of transcription factor involved in various biological processes, including cell growth and survival, cell development, immune response and inflammation (33). In particular, NF- $\kappa$ B is divided into two major signaling transduction pathways, which are the classical pathway (canonical pathway), and the alternative pathway (non-canonical pathway) (34) (Fig. 3).

#### a) Canonical NF- $\kappa$ B pathway

Canonical NF- $\kappa$ B pathway is activated by numerous signals, including those mediated by innate and adaptive immune receptors (35). It plays critical role in osteoclastogenesis which proceeded by TRAF6 activation, a cytoplasmic domain. TRAF6 activates I $\kappa$ B kinase (IKK) complex which is an adaptor protein complex leading to phosphorylation and proteasome degradation of I $\kappa$ B $\alpha$  (19, 32). I $\kappa$ B $\alpha$  is inhibitory factor for RelA (p65)/p50 when NF- $\kappa$ B is activated, the proteasome degradation of I $\kappa$ B leads to conduct nuclear translocation of RelA/p50 (36).

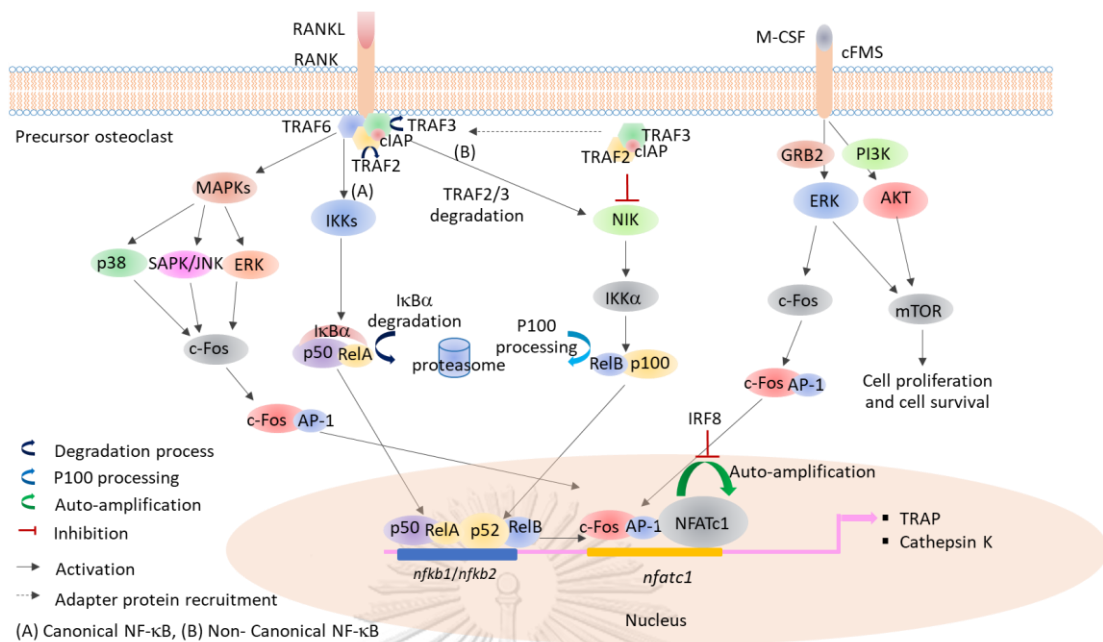


**Figure 3. Major signaling pathways governing osteoclast formation and activation.**

Binding between M-CSF and cFMS enhances cell proliferation and cell survivor through ERK, Akt and mTOR pathways. TRAF6, a transduction molecule, activates MAPKs family including p38, SAPK/JNK and ERK. These kinases activate c-Fos; and, activated c-Fos forms dimer with AP-1, and translocate to the nucleus. They bind to the *nfactc1* promoter. Furthermore, TRAF6 stimulates canonical NF- $\kappa$ B (RelA/p50) via IKKs complex activation and I $\kappa$ B $\alpha$  degradation. On the other hand, TRAF2 and TRAF3 involve in non-canonical NF- $\kappa$ B pathways. TRAF2/TRAF3/cIAP complex regulate the activation of NIK. In the case of RANKL stimulation, this complex is ubiquitinated and degraded by cIAP leading to signaling cascade via NIK. IKK $\alpha$  triggers phosphorylation of p100 and processing into p52, a mature form of p100. Both RelA/p50 and RelB/p52 drive the activation of *nfactc1* promoter. Taken together, c-Fos/AP-1 and NF- $\kappa$ B support the auto-amplification of NFATc1 leading to the expression of osteoclast-related genes; TRAP and cathepsin K. Interferon regulator factor-8 (IRF8) plays a key modulatory role in auto-amplification of NFATc1 by inhibiting the expression of NFATc1 (Modified from Takayanagi (2007) (7), Boyce *et al.* (2015) (37) and Aeschlimann and Evans (2004) (38)).

b) Non-canonical NF- $\kappa$ B pathway

Non-canonical NF- $\kappa$ B is one of arms in NF- $\kappa$ B signaling which plays an important role in osteoclastogenesis as well (39). This process initiated by pass-through cytoplasmic domains; TRAF2 and TRAF3. TRAF3 is a major negative regulator that suppress the activation of NIK by ubiquitination and degradation (40). In TRAF3 knockout cells, NIK is accumulated leading to un-processed of p100 (41). Upon RANKL stimulation, TRAF3 is ubiquitinated and degraded by cellular inhibitor of apoptosis (cIAP) leading to accumulate of NIK and activate IKK $\alpha$ , respectively (39). Subsequently, IKK $\alpha$  triggers phosphorylation of p100 leading to process into the mature form of p100 (p52). Finally, p52 binds with RelB, translocate to nucleus and activates the gene transcription (42, 43).

### 2.3.3 Transcription factors regulating osteoclast differentiation

Association of TRAFs leads to activation of transcription factors, which induces expression of osteoclast related genes (19, 32). RANK mutant (*tnfrsf11a*<sup>-/-</sup>) exhibits completely lacking TRAF6 leading to abrogate osteoclastogenesis (44).

Activation of transcription factors including NF- $\kappa$ B, AP-1 and NFATc1, is necessary for osteoclast differentiation. NFATc1 plays an important role as a master transcription regulator of osteoclast differentiation (32). In *nfatc1*<sup>-/-</sup> embryonic stem cells could not differentiate into mature osteoclasts (45). NFATc1-deficient mice exhibited osteopetrosis phenotype owing to malformation in osteoclastogenesis process (46). Furthermore, mice lacking c-Fos developed osteopetrosis and problem with tooth eruption (47). AP-1 is transcription factor binds to c-Fos and forms dimeric complex. Consequently, the component of AP-1 and c-Fos is necessary for RANKL-mediated induction of NFATc1 (48).

## 2.4 Bone turnover marker (BTMs)

### 2.4.1 Bone resorption markers

#### a) TRAP

TRAP encoding by *acp5*, indicates critical condition for skeleton development. TRAP deficient mice (*acp5<sup>-/-</sup>*) exhibited the reducing of bone resorption activity leading to osteopetrosis phenotype. Therefore, TRAP is useful as biomarker for osteoclast function and level of bone resorption (49).

#### b) Cathepsin K

During bone resorption process, cathepsin K plays an important role in collagen and matrix protein degradation. Cathepsin K is secreted by mature osteoclast from ruffled border area into resorption lacunae. This enzyme encoded by *ctsk*. Cathepsin k (*ctsk<sup>-/-</sup>*) knockout mice contribute the osteopetrosis phenotype due to decreasing in bone resorption (50).

#### c) IRF8

IRF8 is a negative regulator, encoding by *irf8*. It is involved in osteoclast differentiation and function. *irf8* is a key modulatory for osteoclast differentiation by suppressing the function and expression of NFATc1. Mice lacking IRF8 (*irf8<sup>-/-</sup>*) exhibited a severe osteoporosis due to osteoclast number increasing (51).

### 2.4.2 Bone formation markers

#### a) Bone sialoprotein (BSP)

BSP is encoded by *ibsp* and secreted by chondrocytes, a subset of osteoblasts, and osteoclasts. BSP deficient mice (*ibsp<sup>-/-</sup>*) diminished bone growth and mineralization leading to reduction in bone formation (52). Furthermore, BSP is an important for bone mineralization and bone formation. Therefore, BSP is useful diagnostic marker of bone resorption reflected osteoclast activity in human or animal serum (53).

#### b) Osteocalcin (OC)

OC is the most plentiful non-collagenous extracellular matrix protein in bone which produced by osteoblast. OC is encoded by *bglap* and can be used to evaluate bone formation rate. Furthermore, OC plays an important role in

differentiation of mesenchymal stromal cells (MSCs) leading to osteogenic process (54).

c) Bone-specific alkaline phosphatase (BSAP)

BSAP, non-collagen marker, is an isoenzyme of total alkaline phosphatase (ALP), BSAP is enrolled in osteoblast differentiation and specifically produced by osteoblasts while ALP expresses in liver and kidney as well (3). BSAP is encoded by *pax5*; and, in mice lacking in *pax5* gene (*pax5*<sup>-/-</sup>) resulting in osteopenia phenotype and increased osteoclast progenitors (55).

## 2.5 Senile osteoporosis mouse models

Senescence Accelerated Mouse Prone (SAMP) was developed by Takada *et al.* (1981) (56) from AKR/J strain. In 1968, after 24 inbreeding cycles between brothers and sisters of AKR/J strain mice, they observed some abnormality in AKR/J mice owing to some of the mice exhibiting severe degree of senescence such as hair loss and early death. In 1975, the severe senescence mice or others normal senescence mice were chosen as P and R series mouse strain, respectively. In 1999, they successfully developed new mouse strain which are senescence-prone inbred strains (SAMP) and senescence-resistant inbred strains (SAMR) (57).

SAMP6 is the one of SAMP mice exhibited senile osteoporosis and secondary amyloidosis. SAMP6 mice were developed after 110 generations of inbreeding cycles from AKR/J strains R-3. In SAMP6 mice, the peak of bone mass was clearly lower than other strains (58). They were characterized by a low peak in bone mass after 16-week-old (58, 59). Decreasing in bone formation and increasing in bone resorption in SAMP6 mice are caused by deficiency in osteoblast progenitor cell (57) and higher maturation of osteoclasts, respectively (60). In a study by Shimizu *et al.* (2001), they proved that an abnormality in SAMP6 mice were controlled by a group of genes which located at *Pbd2* locus, on chromosome 13 by using cross-mating between SAMP2 and SAMP6 (61). Furthermore, Nakanishi *et al.* (2006), found that the expression of *sfrp4* encoding secreted frizzled-related protein 4 (Sfrp4) increased in SAMP6 mice. Sfrp4 is a negative regulator in Wnt- $\beta$ -catenin signaling which plays an important role in bone formation by competition with Wnt ligand (62). Thus, osteoporosis symptom of SAMP6 mice might be related to the increasing of *sfrp4*.

The appearance of symptom of SAMP6 mice is similar to senile human with type B fracture (57, 58). Therefore, SAMP6 mice are suitable as senile osteoporosis model.

## **2.6 Effects of Thai medicinal plants and their bioactive compounds on osteoclast differentiation**

Natural products from medical plants are invaluable sources for discovery of new compounds for therapies, especially an anti-osteoclastogenesis for osteoporosis treatment. In Table 1, some bioactive compounds which have been used to study for anti-osteoporosis are summarized.

### ***Curcuma comosa* Roxb.**

*C. comosa* (in Thai called Wan-chak-motluk) is one of members in Zingiberaceae. *C. comosa* is an indigenous medicinal plant in Thailand which has been used for postmenopausal state in women (63). The hexane extract from the rhizomes of *C. comosa* increases bone mass density in estrogen deficiency rat model (64). Diarylheptanoids are major compound isolated from a rhizomes of *C. comosa*. Diarylheptanoid not only enhances osteoblast-related genes in human osteoblast cells (65) but also increases bone volume and thickness in ovariectomized rat model with estrogen treatment (66). Furthermore, this compound inhibits nitric oxide production in RAW264.7 cell induced by LPS (67).

### ***Tiliacora triandra* (Colebr.) Diels**

*T. triandra* (in Thai called Ya-nang) is familial with Menispermaceae. This plant is used widely as a traditional medicine in Southeast Asia for anti-inflammation and anti-cancer (68). The leaves extract of *T. triandra* inhibits oxidative stress, suppresses acetylcholinesterase (AChE) and also improves memory in acholic-induced rats (69). Tilliacorinine is belong to the major alkaloid isolated from a roots and stems of *T. triandra*. This compound inhibits human cholangiocarcinoma (CCA) via apoptosis through caspase activity with an increasing pro-apoptotic protein and decreasing anti-apoptosis proteins. In addition, tilliacorinine reduces the tumor growth in CCA xenografted mice (70).

***Curcuma longa* L.**

*C. longa* (in Thai called Khamin-chan) belonged to Zingiberaceae has been used for anti-inflammatory, anti-fungal and abdominal pain in a traditional household treatment (71, 72). The roots extract from *C. longa* exhibits anti-fungal and anti-aflatoxigenic on *Aspergillus flavus*. The crude extract also reduces the contamination in maize seeds (73). Furthermore, the essential oil extracted from rhizomes *C. longa* exhibits anti-oxidant activity; and, it decreases in paw thickness in formalin-induced inflammatory mouse model. Therefore, the essential oil from *C. longa* has potential for anti-inflammation and anti-nociceptive activity (71).

***Croton crassifolius* Geiseler**

*C. crassifolius* (Euphorbiaceae) is a medicinal plant distributed in Asia especially Thailand, Laos, Vietnam and China. The ethanol extract from *C. crassifolius* shows potential to be an anti-nociceptive and anti-inflammatory effects in animal model (74). The main phytochemical compound in *C. crassifolius* consists of diterpenoids (75) and sesquiterpenes. Cyperenoic acid is belong to a major sesquiterpene isolated from the roots of *C. crassifolius* which has been found by Boonyarathanakornkit *et al* (1987) (76). Cyperenoic acid shows anti-angiogenesis in the zebrafish embryo model by downregulating angiogenic genes (77). Furthermore, cyperenoic acid suppresses the releasing of vascular endothelial growth factor (VEGF) regulated angiogenesis in MCF-7 and HepG2 cancer cells line (78).



**Table 1. Anti-osteoclastogenic compounds isolated from medical plants**

| Scientific name<br>/compound<br>group | Bioactive<br>compound  | Anti-osteoclastogenic activity   | Reference |
|---------------------------------------|--|--|-----------|
| <i>Curcuma<br/>comosa</i>             | Diarylheptanoid<br>(3 <i>R</i> )-1,7-diphenyl-<br>(4 <i>E</i> ,6 <i>E</i> )-4,6-<br>heptadien-3-ol<br>(DPHD) | enhances <i>coll α1</i> , and <i>bglap</i><br>osteoblast-related gene in<br>human osteoprogenitor cells<br>further increases bone mineral<br>density (BMD) and reduces<br>bone turnover marker<br>(osteocalcin and TRAP<br>activity) in ovariectomized<br>(OVX) rat. | (65, 66)  |
| <i>Rehmannia<br/>glutinosa</i>        | Aceoside   | inhibits activation of MAPK<br>and NF-κB by suppression<br>p38 and p65 and also<br>attenuates c-Fos and NFATc1<br>further reduces bone loss in<br>OVX mice.  | (79)      |
| <i>Xylocarpus<br/>moluccensis</i>     | 7-oxo-<br>deacetoxygedunin   | suppresses osteoclast<br>differentiation via MAPKs<br>(p38 and ERK) and nuclear<br>translocation of p65 in<br>RAW264.7 cells.  | (80)      |
| <i>Vigna angularis</i>                | Oleanolic acid<br>acetate  | impairs RANKL-stimulated<br>BMMs by pass through<br>PLCγ2-Ca <sup>2+</sup> signaling and<br>suppresses inflammation bone<br>loss in LPS induced mice.  | (81)      |

|                             |                  |   |          |
|-----------------------------|------------------|---|----------|
| <i>Sinomenium acutum</i>    | Sinomenine       | decreases the expression of AP-1 and NFATc1 via MAPKs (p38 and JNK) in BMMs further reduces TRACP5, RANKL and increase OPG in serum of Mt-induced bone loss rat.              | (82)     |
| <i>Rhizoma Curcumae</i>     | Curcumol         | impairs on osteoclast formation both RAW264.7 cells and BMMs; and, also downregulate osteoclast-specific genes and activation of JNK/AP-1 signaling in RANKL-stimulated BMMs. | (83)     |
| <i>Hydratis canadensis</i>  | Berberine        | enhances osteoblast differentiation by increasing the expression of RUNX2 via MAPK (p38) and further increase BMD and decreases bone resorption marker in SAMP6 mice.         | (84, 85) |
| <i>Gardenia jasminoides</i> | Chlorogenic acid | suppresses the MAPKs activation (p38 and ERK) and osteoclast-related genes, attenuates LPS-induced bone loss in mice.   | (86)     |
| Polyphenolic flavonoids     | (1)-Catechin     | enhance cell proliferation and function in MC3T3-E1 pre-osteoblast cell by increasing ALP activity.   | (87)     |

|                                |                 |  |      |
|--------------------------------|-----------------|--|------|
| <i>Humulus lupulus</i>         | Xanthohumol     | increases ALP activity and RUNX2 expression by activation of MAPKs signaling (p38 and ERK).  | (88) |
| <i>Platycodon grandiflorum</i> | Saponins        | increases the expression of osteogenic marker genes, master transcription factor RUNX2 and also ALP activity in C2C12 cells.                   | (89) |
| <i>Panax ginseng</i>           | Ginsenoside-Rb2 | improves ALP activity and enhances osteoblast-related genes ( <i>alp</i> , <i>coll α1</i> and <i>bglap</i> ) further increase BMP in OVX-mice. | (90) |

---

## 2.7 Currently available agents to target bone loss and osteoporosis

### Bisphosphonates

Bisphosphonates are anti-resorption drug with specific binding to bone matrix. The chemical structure is similar to pyrophosphate. Bisphosphonates generate adenosine triphosphate analog leading to apoptosis of osteoclasts (91). They effect to mature osteoclasts when they bind to the bone matrix for bone resorption process while osteoclast differentiation does not impact. However, there are side effects on gastrointestinal tract and kidney function (92). Furthermore, long-term of bisphosphonates treatment impairs bone turnover (93) because they might affect to either osteoblasts or osteocytes (94).

### Denosumab (DMAb)

DMAb is a humanized monoclonal antibody against RANKL (95). It binds specifically to RANKL. The main mechanism of DMAb is a prevent the interaction between RANKL and RANK receptor similar to OPG which also inhibits binding between RANKL/RANK in natural environment. In addition, osteoclast differentiation and bone resorption are inhibited by denosumab (94, 96). However, DMAb has some side effects such as skin problem and bone, joint or muscle pain but not on kidney

function. And the cost of DMAB is probably high because patients should take DMAB every 6 months (97).

### **Odanacatib (ODN)**

ODN is a cathepsin K inhibitor and one of anti-resorption reagents. Cathepsin K is secreted by mature osteoclasts plays an important role in bone resorption by degradation of type I collagen. ODN binds to cathepsin K resulting in reduction of bone resorption (98). In cathepsin k deficiency mice (*ctsk<sup>-/-</sup>*) exhibit an increasing in bone mass at trabecular thickness (99). ODN does not show side effect in phase I or II clinical trial but after 5 years treatment, the level of BSAP is slightly decreased in some patients (100).

### **Hormone therapy**

Hormone therapy is a group of enhancement osteoblast function agent based on directly effect to osteoblasts via these receptors.

- a) Teriparatide is a recombinant fragment of parathyroid hormone. It enhances osteoblast activity and bone formation (96).
- b) Estrogen replacement activates osteoblast proliferation and increases apoptosis rate in osteoclast like estrogen hormone (96).

## CHAPTER III

### MATERIAL AND METHODS

#### 3.1 Bioactive compounds

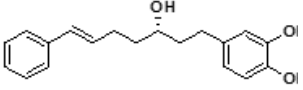
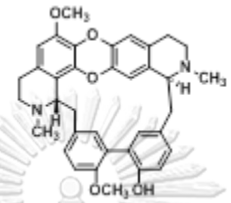
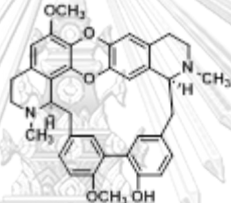
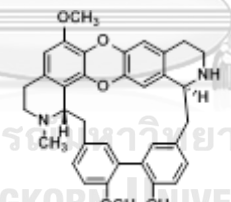
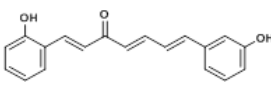
All compounds used in this study were summaries in Table 2. They were provided by Professor Apichart Suksamrarn, Ph.D., Department of Chemistry and Center of Excellence for Innovation in Chemistry, Faculty of Science, Ramkhamhaeng University. Diarylheptanoid (3*S*)-1-(3,4-dihydroxyphenyl)-3-hydroxy-7-phenyl-(6*E*)-6-heptene (DHPH, code name ASTP019) was isolated from the Rhizomes of *Curcuma comosa* which purchased from Kampaengsaen District, Nakorn Pathom Province, Thailand. The voucher herbarium specimen (SCMU no. 300) was deposited at the Department of Plant Science, Faculty of Science, Mahidol University (Thailand).

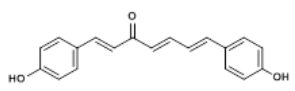
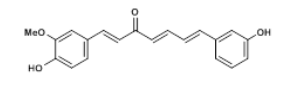
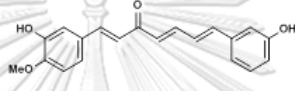
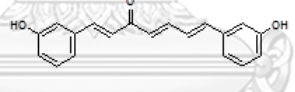
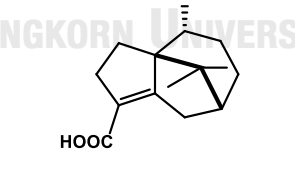
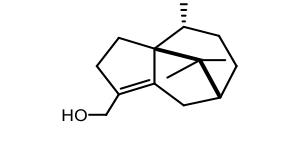
Tiliacorinine, tiliacorine and nortiliacorinine (code name ASTP040-042) were isolated from roots and stems of *Tiliacora triandra* which collected from Krasae Sin district, Songkhla province. A voucher specimen (Apichart Suksamrarn, No. 067) is deposited at the Faculty of Science, Ramkhamhaeng University.

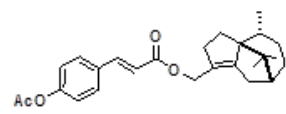
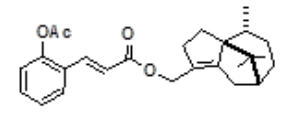
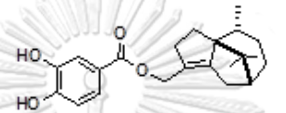
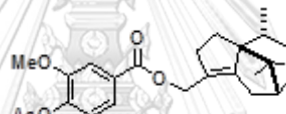
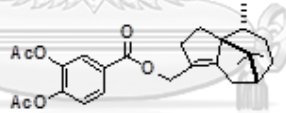
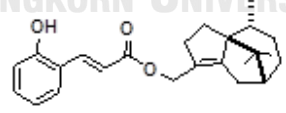
The trienone analogs (code name ASTP045-049) were synthesized as analogs of curcuminoids, which were isolated the rhizome of *Curcuma longa*. The synthesis of the trienone analogs were described by Chuprajob *et al.* (2014) (101).

Cyperenoic acid (code name ASTP053) was isolated from roots of *Croton crassifolius*. The roots of *C. crassifolius*. were collected from Nacharoen, Dech Udom district, Ubon Ratchathani province, Thailand, in December 2009. A voucher specimen (Apichart Suksamrarn, No. 062) was deposited at the Faculty of Science, Ramkhamhaeng University. Cyperenol (ASTP054) was modified from cyperenoic acid as a synthetic analog of cyperenoic acid. and other six ester analogs (code name ASTP055-060) were synthesized from cyperenol by esterification of cyperenol with appropriate carboxylic acids or acid chlorides.

**Table 2. Bioactive compounds used in this study**

| Sample name (code name)  | Structure/ Formula/<br>M.W.  | Sources                               | Part used     |
|--|--|---------------------------------------|---------------|
| Diarylheptanoid (3 <i>S</i> )-1-(3,4-dihydroxyphenyl)-3-hydroxy-7-phenyl-(6 <i>E</i> )-6-heptene (DHPH) (ASTP019)                          | <br>$C_{19}H_{22}O_3$ , 298.38     | <i>C. comosa</i>                      | Rhizome       |
| Tilliacorinine (ASTP040)   | <br>$C_{36}H_{36}N_2O_5$ , 576.26   | <i>T. triandra</i>                    | Root/<br>stem |
| Tiliacorine (ASTP041)  | <br>$C_{36}H_{36}N_2O_5$ , 576.26  | <i>T. triandra</i>                    | Root/<br>stem |
| Nortiliacorinine (ASTP042)   | <br>$C_{35}H_{34}N_2O_5$ , 562.65 | <i>T. triandra</i>                    | Root/<br>stem |
| 1-(2-hydroxyphenyl)-7-(3-hydroxyphenyl)-(1 <i>E</i> ,4 <i>E</i> ,6 <i>E</i> )-1,4,6-heptatrien-3-one or the trienone analog 045/ (ASTP045) | <br>$C_{19}H_{16}O_3$ , 292.33    | Synthetic<br>analog of<br>curcuminoid |               |

|   |   |   |
|---|---|---|
| 1,7-bis(4-hydroxyphenyl)<br>(1 <i>E</i> ,4 <i>E</i> ,6 <i>E</i> )-1,4,6-heptatrien-<br>3-one) or the trienone analog<br>046 (ASTP046)                                   | <br>$C_{19}H_{16}O_3$ , 292.33   | Synthetic<br>analog of<br>curcuminoid     |
| 1-(3-methoxy-4-<br>hydroxyphenyl)-7-(3-<br>hydroxyphenyl)- (1 <i>E</i> ,4 <i>E</i> ,6 <i>E</i> )-<br>1,4,6-heptatrien-3-one)<br>or the trienone analog 047<br>(ASTP047) | <br>$C_{20}H_{19}O_4$ , 322.12   | Synthetic<br>analog of<br>curcuminoid     |
| 1-(3-hydroxy-4-<br>methoxyphenyl)-7-(3-<br>hydroxyphenyl)- (1 <i>E</i> ,4 <i>E</i> ,6 <i>E</i> )-<br>1,4,6-heptatrien-3-one)<br>or the trienone analog 048<br>(ASTP048) | <br>$C_{20}H_{19}O_4$ , 322.12   | Synthetic<br>analog of<br>curcuminoid     |
| 1,7-bis(3-hydroxyphenyl)-<br>(1 <i>E</i> ,4 <i>E</i> ,6 <i>E</i> )-1,4,6-heptatrien-<br>3-one) or the trienone analog<br>049 (ASTP049)                                  | <br>$C_{19}H_{16}O_3$ , 292.33 | Synthetic<br>analog of<br>curcuminoid     |
| Cyperenoic acid<br>(ASTP053)  | <br>$C_{15}H_{22}O_2$ , 234.33 | <i>C. crassifolius</i> Root               |
| Cyperenol<br>(ASTP054)  | <br>$C_{15}H_{24}O$ , 220.35   | Synthetic<br>analog of<br>cyperenoic acid |

|   |   |  |
|---|---|--|
| <p>Cyperenyl 10-<i>O</i>-(4-acetoxy-<i>trans</i>-cinnamate)<br/>or the ester analog 055<br/>(CATC) (ASTP055)</p>    | <br>$C_{26}H_{32}O_4$ , 408.53   | <p>Synthetic ester<br/>analog of<br/>cyperenol</p> |
| <p>Cyperenol 10-<i>O</i>-(2-acetoxy-<i>trans</i>-cinnamate)<br/>or the ester analog 056<br/>(ASTP056)</p>           | <br>$C_{26}H_{32}O_4$ , 408.53   | <p>Synthetic ester<br/>analog of<br/>cyperenol</p> |
| <p>Cyperenol 10-<i>O</i>-(3,4-dihydroxy-<i>trans</i>-cinnamate)<br/>or the ester analog 057<br/>(ASTP057)</p>       | <br>$C_{22}H_{28}O_4$ , 356.46   | <p>Synthetic ester<br/>analog of<br/>cyperenol</p> |
| <p>Cyperenol 10-<i>O</i>-(3-methoxy-4-acetoxy-<i>trans</i>-cinnamate)<br/>or the ester analog 058<br/>(ASTP058)</p> | <br>$C_{25}H_{32}O_5$ , 412.52  | <p>Synthetic ester<br/>analog of<br/>cyperenol</p> |
| <p>Cyperenol 10-<i>O</i>-(3,4-dihydroxy-<i>trans</i>-cinnamate)<br/>or the ester analog 059<br/>(ASTP059)</p>       | <br>$C_{26}H_{32}O_6$ , 440.53 | <p>Synthetic ester<br/>analog of<br/>cyperenol</p> |
| <p>Cyperenol 10-<i>O</i>-(2-hydroxy-<i>trans</i>-cinnamate)<br/>or the ester analog 060<br/>(ASTP060)</p>           | <br>$C_{24}H_{30}O_3$ , 366.49 | <p>Synthetic ester<br/>analog of<br/>cyperenol</p> |

---



## **3.2 Cell cultures**

### **3.2.1 RAW264.7 cell line**

A macrophage like cell line, RAW264.7 (ATTC TIB-71) was cultured in Dulbecco's Modified Eagle's Medium (DMEM) (Thermo Fisher Scientific, UK) containing 10% fetal bovine serum (FBS) (GIBCO-Invitrogen, USA), 1% HEPES free acid, 1% sodium pyruvate and 1% penicillin-streptomycin (Thermo Fisher Scientific, UK) at 37°C with 5% CO<sub>2</sub> incubator (Thermo Electron Corporation, USA).

### **3.2.2 Bone marrow derived macrophage (BMMs)**

Osteoclast differentiation, BMMs were isolated from humerus, femur and tibia of 6-8-week-old BALB/c female mice (National Laboratory Animal Center, Mahidol University). Cells were cultured with recombinant M-CSF (rM-CSF) (Immunotools, Germany) (25 ng/ml) for 48 hrs. BMMs were further cultured with rM-CSF (25 ng/ml) and recombinant RANKL (rRANK) (Biolegend, USA) (100 ng/ml) for another 5 days. Media were changed every 2 days during investigation. All procedures involving laboratory animals were approved by the Animal Care and Use Committee of Faculty of Science, Chulalongkorn University (Protocol review No.1423012 and 1623015).

### **3.2.3 Pre-osteoblast cell line (MC3T3-E1)**

Pre-osteoblast cell line, MC3T3-E1 (RBRC-RCB1126), was purchased from RIKEN Bioresource Center (Ibaraki, Japan). Cells were maintained in  $\alpha$ -Minimum Essential Media (MEM) (Gibco-Invitrogen, USA). For osteoblast differentiation assay, cells were seeded at  $2.5 \times 10^4$  cells/well in 12 well plates and induced by using ascorbic acid 200 mM (Sigma-Aldrich, USA) for 10 days. Media were changed every 3 days during investigation.

## **3.3 Cell viability assay**

### **3.3.1 Thiazolyl blue tetrazolium bromide (MTT) assay**

RAW264.7 or MC3T3-E1 cells line were seeded at  $1 \times 10^4$  cells/well in 96 well-plates for overnight and treated with bioactive compounds which were dissolved in DMSO at indicated concentrations (0.316, 1, 3.162, 10, 31.62 and 100  $\mu$ M) for 24 hrs. MTT solution (Alfa Aesar, England) (5 mg/ml in PBS) was added to treated cells for 4 hrs. at 37°C. After incubation, DMSO was added to dissolve the insoluble formazan;

and, absorbance was measured at 540 nm by microplate reader (Biochom Anthos, UK). Cell viability was calculated by using the following formula.

$$\% \text{ cell viability} = \frac{((\text{Absorbance of treated cells}) - (\text{Absorbance of blank}))}{((\text{Absorbance of vehicle control treated cells}) - (\text{Absorbance of blank}))} \times 100$$

The 50% and 20% inhibition concentration (IC<sub>50</sub>, IC<sub>20</sub>) were calculated using a GraphPad Prism 5.03.

### 3.3.2 Methyl tetrazolium salt (MTS) assay

RAW264.7 or MC3T3-E1 cells were seeded at  $3 \times 10^6$  cells/well in 60 mm<sup>2</sup> culture dish for 48 hrs. After, precursor osteoclasts were collected, seeded in 96 well-plate ( $2.5 \times 10^5$  cells/well) and treated with bioactive compounds at indicated concentrations for 24 hrs. Then, 10  $\mu$ l/well of MTS solution (Promega, USA) was added to treated cells for 4 hrs. and incubated at 37°C. Absorbance was measured at 490 nm by microplate reader. Cell viability was calculated by using the similar formula as 3.3.1.

### 3.4 Anti-inflammatory activity assay

RAW264.7 cells were seeded at  $2 \times 10^5$  cells/well in 96 well-plates overnight. Cells were pretreated with bioactive compounds at indicated concentrations for 1 hr. and stimulated with lipopolysaccharide (LPS) (Sigma Aldrich, USA) (100 ng/ml) and IFN- $\gamma$  (BioLegend, USA) (10 ng/ml) for 24 hrs. Amount of nitric oxide production in culture supernatant of treated cell was measured by Griess reaction (102). Sulfanilamide (Sigma Aldrich, USA) and *N*-(1-naphthyl-ethylenediamine dihydrochloride (NED) (Sigma Aldrich, USA) were added to the culture supernatant (50  $\mu$ l/well); and, the reaction was incubated for 10 min at room temperature in the dark. The absorbance was measured at 540 nm by microplate reader. Standard was generated by nitrite. The relative nitric oxide productivity (%) was calculated as a percentage relative to the untreated control.

### 3.5 Anti-osteoclastogenesis activity screening assay

The assay was performed as described by Bradley and Oursler, (2008) (103). Briefly, BMMs were seeded at  $3 \times 10^6$  cells/well in 60 mm tissue culture dish for 48 hrs. The precursor osteoclasts were harvested and seeded at  $2.5 \times 10^5$  cells/well in 96 well-plates. They were pre-treated with bioactive compounds at indicated concentrations for 30 min and stimulated with rM-CSF (25 ng/ml) and rRANKL (100 ng/ml) for 5 days.

Cells were washed with 1xPBS, fixed with 10% formaldehyde for 10 min, permeated with 95% ethanol for 2 min and washed with 1xPBS. Finally, cells were stained with a TRAP-staining solution (50 mM acetate buffer, 50 mM sodium tartrate, naphthol AS-MX phosphate (Sigma Aldrich, USA) (0.1 mg/ml) and Fast red violet LB salt (Sigma Aldrich, USA) (0.6 mg/ml). TRAP-positive multinucleated cells with three or more nuclei were counted as mature osteoclasts under light microscope (Olympus, Tokyo, Japan). TRAP enzyme activity was measured by using TRAP activity solution containing 50 mM citrate buffer with 10 mM *p*-nitrophenylphosphate (Sigma Aldrich, USA). The reaction was stopped by using 0.1 N NaOH (1:1 v/v). The absorbance was measured at 410 nm by microplate reader. The relative TRAP activity (%) was calculated as a percentage relative to the vehicle control.

### **3.6 Qualitative reverse transcription polymerase chain reaction (RT-qPCR)**

BMMs were seeded at  $7.6 \times 10^5$  cells/well in 24 well-plates and cultured with rM-CSF (25 ng/ml) for 48 hrs. After the incubation, BMMs were pre-treated with bioactive compounds at indicated concentrations for 30 min. This step was followed by the stimulation with rM-CSF (25 ng/ml) and in the present of rRANKL (100 ng/ml) and for 6, 12, 24, 48 and 72 hrs.

#### **3.6.1 RNA extraction**

Total RNA was isolated by using Trizol reagent (Thermo Fisher Scientific, UK) or RNAsiso reagent (Takara-Bio, Japan) according to the manufacturer's instruction RNA was measured using Quant iT assays (Thermo Fisher Scientific, UK).

#### **3.6.2 Reverse transcription and quantitative polymerase chain reaction (qPCR)**

Total RNA was mixed with random hexamer (Qiagen, Hilden, Germany) 0.01 ng/ $\mu$ l, and heated at 65°C for 5 min. The reverse transcription reagents contained 1x reverse transcriptase buffer, 1 mM dNTP mix, 20 U RNase inhibitor and 200 U Reverse transcription (Fermentas, Canada). The reaction was performed with the following condition in 25°C for 10 min, 42°C for 60 min and 70°C for 10 min. In other experiments the total RNA was converted by using ReverTra Ace® qPCR RT master mix with gDNA remover (TOYOBO, Japan).

A SYBR<sup>®</sup> Green (Bio-Rad Laboratories, USA) or Kapa SYBR (Kapa Biosystems, USA) was used for qPCR. Relative expression of osteoclast-related, osteoblast-related and pro-inflammatory genes (primer sequences and conditions for amplification of each gene are shown in Table 3) were determined and normalized, using the expression levels of *β-actin*. Relative fold experiment was calculate by  $2^{-\Delta\Delta CT}$  method as described by Livak and Schmittgen, (2001) (104).

### **3.7 Western blot**

BMMs were seeded at  $7.6 \times 10^5$  cells/well in 24 well-plates and cultured with rM-CSF 25 ng/ml for 48 hrs. After that BMMs were pre-treated with bioactive compounds at indicated concentrations for 30 min. Cells were further stimulated with rRANKL (100 ng/ml) and rM-CSF (25 ng/ml) for 0, 5, 15, 30 and 60 min for MAPKs, canonical NF- $\kappa$ b or non-canonical NF- $\kappa$ B expression, or 0, 6, 12, 24, 48, 72 and 96 hrs for c-Fos or NFATc1 expression.

#### **3.7.1 Cell lysate preparation and sodium dodecyl sulfate-polyacrylamide gel electrophoresis (SDS-PAGE)**

Cell lysate were extracted by using RIPA buffer containing 1x protease inhibitor (Roche, Germany) and 1% (v/v) phosphatase inhibitor (Cell signaling technology, USA). The protein concentration was measured by using BCA assay (Thermo Fisher Scientific, UK). The cellular protein was resolved by 8-12% SDS-PAGE and transferred to PVDF membrane (GE Healthcare, USA) by using Trans-Blot<sup>®</sup> SD Semi-Dry Transfer Cell (Bio-rad, USA). The membranes were blocked twice with 3% skim milk in PBS-T for 5 min and probed with primary and secondary antibodies, respectively (Table 4).  $\beta$ -actin used as a protein loading control. Protein bands were visualized with high performance chemiluminescence X-ray film (Amersham Bioscience, UK) and density of the protein band was measured by using Image-J software.

**Table 3. List of primers used in this study**

| Gene           | Primer sequence (from 5' to 3') |                 | Annealing temp. (°C) | Product size (bp) |
|----------------|---------------------------------|-----------------|----------------------|-------------------|
|                | Forward                         | Reverse         |                      |                   |
| <i>irf8</i>    | GGAAAGCCTT                      | AAGGTCACC       | 55                   | 112               |
|                | ACCTGCTGAC                      | GTGGTCCTT       |                      |                   |
| <i>ctsk</i>    | GGCCAAGCTC                      | GTACCCTCT       | 58                   | 225               |
|                | AAGAAGAAA                       | GCATTTAGC       |                      |                   |
| <i>nfatc1</i>  | GGTAACTCTGTCTT                  | GTGATGACCCCAGCA | 62                   | 240               |
|                | TCTAACCTTAAGCTC                 | TGCACCAGTCACAG  |                      |                   |
| <i>actb</i>    | ACCAACTGGGAC                    | GTGGTGGTGA      | 55                   | 380               |
|                | GACATGGAGAA                     | AGCTGTAGCC      |                      |                   |
| <i>il-6</i>    | AGTCCGGAGA                      | ATTTCCACGA      | 58                   | 108               |
|                | GGAGACTTCA                      | TTTCCAGAG       |                      |                   |
| <i>tnf-α</i>   | GGCAGGTCTACT                    | ACATTTCGAGGCT   | 60                   | 300               |
|                | TTGGAGTCATTGC                   | CCAGTGAATTCGG   |                      |                   |
| <i>coll α1</i> | CTTGGTGGTTTT                    | GCGAAGGCA       | 55                   | 101               |
|                | GTATTCGATGAC                    | ACAGTCGCT       |                      |                   |
| <i>lbsp</i>    | GCACTCCAAC                      | TTTTGGAGCC      | 60                   | 51                |
|                | TGCCCAAGA                       | CTGCTTTCTG      |                      |                   |
| <i>bglap</i>   | CTGACAAAGCC                     | GCGGGCGAGT      | 50                   | 59                |
|                | TTCATGTCCAA                     | CTGTTCACTA      |                      |                   |
| <i>mmp9</i>    | GTCTTCCTGG                      | CTGGACAGAA      | 58                   | 115               |
|                | GCAAGCAGTA                      | ACCCCACTTC      |                      |                   |
| <i>acp5</i>    | CCAATGCCAA                      | TCTGTGCAGAG     | 56                   | 216               |
|                | AGAGATCGCC                      | ACGTTGCCAAG     |                      |                   |
| <i>actb</i>    | CACTATTGGCA                     | ACTTGCGGTG      | 55                   | 249               |
|                | ACGAGCGGTTC                     | CACGATGGAG      |                      |                   |

### 3.8 Immunofluorescence staining

BMMs ( $7.6 \times 10^5$  cells/well, 8 well-plates) were cultured in the presence of rM-CSF (25 ng/ml) for 48 hrs to generate the osteoclast precursors. To examine mature osteoclasts, precursor osteoclast precursors were treated with rM-CSF (25 ng/ml) and rRANKL (100 ng/ml) for 24 and 48 hrs. They were washed with PBS, fixed with 4% paraformaldehyde for 10 min, permeated with 0.2 triton-X100 in PBS for 2 min and

washed four-times with PBS, respectively. Furthermore, Fc receptor on the cell surface was blocked by using 2.4G2 supernatant. Finally, they were stained with a rabbit anti-NFATc1 (1:100) for 1 hr, followed by anti-rabbit IgG conjugated with Alexa Fluor® 555 (1:1000) for 45 min and DAPI, respectively. The nuclear translocation of NFATc1 was visualized and counted (n = 100 cells/condition) under FV10i confocal laser scanning microscope (Olympus scientific solutions America corporation, US).

**Table 4. List of primary antibodies used in this study**

| Antigen             | Working Dilution | Exposure time for x-ray film (min) | Manufacturer                         |
|---------------------|------------------|------------------------------------|--------------------------------------|
| NFATc1              | 1:1000           | 5                                  | Cell Signaling Technology (CST), USA |
| c-Fos               | 1:1000           | 5                                  | CST                                  |
| Phospho-p38 (Pp-38) | 1:2000           | 5                                  | CST                                  |
| total p38 (p38)     | 1:2000           | 2                                  | CST                                  |
| P-pSAPK/JNK         | 1:2000           | 5                                  | CST                                  |
| SAPK/JNK            | 1:2000           | 2                                  | CST                                  |
| P-p44/42            | 1:2000           | 5                                  | CST                                  |
| p44/42              | 1:2000           | 2                                  | CST                                  |
| P-p65               | 1:2000           | 5                                  | CST                                  |
| p65                 | 1:2000           | 2                                  | CST                                  |
| P-p100              | 1:1000           | 30                                 | CST                                  |
| p100                | 1:1000           | 30                                 | CST                                  |
| TRAF3               | 1:2000           | 15                                 | CST                                  |
| Rel-B               | 1:2000           | 15                                 | CST                                  |
| β-actin             | 1:10000          | 1                                  | Merck Millipore, Germany             |
| mouse IgG           | 1:4000           |                                    | CST                                  |
| rabbit IgG          | 1:4000           |                                    | CST                                  |

### 3.9 Bone resorption assay

The bone resorption assay was modified from Bradley and Oursler (2008) (103). To investigate the effect of bioactive compounds on osteoclast-mediated bone resorption, BMMs were seeded at  $3 \times 10^6$  cells/well in 60 mm tissue culture dish for 48 hrs. Precursor osteoclasts were harvested and seeded at  $7.6 \times 10^5$  cells/well in 96 well-plates containing bone slices (Immonodiagnosticsystems, London or dentin slices. Cells were pre-treated with bioactive compounds at indicated concentrations for 30 min and cultured in appropriate media containing rRANKL (100 ng/ml) and rM-CSF (25 ng/ml) for 14 days at 37°C. Thereafter, cells were removed by sonication twice for 15 seconds in concentrated ammonium hydroxide. The bone slices or dentin slices were stained for 10 min by Toluidine Blue (1 mg/ml) (Sigma Aldrich, USA). The resorption pits were examined by a light microscope and photographed. Percentage of resorption area was determined by using area measurement function in Image-J software at 200-fold magnification. And calculation using the following formula Resorption area (%) = ((resorption area of treated cells) - (background of unstimulated control)) / ((resorption area of vehicle control treated cells) - (background of unstimulated control))  $\times$  100.

### 3.10 Alkaline phosphatase activity assay (ALP) for osteoblast differentiation.

ALP activity assay was performed as described by Yazid *et al.*, (2010) (105). Briefly, MC3T3-E1 cell line was washed and harvested with 1xPBS and 0.1% triton x-100 for 10 min, respectively. Amount of all protein lysate was measured by using the BCA assay and used to normalize the enzymatic activity. Cell lysate incubated with 0.1 M sodium bicarbonate-carbonate buffer (pH 10), containing 2 mM MgSO<sub>4</sub> and 6 mM *p*-nitrophenyl phosphate (pNPP) (Sigma Aldrich, USA) for 30 min at 37°C. The reaction was stopped by using 1.5 M NaOH (1:1), and the absorbance was measured at 405 nm by microplate reader.

### 3.11 *In vivo* study using Senescence Accelerated Mouse Prone 6 (SAMP6) mice

#### 3.11.1 Standard diet food AIN-93M

The preparation of standard diet food AIN-93M was modified from Katayama *et al.*, (2016) (106). Standard diet food AIN-93M obtained from Oriental Yeast (Tokyo, Japan) was crushed into ground pieces by using mixer. The crushed diet food AIN-93M (1 kg) was mixed with 0.01% bioactive compounds which dissolved in of absolute

ethanol 50 ml and DW water 500 ml was added. The mixed diet food AIN-93M was kneaded, molded and dried out by using incubator (50 °C) for two days. The diet was stored at 4 °C until use.

### 3.11.2 Animal treatment

SAMP6 mice were purchased from Japan SLC, Inc. (Shizuoka, Japan) and allowed to acclimatize for 1 week before the experiment. Mice were randomly assigned into 2 group based on body weight. Twelve SAMP6 mice were randomly assigned into control and cyperenoic acid treated group, respectively. The control group was fed with a standard diet food AIN-93M; and, cyperenoic acid treated group was fed with a standard diet mixed with 0.01 % cyperenoic acid powder. Mice were enable free access to the diet and tap water. Food intake and body weight were measured once a week. Mice were scarified after 19 weeks, long bones (humorous and tibia) were used for BMMs separation. Other bones were used for bone histomorphometry. In addition, serum was collected for ELISA. All experiments involved SAMP6 mice were conducted in accordance with the institutional guideline established by Shinshu University for laboratory animals (Shinshu Animal Protocol No. 280091).

### 3.11.3 Bone histomorphometry

The bone histomorphometry was modified from Orriss and Arnett (2012) (107) Briefly, mice femur bones were fixed with 4.5% formaldehyde (pH 7.2) for 2 days, decalcified with 14% EDTA (pH 7.2) for 14 days and dehydrated with 70%, 80%, 96% and 100% ethanol, respectively. The processed bones were transferred into a tissue embedding console and embedded in paraffin. The bone embedding was cut by using microtome (5 µm thickness). In addition, the bone tissue sections were stained with hematoxylin, fast green CFC and safranin O and examined by a light microscope. The percentages of bone area (BA) and trabecular area (TbA) were determined using Image-J software, at 200-fold magnification. The histomorphometric parameters both % BA and % TbA were calculated according to the formula described by Vidal *et al*, 2012 (108).

% BA = ((total bone area/total tissue area (TA)) \*100) and

% TbA = ((trabecular area/ total bone area) \*100)



#### 3.11.4 ELISA for serum bone sialoprotein

Mouse Bone Sialoprotein (BSP) ELISA Kit (CUSABIO, USA) was used in this study. First, the standard solution and SAMP6 serum sample were added in BSP coated microwells (100  $\mu$ l/well, 37 °C, 2 hrs); and, biotin-antibody was added into each well (100  $\mu$ l/well, 37 °C, 1 hr). After remove sample, wells were washed by using wash buffer (200  $\mu$ l/well, 2 times). HRP-avidin was added into each well (100  $\mu$ l/well) and incubated 1 hr at 37 °C.); and, all of wells were washed with wash buffer (200  $\mu$ l/well, 5 times). Finally, TMB substrate (90  $\mu$ l/well, 37 °C, 15-30 min) and stop solution (50  $\mu$ l/well) were added to each well. Determine the optical density of each well within 5 min by using microplate reader at 450 nm.

#### 3.12 Statistical analyses

All experiments were done in triplicate with at least two independent experiments. Results were expressed as the mean  $\pm$  standard deviation (S.D.). The statistical significance of difference between an experimental group and the its corresponding control were evaluated by one-way ANOVA or Student's T-test (GraphPad Prism 5.03). All comparisons were made as specified, and \*\*\* $p$  < 0.001, \*\* $p$  < 0.01 and \* $p$  < 0.05. were considered statistical significance.

## CHAPTER IV

### RESULTS

#### 4.1 Screening compounds from Thai medicinal plants with anti-osteoclastogenic activity

##### 4.1.1 The effect of pure compounds from Thai medicinal plants on cell viability in RAW264.7 cells

To determine the effect of toxicity pure compounds from three different plants and synthetic analog of curcuminoid on cell viability, RAW264.7 cells were treated with pure compound at indicated concentrations (0-100  $\mu\text{M}$ ) for 24 hrs. The cell viability (%) was using MTS or MTT assay. The half maximum inhibitory concentration ( $\text{IC}_{50}$ ) or twenty inhibitory concentration ( $\text{IC}_{20}$ ) for each compound was summarized in Table 5. Based on these preliminary results, the concentrations of these pure compounds at  $\text{IC}_{20}$  or maximum concentration (100  $\mu\text{M}$ ) were chosen for further study.

##### 4.1.2 Effect of pure compounds on nitric oxide production in LPS and IFN- $\gamma$ stimulated RAW264.7 cells

Because osteoclast differentiation and inflammatory signaling share same common signaling pathways, pure compounds that have ability to suppress inflammation might interfere with osteoclast differentiation. To determine whether these compounds have anti-inflammatory activity, RAW264.7 cells were stimulated with or without LPS from *E. coli* (100 ng/ml) and IFN- $\gamma$  (10 ng/ml) and treated with these pure compounds at indicated concentrations. The amount of nitric oxide in culture supernatant was measured by using Griess assay. The results indicated that ASTP019 and ASTP045 suppressed the nitric oxide production with an  $\text{IC}_{50}$  of  $1.012 \pm 1.63 \mu\text{M}$  and  $10.32 \pm 1.46 \mu\text{M}$ , respectively (Fig. 4). Therefore, ASTP019 and ASTP045 might have impact on osteoclast differentiation.

**Table 5. IC<sub>50</sub> and IC<sub>20</sub> for cell viability in RAW264.7 cells**

| Source                          | Code name | compounds  | IC <sub>50</sub> (μM) | IC <sub>20</sub> (μM) |
|---------------------------------|-----------|--|-----------------------|-----------------------|
| <i>C. comosa</i>                | ASTP019   | Diarylheptanoid: (3 <i>S</i> )-1-(3,4 dihydroxyphenyl)-3-hydroxy-7-phenyl-(6 <i>E</i> )-6-heptene; (DHPH)                                  | 7.055±0.195           | 1.765±0.045           |
| <i>T. triandra</i>              | ASTP040   | Tiliacorinine  | 4.96±0.62             | 1.06±0.50             |
|                                 | ASTP041   | Tiliacorine  | 1.11±0.55             | 0.28±0.14             |
|                                 | ASTP042   | Nortiliacorinine   | 2.37±1.03             | 0.59±0.25             |
| Synthetic analog of curcuminoid | ASTP045   | 1-(2-hydroxyphenyl)-7-(3-hydroxyphenyl)-(1 <i>E</i> ,4 <i>E</i> ,6 <i>E</i> )-1,4,6-heptatrien-3-one) or the trienone analog 045           | 18.48±1.8             | 4.87±2.31             |
| Synthetic analog of curcuminoid | ASTP046   | 1,7-bis(4-hydroxyphenyl)-(1 <i>E</i> ,4 <i>E</i> ,6 <i>E</i> )-1,4,6-heptatrien-3-one) or the trienone analog 046                          | 10.14±2.13            | 2.53±0.53             |
|                                 | ASTP047   | 1-(3-methoxy-4-hydroxyphenyl)-7-(3-hydroxyphenyl)-(1 <i>E</i> ,4 <i>E</i> ,6 <i>E</i> )-1,4,6-heptatrien-3-one) or the trienone analog 047 | 9.17±1.66             | 2.29±0.41             |

|                                     |         |  |            |            |
|-------------------------------------|---------|--|------------|------------|
|                                     | ASTP048 | 1-(3-hydroxy-4-methoxyphenyl)-7-(3-hydroxyphenyl)-(1 <i>E</i> ,4 <i>E</i> ,6 <i>E</i> )-1,4,6-heptatrien-3-one) or the trienone analog 048 | 17.75±1.71 | 4.44±0.43  |
|                                     | ASTP049 | 1,7-bis(3-hydroxyphenyl)-(1 <i>E</i> ,4 <i>E</i> ,6 <i>E</i> )-1,4,6-heptatrien-3-one) or the trienone analog 049                          | 3.26±0.5   | 0.86±0.42  |
| <i>C. crassifolius</i>              | ASTP053 | Cyperenoic acid  | ≥ 100      | -          |
| Synthetic analog of cyperenoic acid | ASTP054 | Cyperenol  | ≥ 100      | -          |
| Synthetic ester analog of cyperenol | ASTP055 | Cyperenyl 10- <i>O</i> -(4-acetoxy- <i>trans</i> -cinnamate) (CATC) or the ester analog 055  | 18.74±3.34 | 4.69±0.84  |
|                                     | ASTP056 | Cyperenol 10- <i>O</i> -(2-acetoxy- <i>trans</i> -cinnamate) or the ester analog 056   | 82.40±0.77 | 14.44±6.81 |
|                                     | ASTP057 | Cyperenol 10- <i>O</i> -(3,4-dihydroxy- <i>trans</i> -cinnamate) or the ester analog 057   | 13±1.25    | 3.25±0.31  |

|         |   |            |           |
|---------|---|------------|-----------|
| ASTP058 | Cyperenol 10- <i>O</i> -(3-methoxy-4-acetoxy- <i>trans</i> -cinnamate)<br>or the ester analog 058 | 12.77±0.3  | 3.3±1.55  |
| ASTP059 | Cyperenol 10- <i>O</i> -(3,4-dihydroxy- <i>trans</i> -cinnamate)<br>or the ester analog 059       | 3.84±1.39  | 0.96±0.35 |
| ASTP060 | Cyperenol 10- <i>O</i> -(2-hydroxy- <i>trans</i> -cinnamate)<br>or the ester analog 060           | 19.63±0.04 | 4.89±2.31 |

---

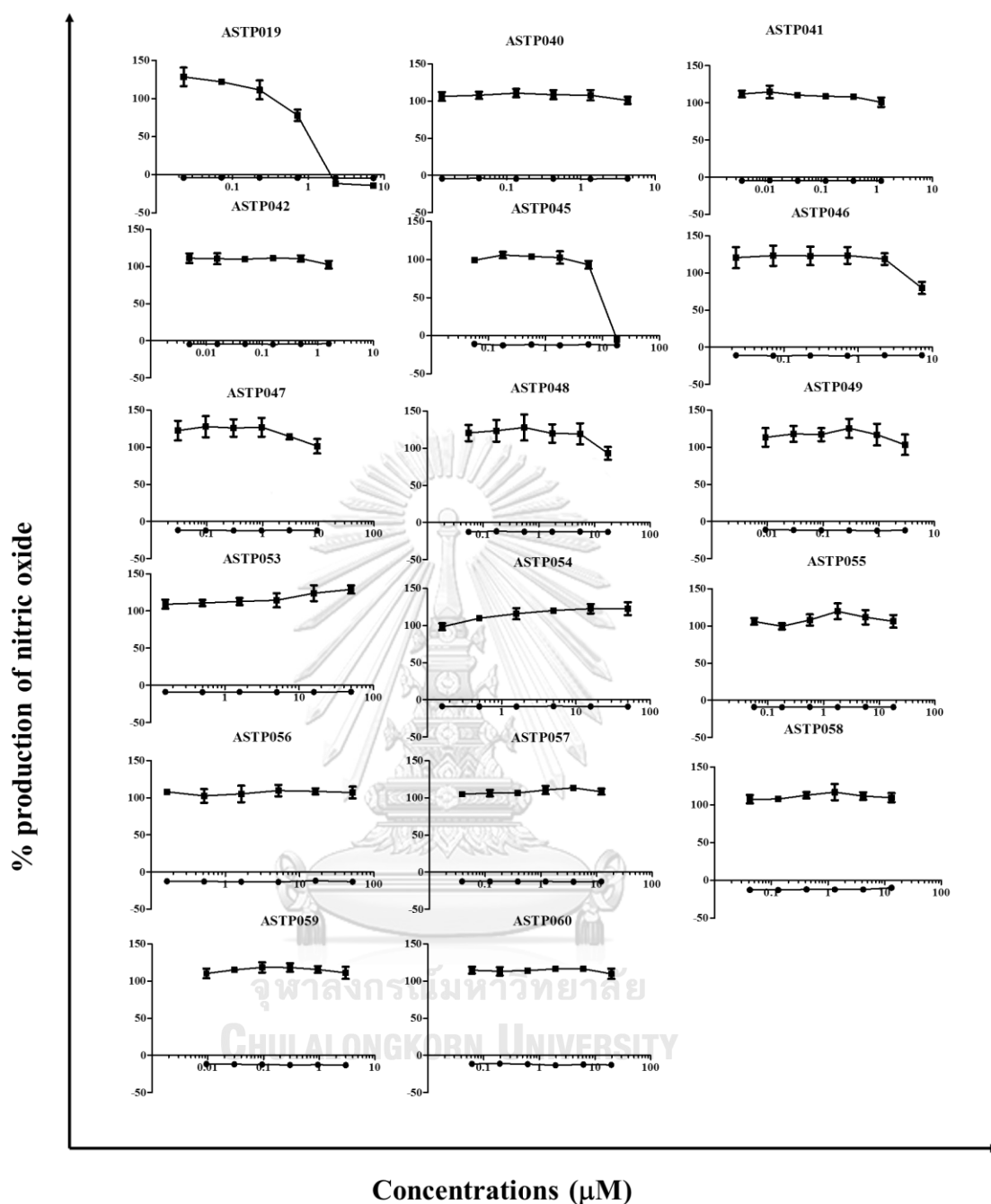


**Figure 4. Anti-inflammation activity in stimulated RAW264.7 cells.**

RAW264.7 cells were stimulated with or without LPS (100 ng/ml) and IFN- $\gamma$  (10 ng/ml) and treated with pure compounds at indicated concentrations (six different concentrations lower than or equal to  $\text{IC}_{50}$  for cell viability). The amount of nitric oxide production was measured by using Griess assay. The data are representative of two independent experiments and presented as mean  $\pm$  S.D.

#### 4.1.3 Effect of pure compounds on RANKL-stimulated osteoclast formation

To investigate whether these pure compounds have activity against osteoclast differentiation, BMMs were stimulated with rRANKL (100 ng/ml) and rM-CSF (25 ng/ml) and treated with each compound at the IC<sub>20</sub> or maximum concentration (100 μM) for cell viability (Table 4). After 5 days, TRAP<sup>+</sup> MNCs were counted and percentage of osteoclast formation was calculated (Fig. 5) The results demonstrated that compounds from *C. comosa* (ASTP019), *T. triandra* (ASTP040, 41 and 42) and *C. crassifolius* (ASTP053, 54, 55 and 59) significantly inhibited osteoclast differentiation by suppressing the formation of TRAP<sup>+</sup> MNCs. Among these, the compounds (ASTP019, 53, 54 and 55) that effectively suppressed TRAP<sup>+</sup> MNCs to be 25% or lower were chosen for further investigation of the effect on the signaling in RANKL/RANK pathway.

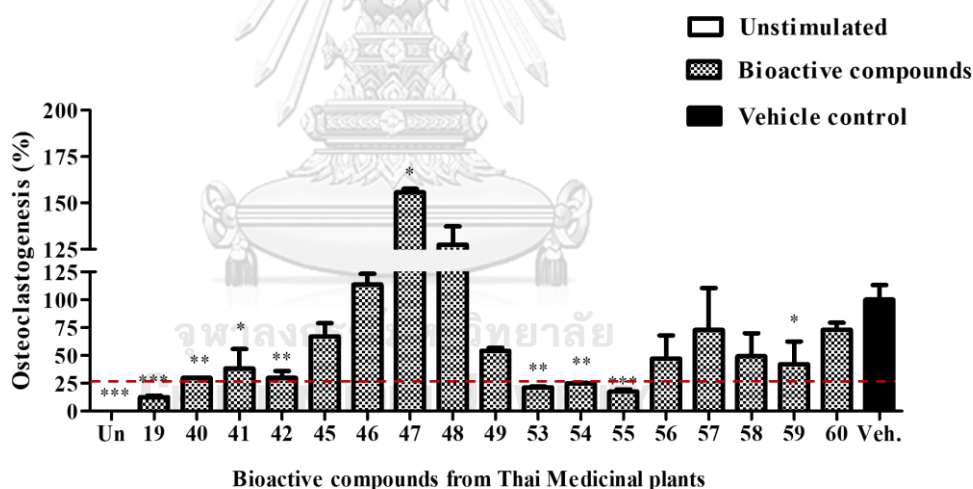


**Figure 5. Effect of plant-derived pure compounds on RANKL-stimulated osteoclast formation.**

BMMs were cultured with rRANKL (100 ng/ml) and rM-CSF (25 ng/ml) in the presence of each compound at the IC<sub>20</sub> or maximum concentration (100 μM) for cell viability for 5 days. TRAP<sup>+</sup>MNCs were stained and counted. Data were expressed as mean ±S.D. from at least two independent experiments. \* $p < 0.05$ , \*\* $p < 0.01$  and \*\*\* $p < 0.001$  indicated statistical significance.

## 4.2 The molecular mechanism of diarylheptanoid (DHPH, ASTP019) from *C. comosa* Roxb. on RANKL-stimulated osteoclast differentiation

### 4.2.1 Effect of DHPH on RANKL-stimulated osteoclast formation

To confirm the effect of DHPH on osteoclast differentiation and calculate the  $IC_{50}$  for this activity, BMMs were stimulated with rRANKL (100 ng/ml) and rM-CSF (25 ng/ml) and treated with  $IC_{20}$  DHPH (1.765  $\mu$ M) (Fig. 6A, B) or indicated concentrations (0-3.53  $\mu$ M) (Fig. 6C). TRAP<sup>+</sup> MNCs were counted in each condition after 5 days of incubation. The representative pictures of TRAP staining were shown in Fig. 6D. The results indicated that DHPH with concentration of 1.765  $\mu$ M or higher clearly inhibited RANKL-stimulated osteoclast formation. Both TRAP<sup>+</sup> MNCs and TRAP enzyme activity were suppressed by DHPH treatment compared with vehicle control. The  $IC_{50}$  of DHPH for osteoclast differentiation was  $325 \pm 1.37$  nM. Therefore, DHPH at the  $IC_{20}$  (1.765  $\mu$ M) was used for further investigation in next series of experiments.

### 4.2.2 Effect of DHPH on the expression of osteoclast-related genes in RANKL-stimulated BMMs

To examine whether DHPH effect the expression of osteoclast-related genes, BMMs were pre-treated with DHPH (1.765  $\mu$ M) or DMSO as the vehicle control for 30 min, and then stimulated with rM-CSF (25 ng/ml) and rRANKL (100 ng/ml) for 0, 6, 12, 24 and 48 hrs. Total RNA was subjected to RT-qPCR analysis for osteoclast-related genes (*nfatc1*, *ctsk* and *irf8*). The relative level of these genes was calculated as fold changes relative to that of the housekeeping gene  *$\beta$ -actin*. The results suggested that expression of *nfatc1* was clearly suppressed by DHPH treatment after 24 hrs of rRANKL stimulation (Fig. 7A). Consistent with this result, the level of *ctsk* encoding cathepsin K which is one of the target genes of NFATc1 was reduced at 24 and 48 hrs (Fig. 7B). However, DHPH did not affect the level of *irf8* (Fig. 7C) which encoded the negative regulator of osteoclast differentiation.

Therefore, DHPH impaired transcription of major osteoclast-related genes. The effect of DHPH at the signaling downstream of RANK/RANKL were investigated in the next experiment.



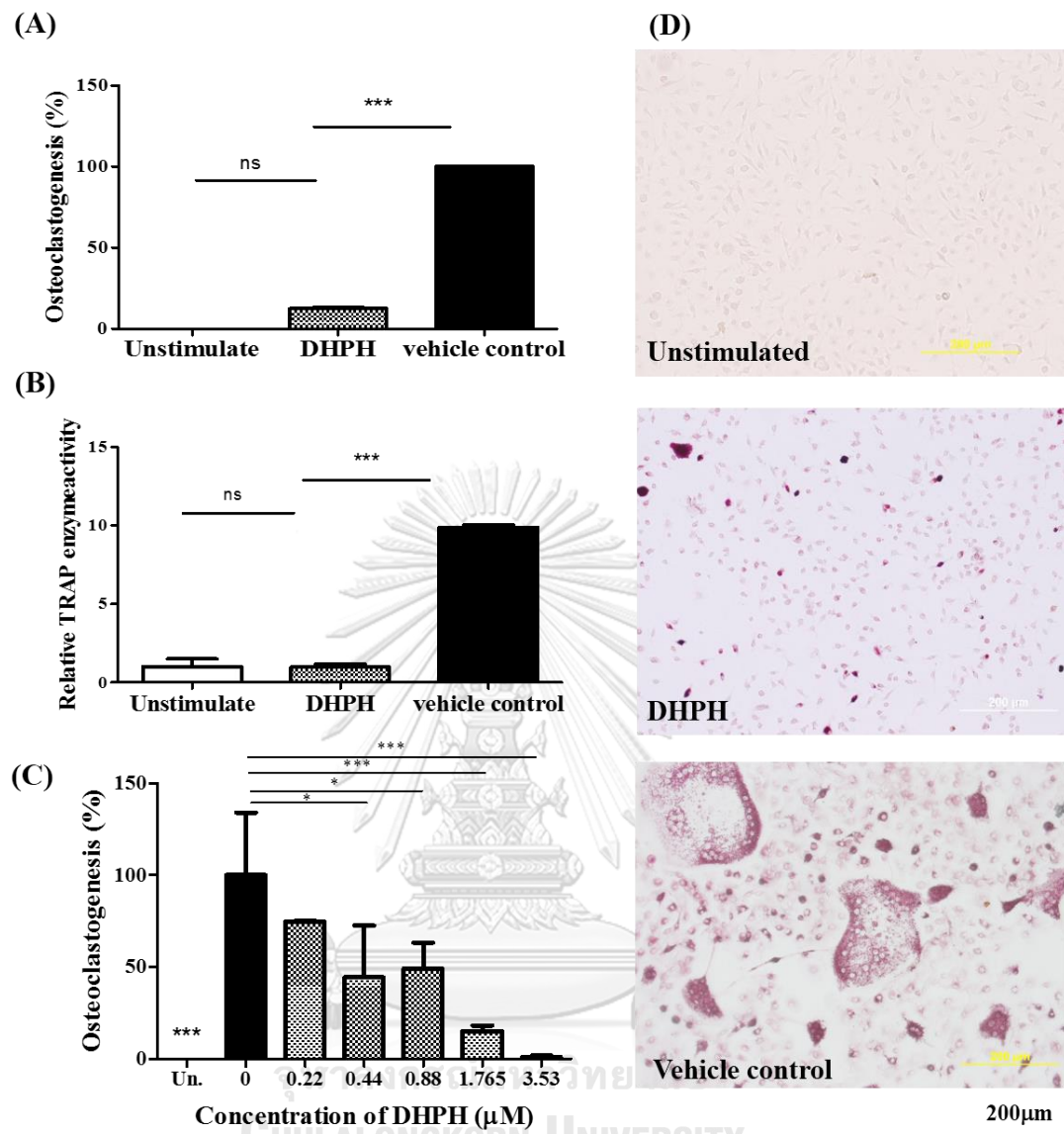


**Figure 6. Effect of DHPH on RANKL-stimulated osteoclast formation.**

BMMs were cultured with rRANKL (100 ng/ml) and rM-CSF (25 ng/ml) in the presence of (A, B) DHPH at 1.765  $\mu\text{M}$  or (C) indicated concentrations for 5 days. (B) TRAP enzyme activity was determined as a relative enzyme activity (D) TRAP<sup>+</sup>MNCs were stained and counted as shown in A or C. Data were expressed as mean  $\pm$  S.D. from at least two independent experiments. N.S., not significant. \*\*\* $p < 0.001$  indicated statistical significance. Scale bar = 200  $\mu\text{m}$ .

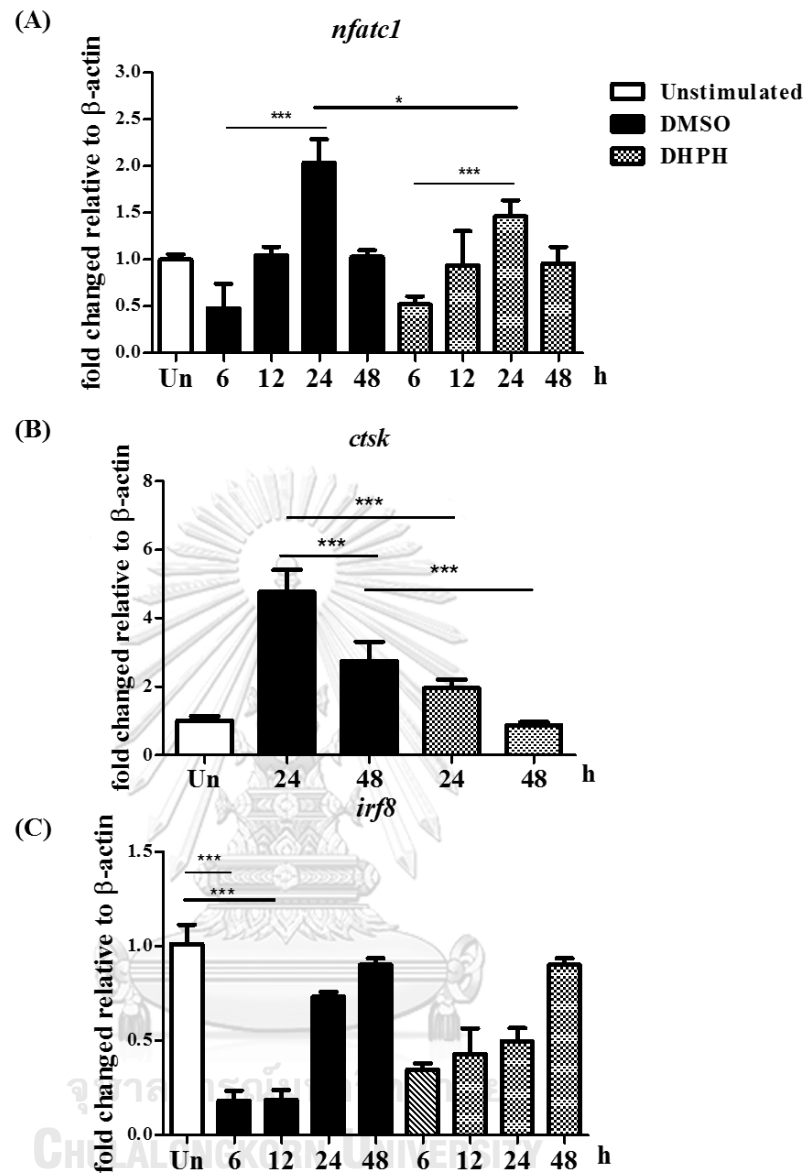


**Figure 7. Effect of DHPH on mRNA expression of osteoclast-related genes in RANKL-stimulated BMMs.**

BMMs were stimulated DMSO without RANKL (opened bar), DMSO as the vehicle control (closed bar) or pre-treated with DHPH (1.765  $\mu$ M) (hatched bar) for 30 min, then stimulated with rRANKL (100 ng/ml) for indicated times. Total RNA was subjected to RT-qPCR. The expression of (A) *nfatc1*, (B) *ctsk*, and (C) *irf8* were calculated as a fold change relative to  $\beta$ -actin. The experiments were performed in triplicate with two independent experiment. Data were expressed as mean  $\pm$  S.D., \* $p$  < 0.05, \*\* $p$  < 0.01 and \*\*\* $p$  < 0.001 indicated statistical significance.

#### **4.2.3 Effect of DHPH on expression of NFATc1 and c-Fos in RANKL-stimulated BMMs**

To investigate the effect of DHPH on protein expression of two transcription factors, NFATc1 and c-Fos, of the RANKL/RANK, BMMs were pre-treated with DHPH (1.765  $\mu$ M) or the vehicle control (DMSO) for 30 min, and then stimulated with rM-CSF (25 ng/ml) and RANKL (100 ng/ml) for 0, 6, 12, 24, 48, 72 and 96 hrs (Fig. 8A, B). Cell lysates were subjected to Western blot. The results indicated that NFATc1 was dramatically reduced in DHPH treated cells after 24 hrs of rRANKL stimulation, consistent with mRNA level. In addition, c-Fos was clearly suppressed by DHPH treatment after 6 and 24 hrs of rRANKL stimulation (Fig. 8A, B). Therefore, DHPH acts by inhibiting NFATc1 and c-Fos expression in RANKL-stimulated BMMs. Both transcription factors play a critical role in osteoclast differentiation.

#### **4.2.4 Effect of DHPH on NFATc1 nuclear translocation in RANKL-stimulated BMMs**

To determine whether DHPH interferes with NFATc1 nuclear translocation, BMMs were pretreated in the presence of DHPH (1.765  $\mu$ M) for 30 min and then stimulated with rM-CSF (25 ng/ml) and RANKL (100 ng/ml) for 24 and 48 hrs. Cells with nuclear translocation of NFATc1 were shown in Fig. 9A and the cell numbers were counted and shown in Fig. 9B, DHPH treatment significantly reduced the percentage cells with nuclear NFATc1 in RANKL-stimulated BMMs.

Taken together, these results strongly suggested that DHPH interfered with RANKL/RANK signaling during osteoclast differentiation and suppressed activation of NFATc1 and c-Fos.

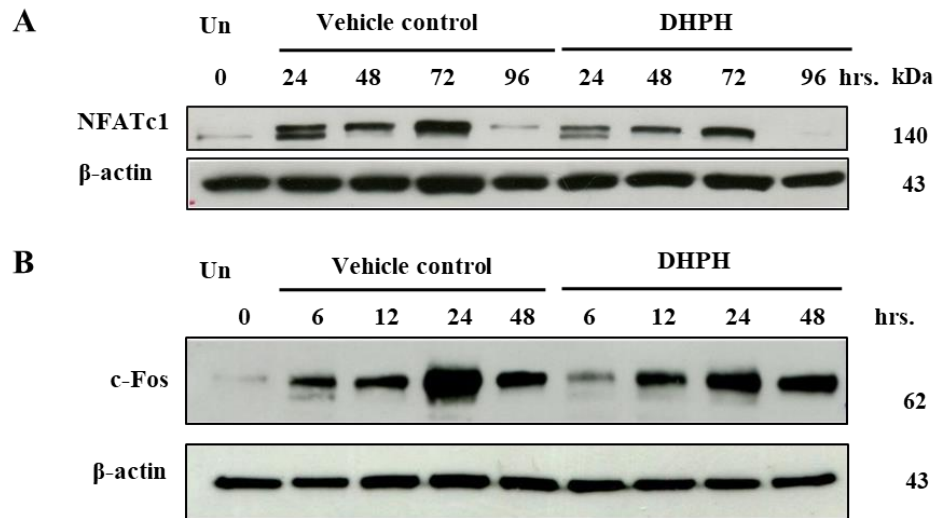


**Figure 8. Effect of DHPH on NFATc1 and c-Fos in RANKL-stimulated BMMs.**

BMMs were pre-treated with DHPH (1.765  $\mu$ M) or vehicle control and stimulated with rRANKL (100 ng/ml) for indicated times. Cell lysates were analyzed for (A) NFATc1 and (B) c-Fos by Western blot.  $\beta$ -actin was used as a loading control. Data were representative of two independent experiments.

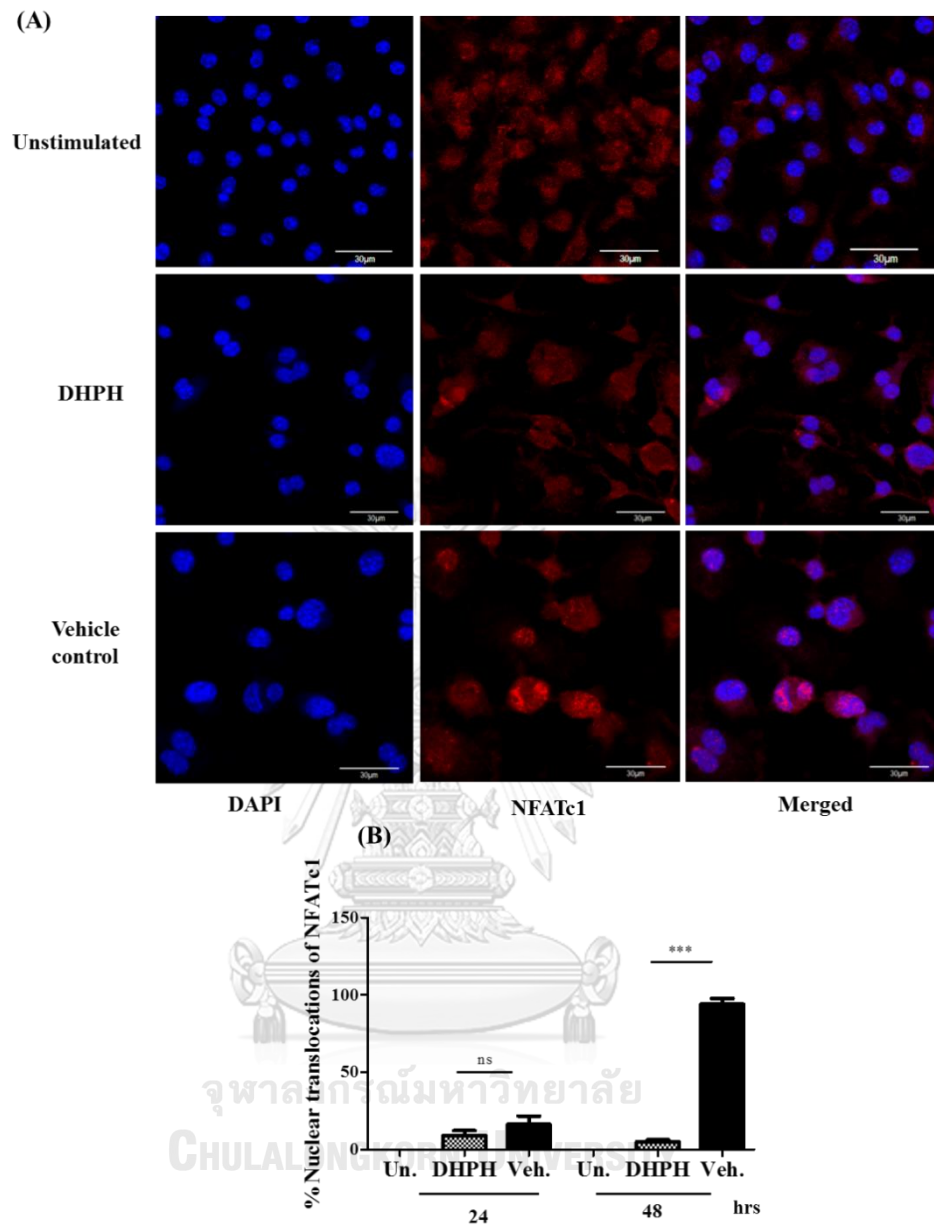


**Figure 9. Effect of DHPH on nuclear translocation of NFATc1 in RANKL stimulated BMMs.**

BMMs were pretreated with DHPH (1.765  $\mu$ M) for 30 min and then stimulated with rM-CSF (25 ng/ml) and RANKL (100 ng/ml) for 48 hrs. Immunofluorescent staining for NFATc1 (red) and nuclei (blue) were shown in A. Cells with NFATc1 nuclear translocation were counted and calculated as % of cells with NFATc1 nuclear translocation in B. Data were expressed as two independent experiments. Scale bar = 30  $\mu$ m, N.S. indicated statistical significance, \*\*\* $p < 0.001$  indicated statistical significance.

#### 4.2.5 Effect of DHPH on downstream signaling of the RANKL/RANK

Because, DHPH interferes with both osteoclast-related genes and transcription with the expression of protein involving osteoclast differentiation, furthermore to examine whether DHPH inhibits activation of the MAPK (p38, ERK, and SAPK/JNK), BMMs were pre-treated with DHPH (1.765  $\mu$ M) or DMSO as the vehicle control for 30 min, and then stimulated with rM-CSF (25 ng/ml) and RANKL (100 ng/ml) for 0, 5, 15, 30 and 60 min (Fig. 10). The results indicated that DHPH diminished the phosphorylation of p38 and ERK (p44/42) after 30 and 60 min after rRANKL stimulation while the phosphorylation of SAPK/ JNK remained unchanged in the DHPH treatment (Fig. 10A).

To investigate the effect of DHPH on canonical NF- $\kappa$ B pathway (p65 and I $\kappa$ B $\alpha$ ), BMMs were stimulated with the two cytokines and treated with DHPH at the same condition as described above. The expression of canonical NF- $\kappa$ B were shown in Fig. 10B; and, the quantitative assay of band density was shown in Fig. 10C. The results indicated that DHPH did not reduce p65 phosphorylation or interfered with I $\kappa$ B $\alpha$  degradation after rRANKL stimulation.

Therefore, DHPH inhibited osteoclast differentiation by inhibiting phosphorylation of p38 and p44/42 in the MAPKs signaling pathway which play a critical role in osteoclastogenesis.

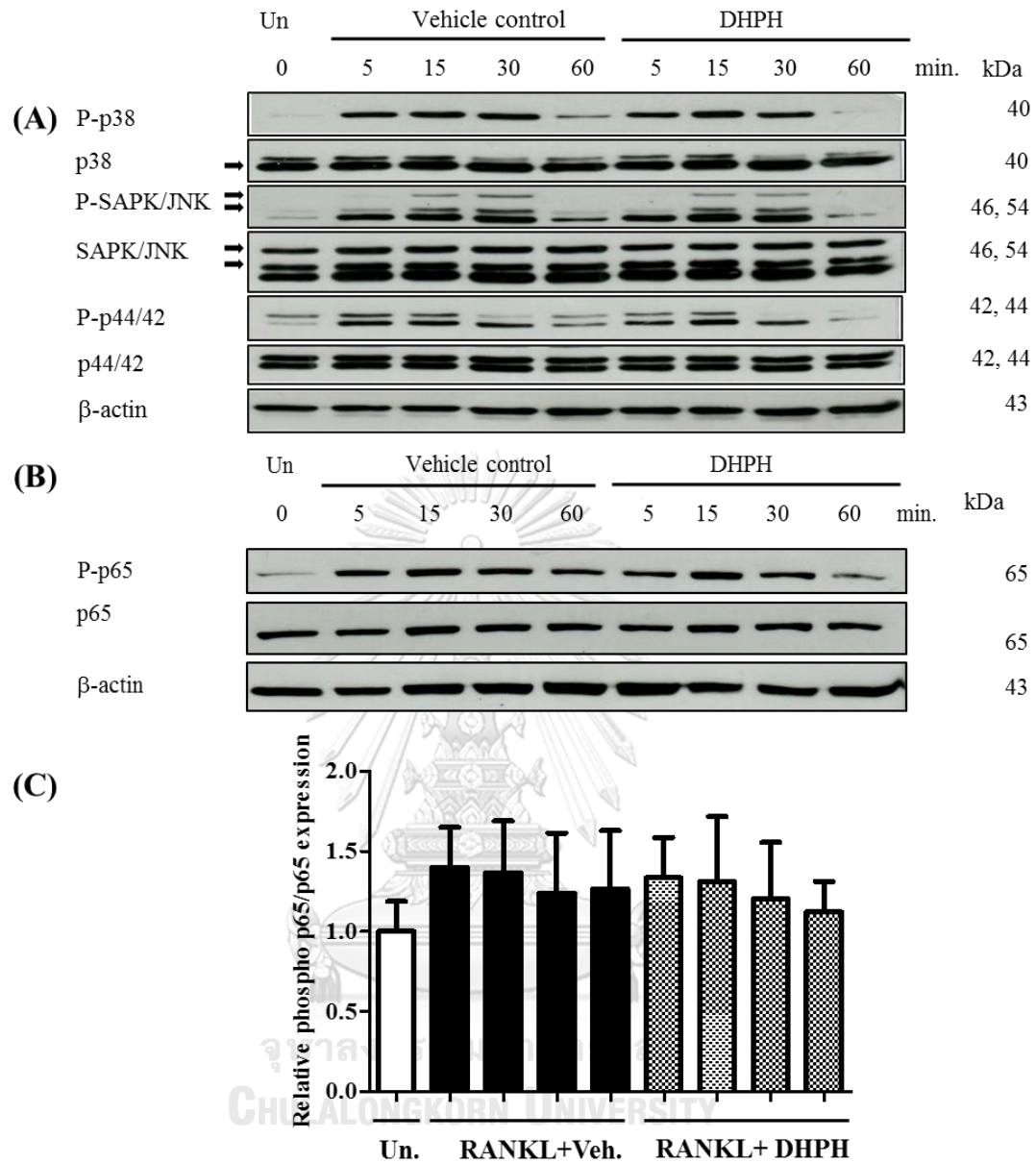


**Figure 10. Effect of DHPH on downstream signaling of the RANKL/RANK.**

BMMs were pre-treated with of DHPH (1.765  $\mu$ M) or vehicle control and stimulated with rRANKL (100 ng/ml) for the indicated times. Cell lysates were analyzed for (A) MAPKs or (B) canonical NF- $\kappa$ B by Western blot. (C) The quantitative band density of phosphorylation p65 normalized by p65 that were quantitated Pp65/p65 expression.  $\beta$ -actin was used as a loading control. The data represent the results obtained from at least two independent experiments.

#### 4.2.6 Effect of DHPH on bone resorption activity or osteoclast activation

To investigate whether DHPH impairs osteoclast functions, bone slices were subjected to a bone absorption assay. Precursor osteoclasts from BMMs were cultured with rM-CSF (25 ng/ml) for 2 days then precursor osteoclasts were unstimulated, stimulated with rRANKL (100 ng/ml) as a vehicle control or treated with DHPH (1.765  $\mu$ M) for 14 days. The bone resorption pits were observed and quantitated (Fig. 11A-D). DHPH treatment clearly decreased the area of osteoclast-mediated bone resorption. Therefore, these results were consistent with the effect of DHPH treatment on osteoclast differentiation.

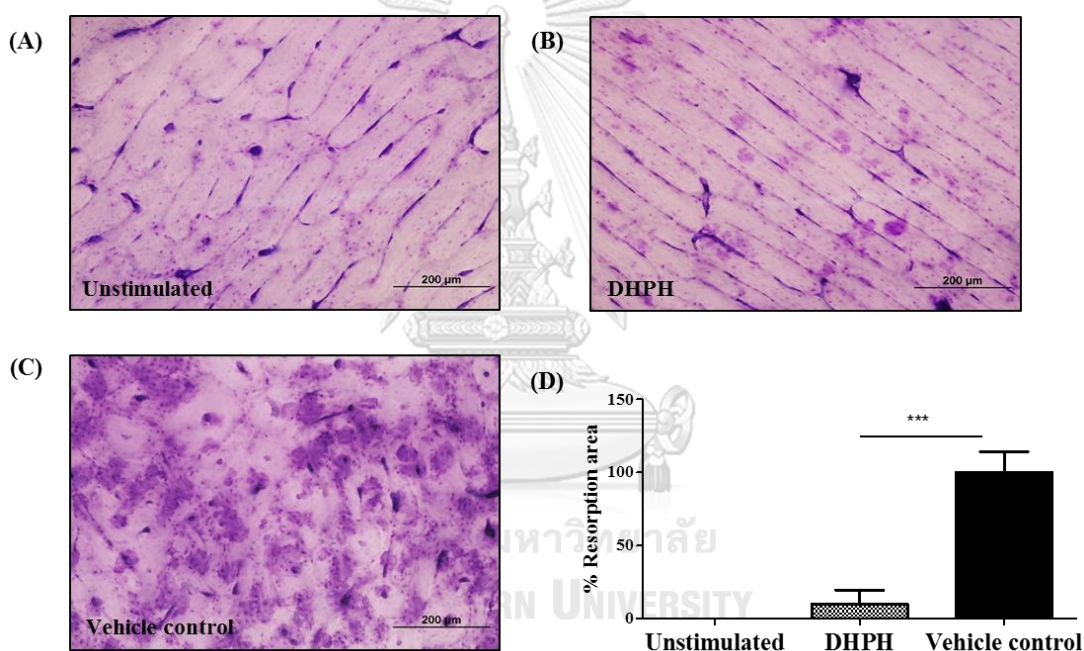


**Figure 11. Effect of DHPH on bone resorption in RANKL-stimulated osteoclasts.**

(A-C) Precursor osteoclasts were either left untreated (A) or cultured with rRANKL (100 ng/ml) and rM-CSF (25 ng/ml) in the presence of DHPH (1.765  $\mu$ M) (B) or vehicle control (C) for 14 days. The resorption area on bone slices were stained with Toluidine Blue and observed by light microscope Scale bar = 200  $\mu$ m. (D) The resorption areas were calculated as a percentage of total area resorbed using Image-J software at 100-fold magnification. \*\*\* $p < 0.001$  indicated statistical significance.



#### 4.2.7 Effect of DHPH on osteoblast differentiation

Because the chemical structure of DHPH is similar to estrogen hormone which can induce osteoblast differentiation and bone formation, the effect of DHPH on cell viability and osteoblast differentiation using pre-osteoblast cell line (MC3T3-E1) was investigated. First, MC3T3-E1 cells were treated with DHPH at indicated concentrations (0-100  $\mu\text{M}$ ) for 24 hrs to evaluate toxicity. The effect of DHPH on cell viability of MC3T3-E1 cells was measured by using MTS assay (Fig. 12A). The results revealed that DHPH did not show any toxicity at tested concentrations. Interestingly, DHPH treatment increased cell numbers at high concentration (10-100  $\mu\text{M}$ ).

Next, to investigate the effect of DHPH on osteoblast differentiation, MC3T3-E1 cells were cultured with DHPH (1.765  $\mu\text{M}$ ) and stimulated with ascorbic acid (200  $\mu\text{M}$ ) for 10 days. The effect of DHPH on osteoblast differentiation was evaluated by measuring the ALP. ALP activity was normalized by 15  $\mu\text{g}$  of protein content. As shown in Fig. 12B, DHPH treatment significantly enhanced ALP activity after ascorbic acid-induced osteoblast differentiation. Therefore, DHPH not only inhibits RANKL-stimulated osteoclast differentiation but also increases ascorbic-induced osteoblast differentiation.

Taken together, DHPH shows both anti-osteoclast differentiation and pro-osteoblast differentiation. Therefore, this compound has potential to become lead compound for osteoporosis treatment.

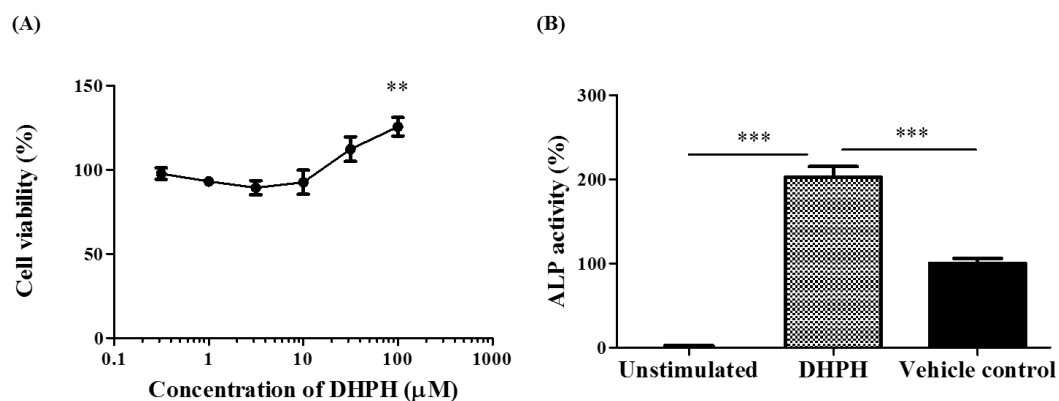


**Figure 12. Effect of DHPH on cell viability and cell differentiation of pre-osteoblast MC3T3-E1 cells.**

(A) MC3T3-E1 cells were treated with various concentration of DHPH for 24 hrs and measured by MTS assay (B) MC3T3-E1 cells were treated with DHPH (1.765 μM) or vehicle control and stimulated with ascorbic acid (200 μM) for 10 days. The alkaline phosphatase activity was measured and normalized by the same protein concentration. The data are representative of two independent experiments and presented as the mean  $\pm$  S.D., \*\* $p < 0.01$  and \*\*\* $p < 0.001$  indicated statistical significance.

### **4.3 The molecular mechanism of cyperenoic acid (ASTP053) from *C. crassifolius* Geiseler on RANKL-stimulated osteoclast differentiation**

#### **4.3.1 Effect of cyperenoic acid, cyperenol and CATC on RANKL-stimulated osteoclast formation.**

To test whether cyperenoic acid, cyperenol or CATC suppress osteoclast differentiation by using the same concentrations as in Fig. 13, BMMs were stimulated with rRANKL (100 ng/ml) and rM-CSF (25 ng/ml) and treated with cyperenoic acid (100  $\mu$ M), or cyperenol (100  $\mu$ M) or CATC (4.69  $\mu$ M) for 5 days. TRAP<sup>+</sup> MNCs were counted and shown in Fig. 13A, B. The representative pictures of TRAP staining were shown in Fig. 13 C. The results indicated that three bioactive compounds isolated from *C. crassifolius* significantly inhibited osteoclast differentiation to the same level (Fig. 13A). Therefore, cyperenoic acid, major compound from *C. crassifolius*, was chosen for detailed study in the next experiment at a concentration of 100  $\mu$ M.

Next, BMMs were stimulated with rRANKL (100 ng/ml) and rM-CSF (25 ng/ml) and treated with cyperenoic acid at several concentrations (0-100  $\mu$ M) for 5 days. TRAP<sup>+</sup> MNCs were counted and valuated for IC<sub>50</sub>. The results suggested that cyperenoic acid clearly inhibited RANKL-stimulated osteoclast formation with the IC<sub>50</sub> of 36.69  $\pm$  1.02  $\mu$ M (TRAP<sup>+</sup> MNCs IC<sub>50</sub>). Therefore, cyperenoic acid at 100  $\mu$ M was used for investigation in the next experiments.

#### **4.3.2 Effect of cyperenoic acid on expression of osteoclast related genes in RANKL-stimulated BMMs**

To examine whether cyperenoic acid affects expression of osteoclast related genes, BMMs were pre-treated with cyperenoic acid (100  $\mu$ M) or DMSO as the vehicle control for 30 min, and then stimulated with rM-CSF (25 ng/ml) and rRANKL (100 ng/ml) for 0, 6, 12, 24 and 48 hrs. Total RNA was subjected to RT-qPCR analysis for osteoclast-related genes (*nfatc1*, *ctsk* and *irf8*). The expression of these genes was indicated as a fold change normalized by the level of  $\beta$ -actin. The results indicated that mRNA of both *nfatc1* and *ctsk*, which encoded positive regulator of osteoclastogenesis, were suppressed by cyperenoic acid after 48 hrs rRANKL stimulation (Fig. 14A, B). Moreover, this compound obviously delayed the reduction of *irf8*, which encoded

negative regulator of osteoclastogenesis (Fig. 14C). Therefore, cyperenoic acid affect the transcriptional level of both positive and negative regulators in osteoclast differentiation.

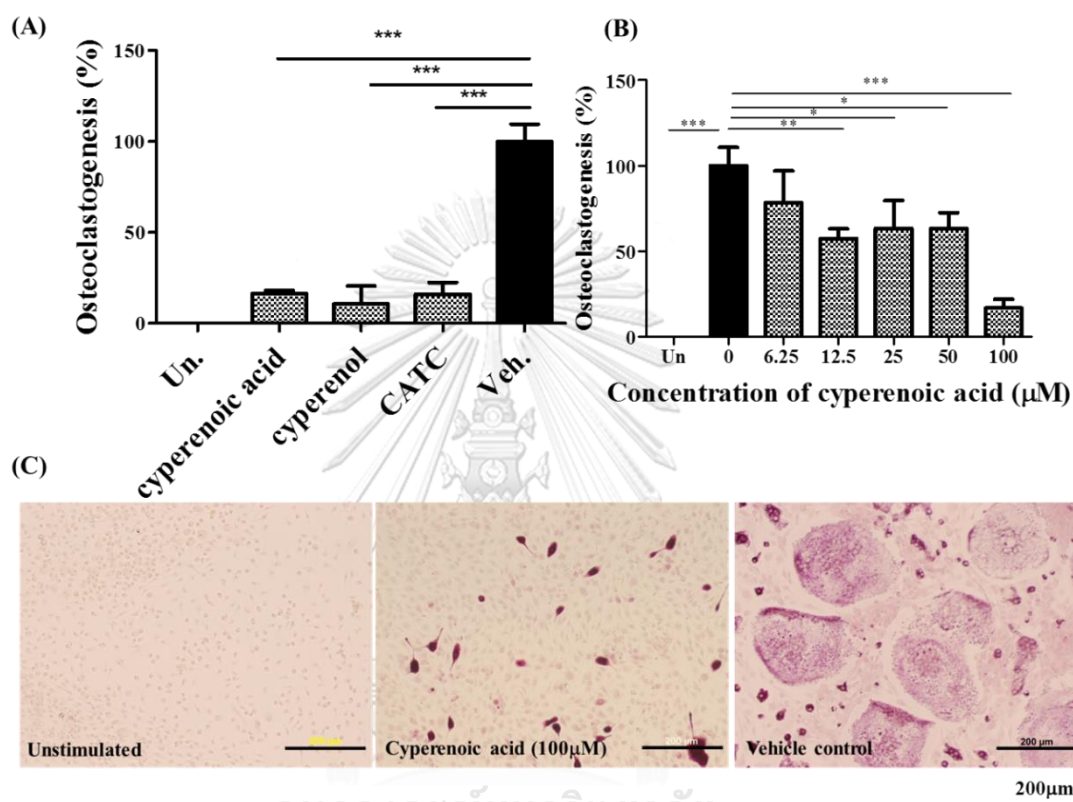


**Figure 13. Effect of cyperenoic acid and other compounds on RANKL-stimulated osteoclast formation.**

BMMs were cultured with rRANKL (100 ng/ml) and rM-CSF (25 ng/ml) in the presence of (A) cyperenoic acid (100 μM), cyperenol (100 μM) and CATC (4.69 μM) or (B) cyperenoic acid at various concentration (0-100 μM) for 5 days. (C) TRAP<sup>+</sup> MNCs were stained for TRAP activity. The data are representative of two independent experiments and presented as mean ± S.D., \*\*\* $p < 0.001$ , \*\* $p < 0.01$  and \* $p < 0.05$  indicated statistical significance.

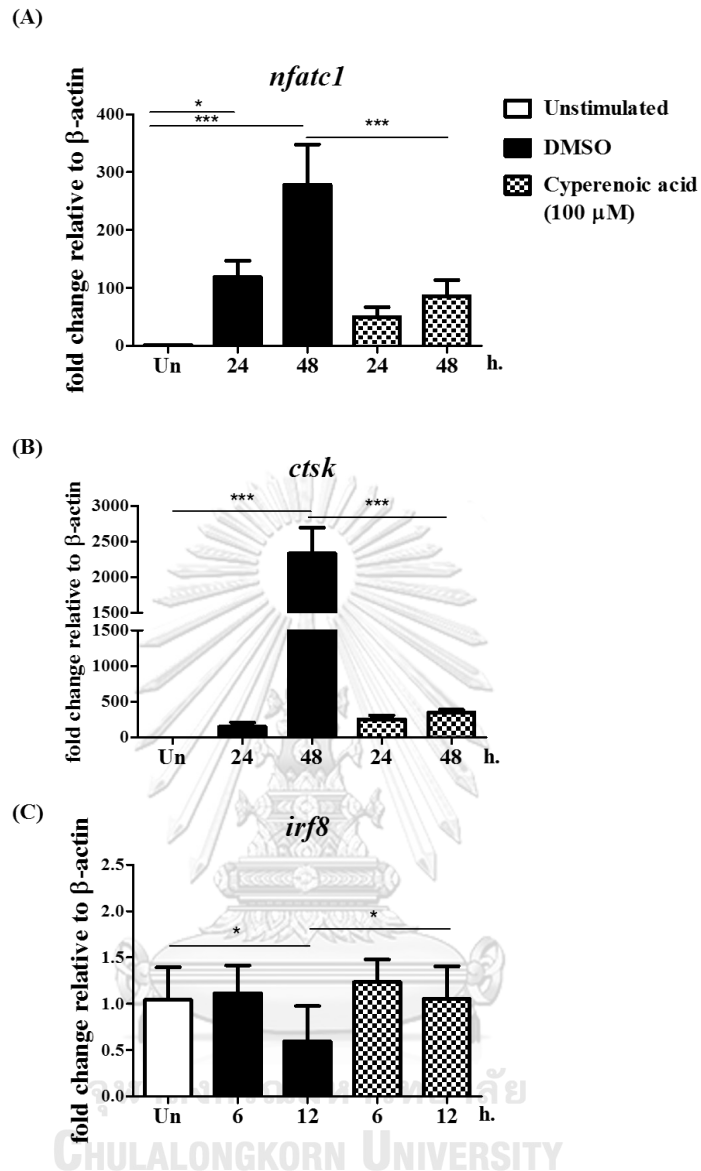


**Figure 14. Effect of cyperenoic acid on expression of osteoclast-related genes in RANKL-stimulated BMMs.**

BMMs were stimulated DMSO without RANKL (opened bars), DMSO as the vehicle control (closed bars) or pre-treated with cyperenoic acid (100  $\mu$ M) (hatched bars) for 30 min, then stimulated with rRANKL (100 ng/ml) for indicated times. Total RNA was subjected to RT-qPCR. The expression of (A) *nfatc1*, (B) *ctsk*, and (C) *irf8* were shown as a fold change relative to  $\beta$ -actin. The experiments were performed in triplicate and two the results were representative of two independent experiments. Data were expressed as mean  $\pm$  S.D., \*\*\* $p$  < 0.001 and \* $p$  < 0.05 indicated statistical significance.

### 4.3.3 Effect of cyperenoic acid on NFATc1 and c-Fos in RANKL-stimulated BMMs.

To investigate whether cyperenoic acid attenuates the expression of NFATc1 and c-Fos, BMMs were pre-treated with cyperenoic acid (100  $\mu$ M) or the vehicle control (DMSO) for 30 min, then stimulated with rM-CSF (25 ng/ml) and RANKL (100 ng/ml) for 0, 6, 12, 24, 48, 72 and 96 hrs. Cell lysates were subjected to Western blot analysis for NFATc1 or c-Fos. The results indicated that cyperenoic acid delayed the pattern of NFATc1 expression after 72 hrs of RANKL stimulated and also clearly suppressed NFATc1 expression at 96 hrs (Fig. 15A). Furthermore, the level of c-Fos expression was significantly impaired by cyperenoic acid at 48 hrs (Fig. 15B).

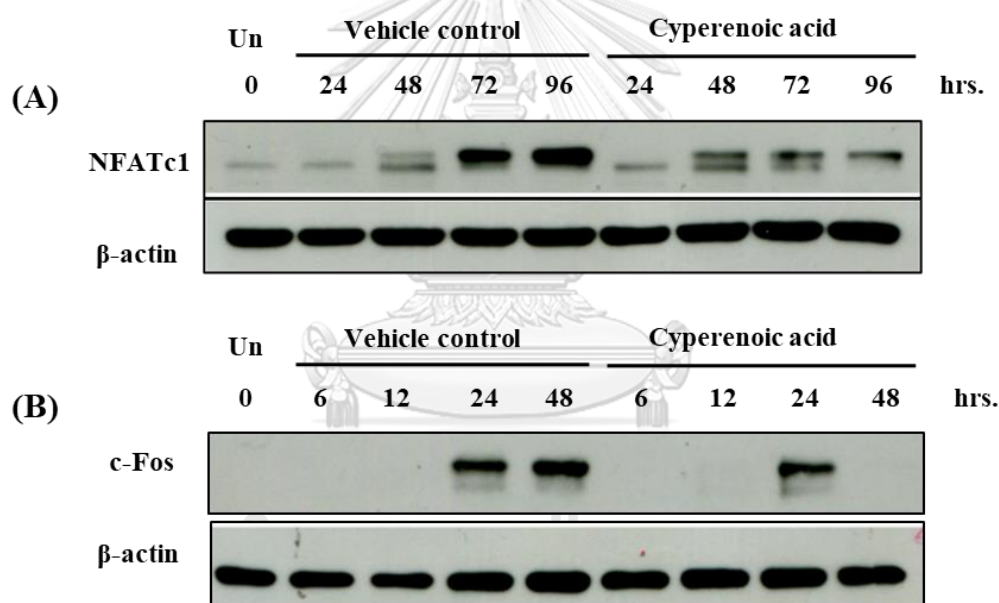


**Figure 15. Effect cyperenoic acid on transcription factor in RANKL-stimulated BMMs.**

BMMs were pre-treated with cyperenoic acid (100  $\mu$ M) or DMSO as a vehicle control and stimulated with rRANKL (100 ng/ml) for indicated times. Cell lysates were analyzed for expression of NFATc1 (A) and c-Fos (B) by Western blot.  $\beta$ -actin was used as a loading control. Data were representative of two independent experiments.

#### **4.3.4 Effect of cyperenoic acid on signaling downstream of RANKL/RANK in RANKL-stimulated BMMs**

Because cyperenoic acid impairs both osteoclast-related genes expression and transcription factors activation, to determine whether cyperenoic acid effects on the activation of MAPKs (p38, ERK, and SAPK/JNK) or canonical NF- $\kappa$ B (p65 and I $\kappa$ B $\alpha$ ), BMMs were pre-treated with cyperenoic acid (100  $\mu$ M) or DMSO as the vehicle control for 30 min, and then stimulated with rM-CSF (25 ng/ml) and RANKL (100 ng/ml) for 0, 5, 15, 30 and 60 min. All phosphorylation of MAPKs and canonical NF- $\kappa$ B signaling were not differed after cyperenoic acid treatment. The results indicated that cyperenoic acid (100  $\mu$ M) did not have any effect neither on MAPKs (Fig. 16A) nor on canonical NF- $\kappa$ B (Fig. 16B). There are reports suggesting that RANK/RANKL activates non-canonical NF- $\kappa$ B pathways (39). Thus, the effect of cyperenoic acid on non-canonical NF- $\kappa$ B pathways was examine in the next experiment.

To examine the effect of cyperenoic acid on non-canonical NF- $\kappa$ B pathway (RelB/p52 and TRAF3), BMMs were pre-treated with cyperenoic acid (100  $\mu$ M) or DMSO and stimulated with RANKL and rM-CSF at the same condition as described above. As shown in Figure 17, cyperenoic acid clearly attenuated the phosphorylation of p100 and also impaired the activation of p52, a processed from of p100, at 60 min after cyperenoic acid treatment. The level of TRAF3 was also reduced after 15 min of cyperenoic acid treatment. However, this compound did not have any effect on RelB level.

Therefore, cyperenoic acid impaired on osteoclast differentiation at least at the p100/52 activation step in non-canonical NF- $\kappa$ B signaling.

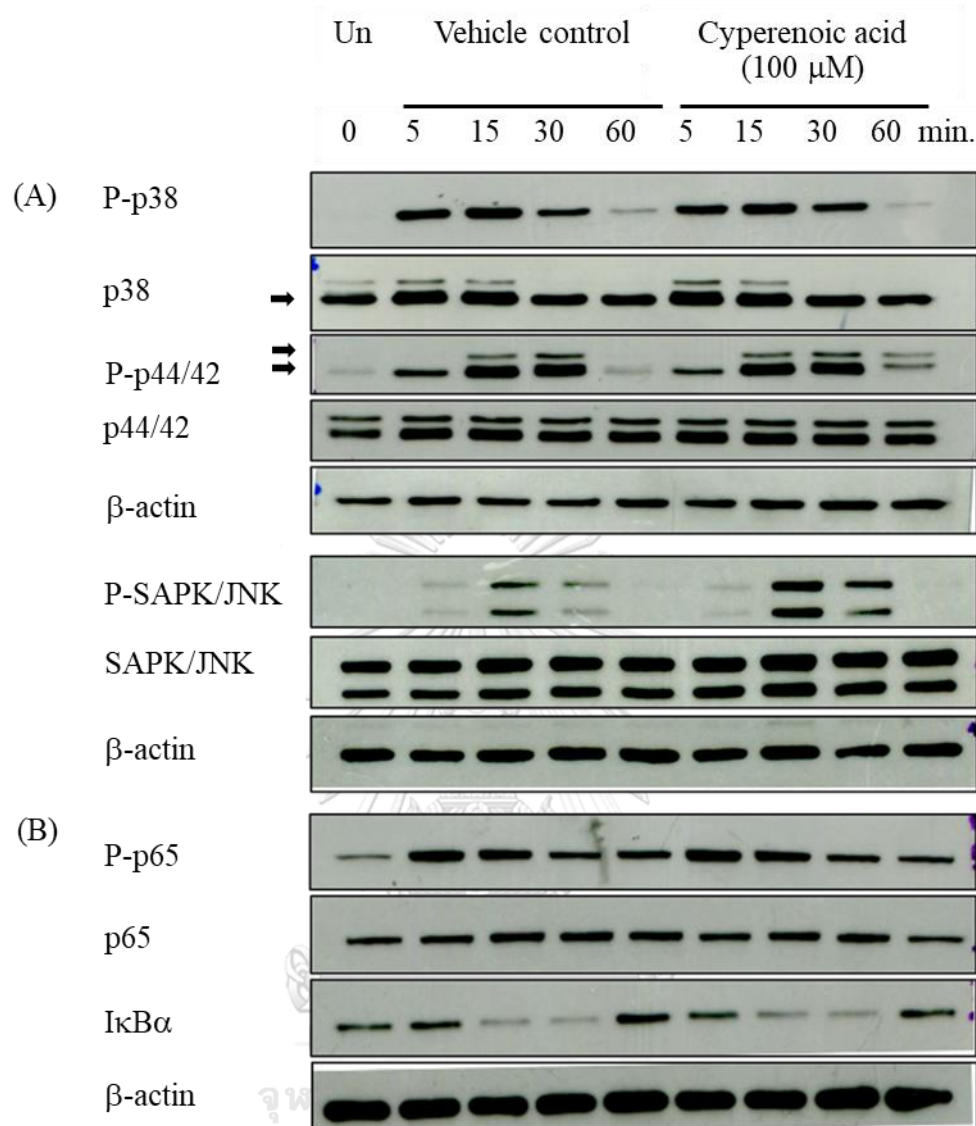


**Figure 16. Effect of cyperenoic acid on MAPK and canonical NF- $\kappa$ B pathway in RANKL-stimulated BMMs.**

BMMs were pre-treated with of cyperenoic acid (100  $\mu$ M) or vehicle control for the indicated times in the present of rRANKL (100 ng/ml). Cell lysates were analyzed for (A) MAPKs and (B) canonical NF- $\kappa$ B by using Western blot.  $\beta$ -actin was used as a loading control. Data were representative of two independent experiments.



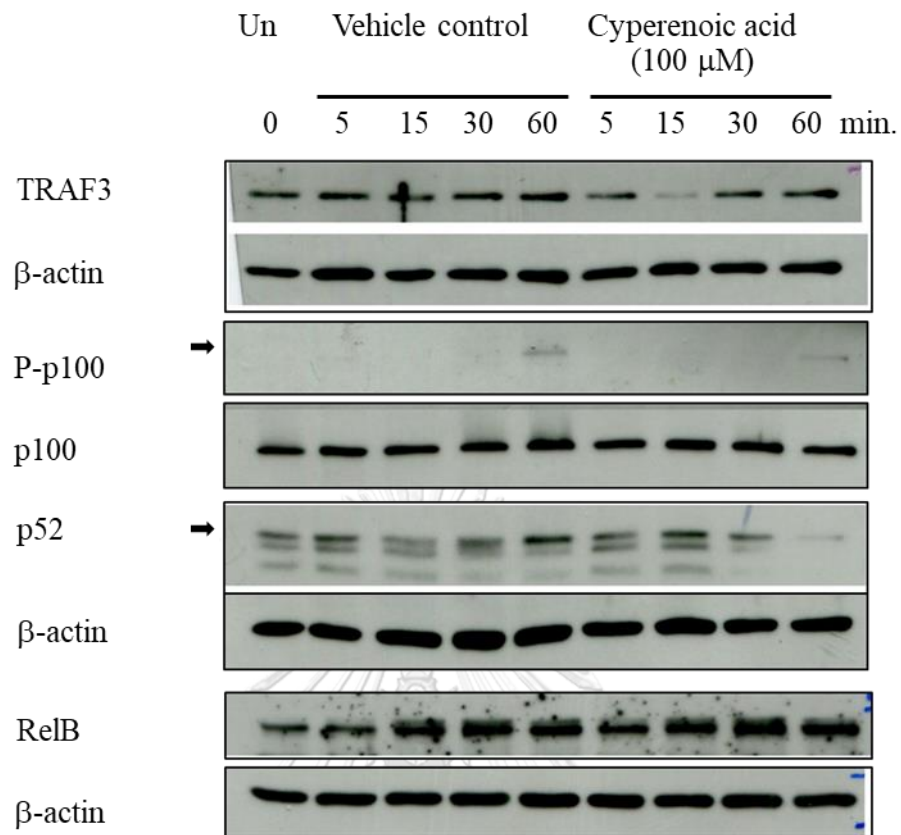


**Figure 17. Effect of cyperenoic acid on non-canonical NF- $\kappa$ B pathway in RANKL-stimulated BMMs.**

BMMs were pre-treated with of cyperenoic acid (100  $\mu$ M) or vehicle control for the indicated times in the present of rRANKL (100 ng/ml). Cell lysates were analyzed for non-canonical NF- $\kappa$ B expression by using Western blot.  $\beta$ -actin was used as a loading control. Data were representative of two independent experiments.

#### 4.3.5 Effect of cyperenoic acid on bone resorption activation in RANKL-stimulated osteoclasts

To investigate whether cyperenoic acid disrupt osteoclast function, dentin slices were subjected to a bone absorption assay. To generate precursor osteoclast, BMMs were cultured with rM-CSF (25 ng/ml) for 2 days; and, precursor osteoclasts were unstimulated, stimulated with rRANKL (100 ng/ml) as a vehicle control or treated with cyperenoic acid (100  $\mu$ M) for 14 days. The bone resorption pits were observed (Fig. 18A-C) and the area of resorption was calculated and shown in Fig. 18D. The results indicated that cyperenoic acid treatment significantly, but partially, reduced the size of the area of osteoclast-mediated bone resorption, consistent with the effect of cyperenoic acid treatment on osteoclast differentiation.

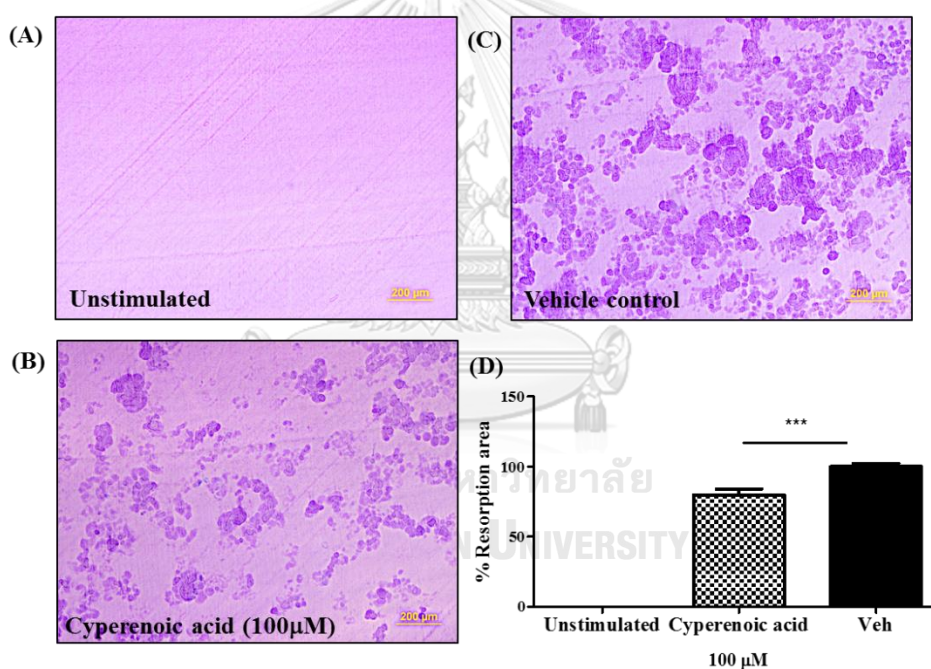


**Figure 18. Effect of cyperenoic acid on bone resorption in RANKL-stimulated osteoclasts.**

(A-C) Precursor osteoclasts were either left untreated (A) or cultured with rRANKL (100 ng/ml) and rM-CSF (25 ng/ml) in the presence of cyperenoic acid (100  $\mu$ M) (B) or vehicle control (C) for 14 days. The resorption area on dentin slices were stained with Toluidine Blue and observed by light microscope Scale bar = 200  $\mu$ m. (D) The resorption areas were calculated as a percentage of total area resorbed using Image-J software at 100-fold magnification. \*\*\* $p$  < 0.001 indicated statistical significance.

#### 4.3.6 Effect of cyperenoic acid on ALP activity in osteoblasts

As DHPH is effective on both osteoclast and osteoblast differentiation, it is an interest to know whether cyperenoic acid has an effect on osteoblast differentiation. MC3T3-E1 cells were treated with cyperenoic acid at various concentrations (0-100  $\mu\text{M}$ ) for 24 hrs. The effect on cell viability in MC3T3-E1 was measured by MTT assay (Fig. 19A). The results indicated that this compound did not show any toxicity at tested concentrations and the  $\text{IC}_{50}$  is more than 100  $\mu\text{M}$ .

To investigate the effect of cyperenoic acid on osteoblast differentiation based on ALP, MC3T3-E1 cells were cultured in the presence of cyperenoic acid (100  $\mu\text{M}$ ), the same concentration which inhibited osteoclast differentiation, and stimulated with ascorbic acid (200  $\mu\text{M}$ ) for 10 days. The effect of cyperenoic acid on osteoblast differentiation was evaluated by ALP activity assay as shown in Fig. 19B. Cyperenoic acid did not have any affect to ALP activity in ascorbic acid-induced osteoblast differentiation, as well. Therefore, cyperenoic acid from did not have any effect on osteoblast differentiation in pre-osteoblast cell.

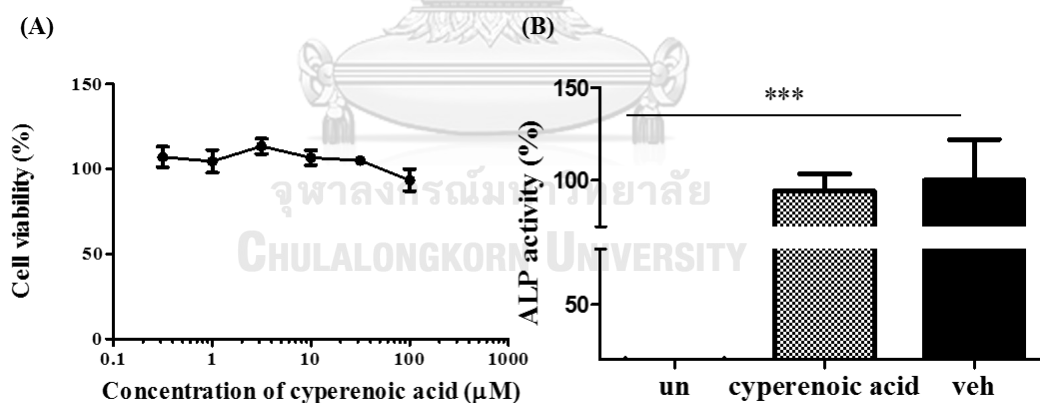


**Figure 19. Effect of cyperenoic acid on cell viability and osteoblast differentiation in MC3T3-E1 cells.**

MC3T3-E1 cells were treated with cyperenoic acid at various concentrations (0-100  $\mu\text{M}$ ) for 24 hrs and measured cell viability by MTT assay. (B) MC3T3-E1 cells were treated with cyperenoic acid (100  $\mu\text{M}$ ) or DMSO as a vehicle control and stimulated with ascorbic acid (200  $\mu\text{M}$ ) for 10 days. The ALP activity was measured and normalized by the protein concentration. The data are representative of two independent

experiments and presented as the mean  $\pm$  S.D.,  $**p < 0.001$  indicated statistical significance.

#### **4.3.7 Effect of cyperenoic acid on SAMP6 mice as a senile osteoporosis model**

As shown above, cyperenoic acid is a strong potentiality of osteoclast differentiation owing to its effect on the activation of both transcriptional and translational level of RANKL-stimulated BMMs. Next, the effect of cyperenoic acid on senile osteoporosis model (SAMP6) were investigated.

To examine whether cyperenoic acid influence bone loss in senile osteoporosis model, SAMP6 mice were randomly assigned into two groups; control and cyperenoic acid treated group by using body weight (Appendix Table 1). Mice were fed with standard diet mixed with 0.01% cyperenoic acid for 19 weeks. The body weight and diet consumption were measured once a week (Fig. 20A-B). The results indicated that there was no difference between body weight and diet consumption between the two groups.

Next, the organ toxicity was examined in liver and kidney sections stained with hematoxylin and eosin (H&E) (Fig. 20C-F). There were no obvious pathological signs in both organs in cyperenoic acid fed mice. The results indicated that cyperenoic acid did not have systemic toxicity even in long-term consumption.

To determine the effect of cyperenoic acid on bone microstructure, femur bones were separated and processed for bone histomorphometry. Bone histomorphometric parameters which are bone area and trabecular area, were used to determine the bone condition. Bone microstructure of control and cyperenoic acid fed group were shown in Fig. 21A, B. The results indicated that cyperenoic acid treatment significantly increased both bone area and the trabecular area in SAMP6 mice as shown in Fig. 21C, D, compared to the control group.

Furthermore, to detect the effect of cyperenoic acid on expression of genes involved in bone formation (*coll1a1*, *bglab* and *ibsp*) or bone resorption (*acp5* and *mmp9*) or pro-inflammatory cytokines (*tnf- $\alpha$*  and *il-6*), BMMs were flushed out of tibia and humerus and total RNA was subjected to RT-qPCR analysis for genes expression. The result demonstrated that cyperenoic acid enhanced the expression of *ibsp*

encoding bone sialoprotein (BSP) compared with the control group (Fig. 22C). BSP is an osteoblast-related protein played an important role in bone formation and bone mineralization. On the other hand, this compound did not have any effect on other genes tested (Fig. 22D-G).

To confirm whether cyperenoic acid influences the serum bone resorption marker, serum was collected from SAMP6 mice after 19 weeks of cyperenoic acid treatment. Amount of BSP in serum was detected by sandwich ELISA. The results indicated that the level of BSP in serum was slightly decreased when compared with control group but did not reach statistical significance (Fig. 23). Therefore, cyperenoic acid treatment by supplement in the normal diet enhanced the expression of *ibsp* and also increased bone microstructure, bone area and trabecular area, in SAMP6 mice.

Taken together, these results strongly suggested that cyperenoic acid from *C. crassifolius* impairs RANKL/RANK signaling via non-canonical NF- $\kappa$ B pathway and might be an effective compound for osteoporosis.

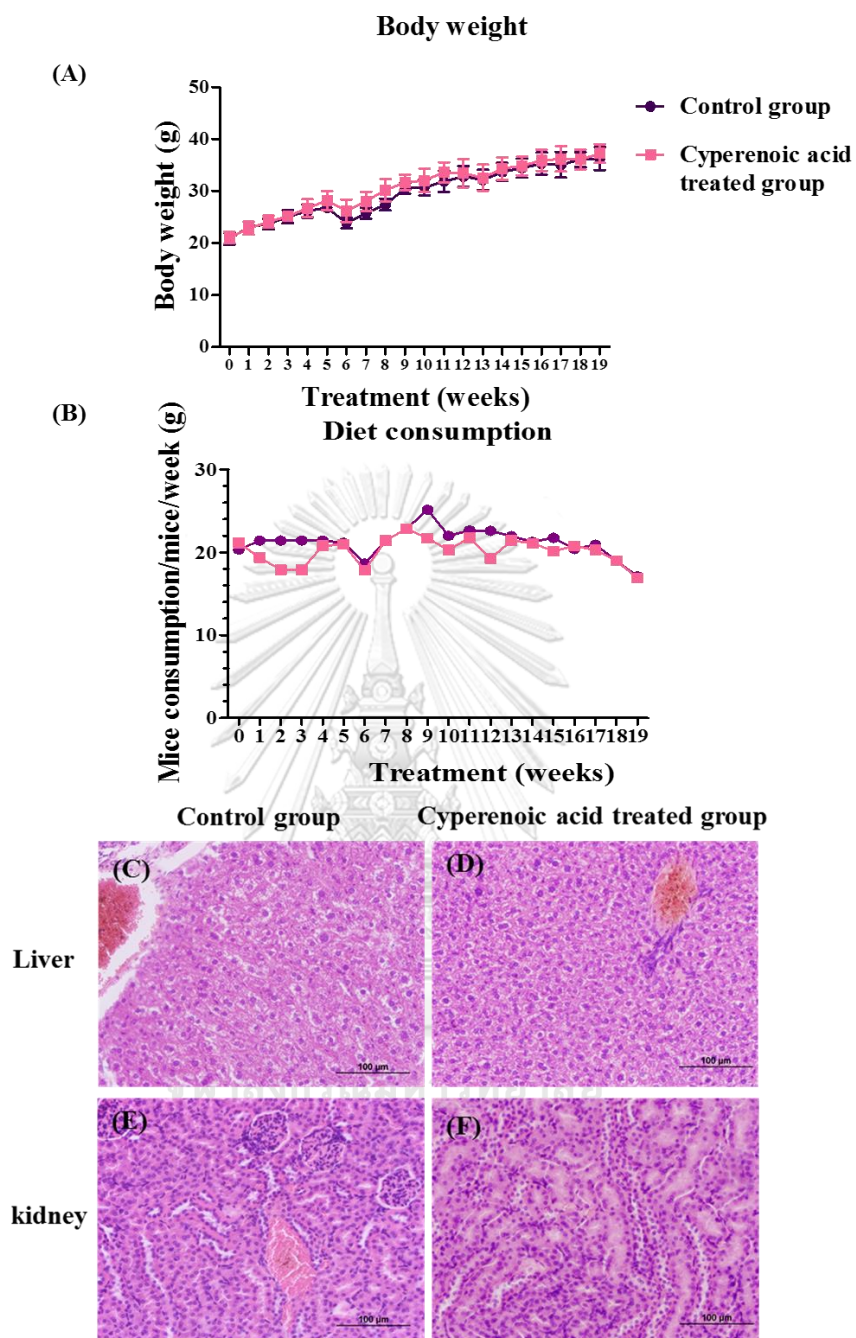


**Figure 20. The body weight, diet consumption and pathology of liver and kidney in SAMP6 mice.**

SAMP6 mice were fed with the standard diet food AIN-93M or mixed with 0.01 % cyperenoic acid for 19 weeks. (A-B) The body weight and diet consumption were measured once a week. Representative liver (C, D) and kidney (E, F) sections with H&E staining from each group. The experiments were performed with six mice per group. Scale bar = 200  $\mu\text{m}$ .

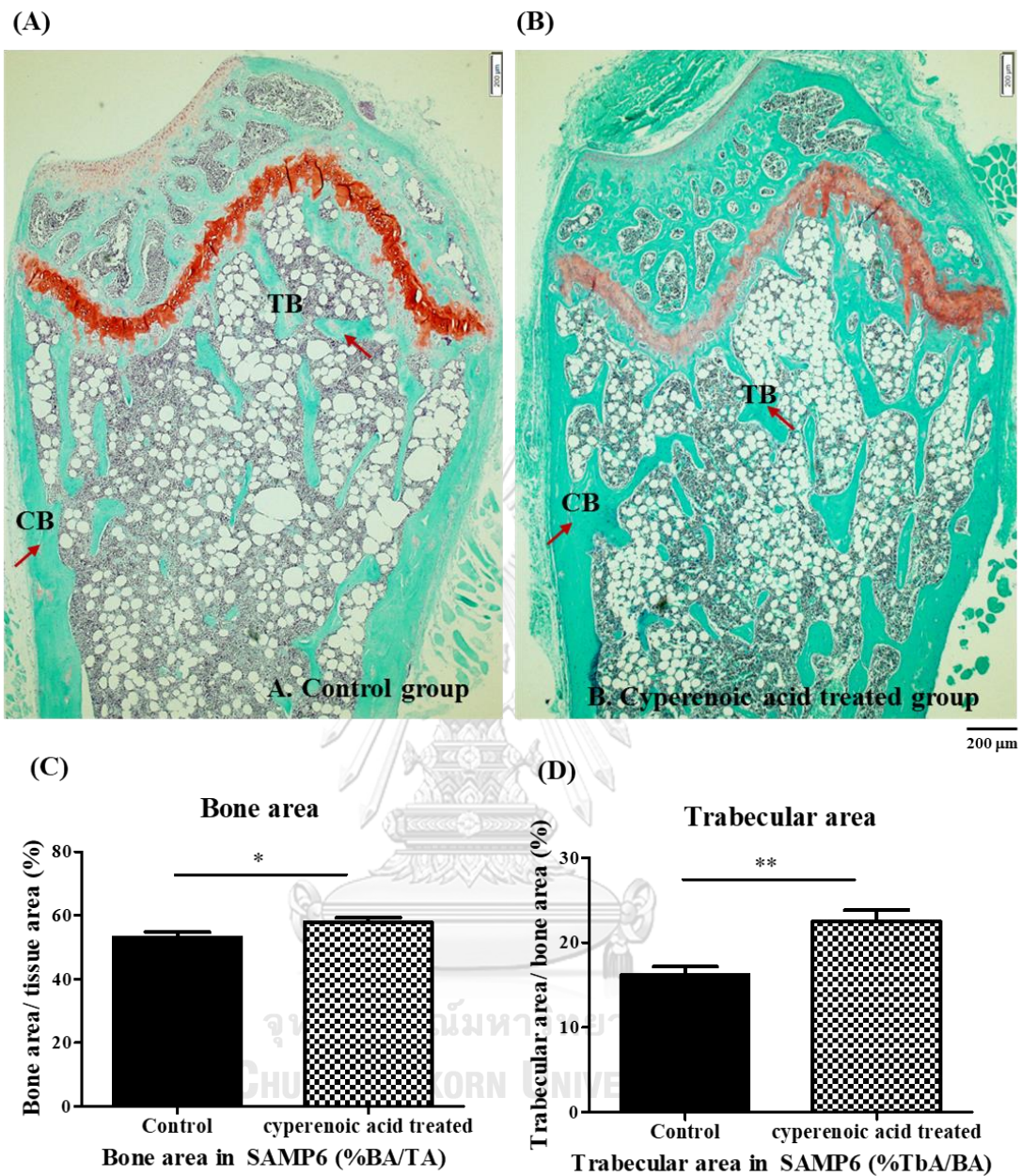


**Figure 21. Effect of cyperenoic acid on bone histomorphometry at distal femur.**

Femur bones of mice were separated and processed for bone histomorphometry. And bone area and trabecular area were used to distinguish the bone condition. (A-B) Representative microscopic image of femoral bone at distal end stained with safranin O (red), fast green (green) and hematoxylin (blue). Bone histomorphometric parameters, the bone area and trabecular area were calculated and shown in C or D. The experiments were performed with six mice per group. Trabecular bone (TB).

Cortical bone (CB), Scale bar = 200  $\mu\text{m}$ .  $**p < 0.01$  and  $*p < 0.05$  indicated statistical significance.

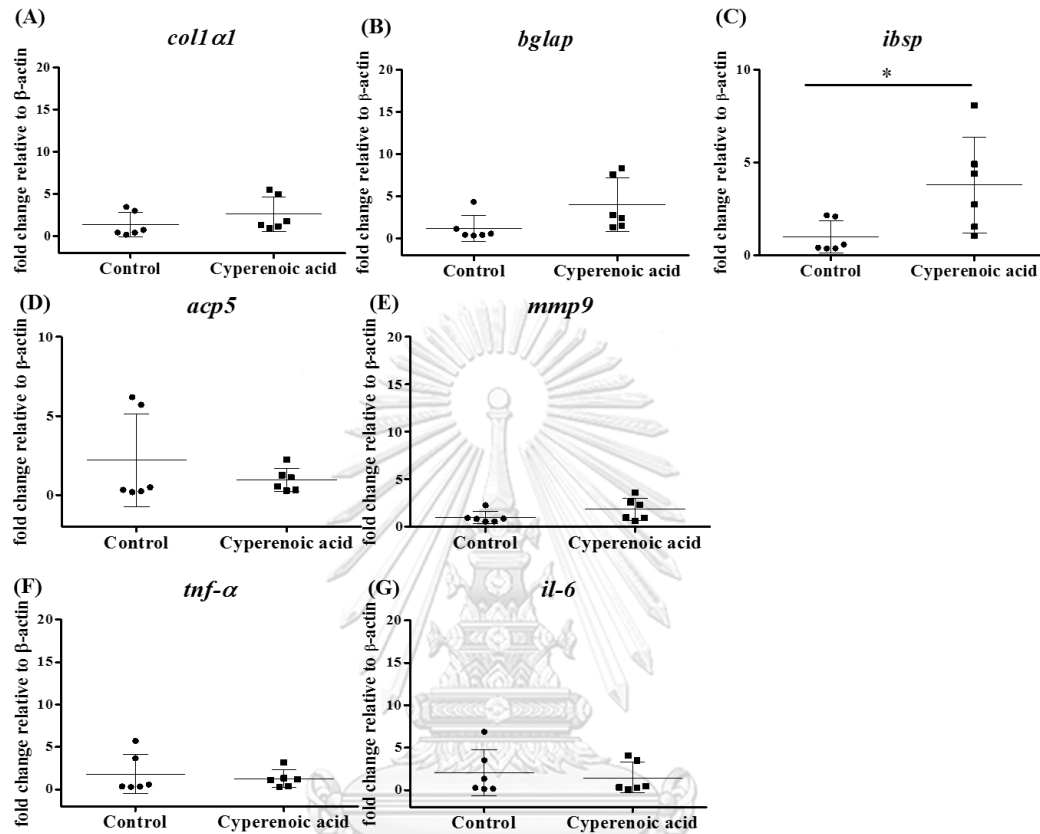


**Figure 22. Effect of cyperenoic acid on expression of bone formation-related genes, bone resorption-related genes and pro-inflammatory cytokine genes in BMMs of SAMP6 mice.**

Total RNA from bone marrow cells was subjected to RT-qPCR analysis for genes expression. The expression of the bone formation-related genes ((A) *coll1a1*, (B) *bglap* and (C) *ibsp*), the bone resorption-related genes ((D) *acp5* and (E) *mmp9*) and pro-inflammatory cytokines ((F) *tnf- $\alpha$*  and (G) *il-6*) were indicated as a fold change relative to  $\beta$ -actin. Each dot represented each mouse. Data were expressed as mean  $\pm$  S.D.,  $**p < 0.01$  and  $*p < 0.05$  indicated statistical significance.



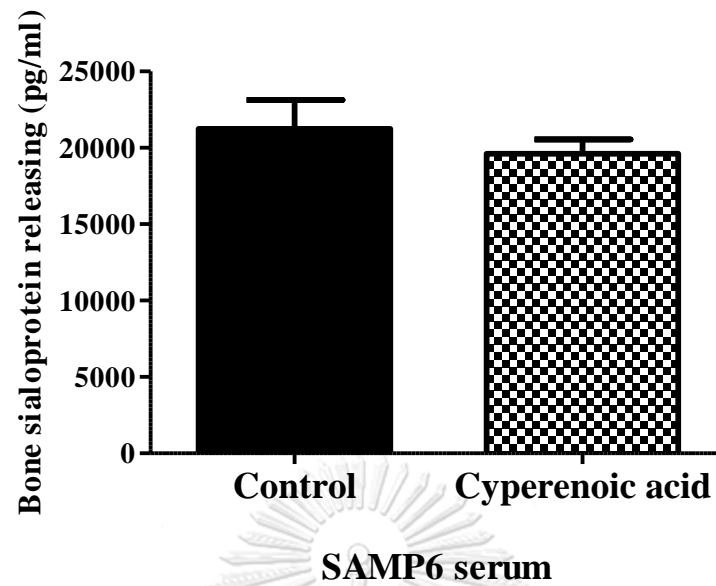


**Figure 23. Effect of cyperenoic acid on bone resorption marker in SAMP6 mice serum.**

Serum was collected from SAMP6 mice in each group. The level of BSP in blood circulation was detected by sandwich ELISA and compared between the two groups. Data were expressed as mean  $\pm$  S.D., \* $p < 0.05$  indicated statistical significance.

## CHAPTER V

### DISCUSSION

This study reported the novel biological activity of natural compounds isolated from medicinal plants on osteoclast differentiation. There are four medicinal plants that were used to investigate in this study. First, *C. comosa* (in Thai called Wan-chak-motluk) has been traditionally used for postmenopausal symptoms in women (63). Recently, the hexane extract from the rhizome of *C. comosa* was reported to increase bone mass density in estrogen deficiency mouse model (64) but its effect on osteoclast was not reported. DHPH is a major phytoestrogen from a rhizomes of *C. comosa*. Therefore, it is hypothesized that DHPH may act as phytoestrogen and improve postmenopause conditions. Second, *T. triandra* (in Thai called Ya-nang) is used widely as a traditional medicine in Southeast Asia for anti-inflammation and anti-malarial treatment (68). The leaves extract of *T. triandra* improves memory via decreasing oxidative stress in alcoholic rats (69). Tilliacorinine belongs to the major alkaloid isolated from roots and stems of *T. triandra*. This compound induced cell death in human cholangiocarcinoma cell via apoptosis through activation of caspase (70). Third, *C. longa* (in Thai called Khamin-chan) has been used for anti-inflammatory, anti-fungal and abdominal pain in a traditional household treatment (71, 72). The root extract from *C. longa* shows activity against *Aspergillus flavus* (73). The essential oil extracted from rhizomes of *C. longa* exhibits anti-inflammation and antinociceptive activity in inflammatory mouse model (71). Fourth, *C. crassifolius* (in Thai called Phang-khi) has been used for anti-cancer in alternative medicine (76). Cyperenoic acid belongs to the major sesquiterpenoids which was isolated from the roots of *C. Crassifolius* (109). Cyperenoic acid was reported to have an anti-angiogenesis in MCF-7 and HepG2 cancer cells line (78).

Osteoclastogenesis and inflammatory signaling share same common pathways. During osteoclastogenesis, pro-inflammatory cytokines such as IL-1, IL-6 and TNF enhance osteoclast activity while osteoblast activity inhibit (58). TNF- $\alpha$  also activates c-Fos and NFATc1 via NF- $\kappa$ B and JNK pathways (110). In the case of chronic inflammation such as in rheumatoid arthritis, synovial tissues produce pro-

inflammatory cytokines that can stimulate osteoclastogenesis (111). Therefore, if compounds have anti-inflammatory activity, they might be effective against osteoclast differentiation. DHPH and ASTP045 isolated from *C. comosa* and curcuminoids of *C. longa*, respectively, clearly suppressed nitric oxide production in macrophages which is an indicator of inflammation while cyperenoic acid and other tested pure compounds did not have any effect on nitric oxide production. Similarly, Sornkaew *et al.* (2015), reported that diarylheptanoids from *C. comosa* inhibited nitric oxide production in RAW264.7 cell induced by LPS (67); and, in a study by Liju *et al.* (2011), the essential oil from *C. longa* reduced acute inflammation in inflammatory mouse model (71). The ethanol extract from *C. crassifolius* showed anti-inflammatory effect in mice (74).

There were some pure compounds that also affect osteoclastogenesis such as tiliacorinine, tiliacorine and nortiliacorinine from *T. triandra*; and, the cyperenol and CATC from *C. crassifolius*. However, they were not study in detail because of the cellular toxicity and the limitation in quantity of the compounds.

TRAP is an enzyme critical for skeleton development (49). Mice with TRAP deficiency (*acp5<sup>-/-</sup>*) exhibited reduction in bone resorption leading to osteopetrosis phenotype (49). Therefore, TRAP activity is useful as an indicator for osteoclast differentiation. In this study, the biological activity of DHPH and cyperenoic acid in osteoclast differentiation model was examined by TRAP enzyme activity. DHPH is a strong inhibitor of osteoclastogenesis with an  $IC_{50}$  of  $325 \pm 1.37$  nM whereas cyperenoic acid has an  $IC_{50}$  of  $36.69 \pm 1.02$   $\mu$ M with no cellular toxicity. The results indicated that DHPH has stronger anti-osteoclastogenic activity than cyperenoic acid. However, DHPH showed cellular toxicity at higher concentrations.

DHPH and cyperenoic acid dramatically decreased the expression of c-Fos at earlier timepoint and decreased NFATc1 expression at late timepoint of RANKL-stimulated osteoclast differentiation. Both compounds reduced both mRNA and protein of NFATc1. The sizes of NFATc1 on Western blot may reflect the post-translational modification by histone acetyltransferase (HATs) in acetylation process (112). DHPH and cyperenoic acid also affect NFATc1 molecular weight pattern. Furthermore, the nuclear translocation of NFATc1 is controlled by dephosphorylation of NFATc1 by activated calcineurin (113) and modification of NFATc1 by poly (ADP-ribose) polymerase 1 (PARP-1) in poly(ADP-ribosyl)ation (114).

NFATc1 is a master regulator of osteoclast differentiation and functions to transcriptional osteoclast-specific gene such as TRAP via c-Fos (45, 115). NFATc1-deficient mice exhibited osteopetrosis phenotype owing to malformation in osteoclastogenesis process. Matsuo *et al.* (2004) (115); and, Takayanagi *et al.* (2002), found that the expression of *nfatc1* was abrogated by *fos* deletion in osteoclast precursors and c-Fos deficient mice showed failure in osteoclast differentiation. Furthermore, c-Fos also bound to *nfatc1* and *acp5* promotor. Thus, the critical role of *nfatc1* auto-amplification might be impacted by cooperation between NFATc1 and c-Fos (45, 46). It was reported that at an early stage of osteoclast differentiation, c-Fos is a necessary factor involved in early activation of NFATc1 in osteoclastogenesis (48). Lee *et al.* (2013) reported that acteoside isolated from *Rehmannia glutinosa*, reduced both c-Fos and NFATc1 expression and might be an effective compound for anti-osteoclast differentiation (79).

Treatment with DHPH or cyperenoic acid reduced the TRAP and transcription factors which play a critical step in osteoclastogenesis and because they are major ingredient from medicinal plants, they were chosen for detailed *in vitro* and *in vivo*.

The osteoclast-specific genes encoding both positive regulators (*nfatc1* and *ctsk*) and negative regulator (*irf8*) were affected by either DHPH or cyperenoic acid. DHPH inhibited the expression of *nfatc1* and *ctsk* but not *ifr8*. On the other hand, cyperenoic acid impacted not only positive regulator genes but also negative regulator gene which involved in osteoclast differentiation and function. These results suggested that these two compounds act differently on RANKL signaling pathway. *irf8* encodes a key modulatory protein for osteoclast differentiation. IRF8 suppresses the expression of NFATc1. Mice lacking *irf8* exhibited severe osteoporosis phenotype because of increasing osteoclast numbers (51).

The molecular mechanism underlying the anti-osteoclastogenic activity of DHPH is proposed in Fig. 24 The phosphorylation of p38 and p44/42 were reduced by DHPH treatment. MAPKs pathway is involved in an early step in osteoclast differentiation. p38 $\alpha$ -deficient monocytes cells exhibited decreasing osteoclast differentiation capacity (30). Furthermore, in a study by Huang *et al.* (2006), the expression of c-Fos and NFATc1 in BMMs were completely blocked by p38 inhibitor (SB203580). Therefore, during osteoclast differentiation, p38 plays a critical role in

regulating both c-Fos and NFATc1 expression (31). There are anti-osteoclastogenic compounds such as the acteoside (79) and a 7-oxo-deacetoxygedunin (80), that suppress both phosphorylation of p38 and phosphorylation of p65 in canonical NF- $\kappa$ B signaling during osteoclast differentiation.

An important finding of this study was that cyperenoic acid was effective in inhibiting RANKL-mediated osteoclast differentiation in BMMs via a non-canonical NF- $\kappa$ B signaling pathway. Cyperenoic acid suppressed both phosphorylation of p100 and p52 processing. The processing of p100 is critical for development of lymphoid organs and bone metabolism (39). NIK is responsible for p100 processing by inducing the Skp1-Cullin-1/Cdc53-F box protein ubiquitin ligase (SCF <sup>$\beta$ TrCP</sup>). Then, SCF <sup>$\beta$ TrCP</sup> binds to  $\beta$ -transducin repeat-containing protein ( $\beta$ -TrCP), a substrate-binding site on NIK-responsive domain (NRD) of p100, resulting in p100 processing (34). NIK induced p100 ubiquitination and processing is blocked by  $\beta$ -TrCP knockdown (116). Furthermore, Iotsova *et al.* (1997), found that p50, p52 double knockout mice ( $p50^{-/-}$   $p52^{-/-}$ ) exhibited an osteopetrosis phenotype while single knockout of  $p50^{-/-}$  or  $p52^{-/-}$  mice, did not show bone malformation. In  $p50^{-/-}$   $p52^{+/+}$  mice, they harbor osteoclast progenitors and precursor osteoclasts but these progenitors could not develop to mature osteoclasts (117). Therefore, both canonical and non-canonical NF- $\kappa$ B are important for bone development. Cyperenoic acid dramatically inhibited osteoclastogenesis based on c-Fos and NFATc1 expression at least through non-canonical NF- $\kappa$ B signaling. Thus, the summarized mechanisms of action cyperenoic acid was proposed in Fig. 24.

On the other hand, cyperenoic acid might affect other signaling pathways downstream of RANK/RANKL signaling. In the studies by Huang *et al.* (2015) (77); and, Chen *et al.* (2017) (78), cyperenoic acid from *C. crassifolius* shows anti-angiogenesis activity. RANKL also induces angiogenesis via ERK1/2 (p44/42) and Src-PLC-Ca<sup>2+</sup> which are also critical downstream molecular in osteoclastogenesis (118). In this study, the effect of cyperenoic acid on ERK was not detected. Therefore, cyperenoic acid might be inhibits osteoclastogenesis via Src-PLC-Ca<sup>2+</sup>. However, the effect of cyperenoic acid on Src-PLC-Ca<sup>2+</sup> pathway in osteoclastogenesis needs further investigation.

DHPH not only enhanced the ALP activity during osteoblast differentiation but also increased cell proliferation in the murine pre-osteoblast cell (MC3T3-E1). Similar to diarylheptanoid 7-(3,4-dihydroxyphenyl)-5-hydroxy-1-phenyl-(1*E*)-1-heptene, this compound also enhances cell differentiation and bone marker-related genes in MC3T3-E1 (119). In a study by Tantikanlayaporn *et al.* (2013), the diarylheptanoid (3*R*)-1,7-diphenyl-(4*E*,6*E*)-4,6-heptadien-3-ol from *C. comosa* enhanced expression of osteoblast-related genes in human osteoblasts (65). In addition, diarylheptanoid has a bone-sparing effect by increasing bone volume and thickness in ovariectomized rat model compared with estrogen treatment (66). In contrast to DHPH, cyperenoic acid has no impact on ALP activity and osteoblast proliferation.

The effect of diarylheptanoid on bone formation might be due to the structure of this compound is similar to estrogen. Estrogen is a stimulator for bone growth and maintain the bone structural (120). DHPH is one of the diarylheptanoids associated with phytoestrogen. In a study by Thongon *et al.*, (2017), a major hydroxyl diarylheptanoid, 7-(3,4-dihydroxyphenyl)-5-hydroxy-1-phenyl(1*E*)-1-heptene was isolated from *C. comosa*. This compound performs as selective estrogen receptor modulators (SERMs) (119). Accordingly, DHPH may bind to estrogen receptor (ER) and perform as SERMs. Nevertheless, the association between cyperenoic acid and its receptor in osteoclasts need further investigation such as structure modeling (121).

Senescence Accelerated Mouse Prone 6 (SAMP6) mice are used as senile osteoporosis model because of the deficiency in osteoblast progenitor cell (57) and increased osteoclast maturation (60) due to the defect in the group of genes located at *Pbd2* locus on chromosome 13 (61). The appearance of symptom is similar to aging human (58). In a study by Li *et al.* (2003), SAMP6 mice were used to determine the effect of berberine, an isoquinoline alkaloid, on dexypyridinoline (Dpd), a bone resorption marker, and procollagen type I carboxyterminal extension peptide (PICP), a bone resorption marker from either urine or serum, respectively (85). Furthermore, Gou *et al.* (2010) also used SAMP6 mice for investigation the bone loss condition in substituted benzothiophene or benzofuran derivatives. Thus, SAMP6 is useful as senile osteoporosis model (122, 123).

In an *in vivo* study of SAMP6 mice, compelling evidence was obtained that cyperenoic acid is effective in preventing osteoporosis in SAMP6 mice. In particular,

cyperenoic acid enhanced the bone sialoprotein (BSP) encoded by the *ibsp* gene. BSP deficiency in mice (*ibsp*<sup>-/-</sup>) resulting in diminishing bone growth and mineralization and reduction of bone formation (52); therefore, BSP is important for bone mineralization and bone formation. Furthermore, BSP is a useful diagnostic marker of bone resorption, reflecting the osteoclast activity in human or animal serum (53). In this study, cyperenoic acid slightly decreased BSP level in SAMP6 mice serum but did not significantly.

Interestingly, cyperenoic acid did not have any effect on *il-6* and *tnf- $\alpha$*  mRNA level which are related to inflammation and bone loss condition (124). A systemic organ toxicity in SAMP6 mice was determined by using histological analysis of H&E staining. After 19 weeks of treatment, there was no evidence for side effect either in the control or cyperenoic acid fed group at least in liver and kidney. Furthermore, histomorphometric parameters are used to distinguish the bone condition. Typically, osteoporosis shows a high level of bone turnover and low level of bone volume (108). Cyperenoic acid clearly increased in bone area and trabecular area.

SAMP6 mice are characterized by both low bone mass and low bone mass density (BMD) after 16 weeks of age (59). In this study, mice were fed with cyperenoic acid (0.01%) supplemented with animal chow before they start showing any sign of osteoporosis symptoms. The treatment period considered a long-term treatment. On the other hand, ovariectomized (OVX) mouse model exhibits bone loss condition within shorter periods (5 weeks) (125). However, it is noted that OVX impacts both hormone and immune systems in mice (126).

Taken together, DPH and cyperenoic acid appear to be a promising candidate for osteoporosis therapeutic based on anti-osteoclastogenic and enrich bone formation in SAMP6 without toxicity.

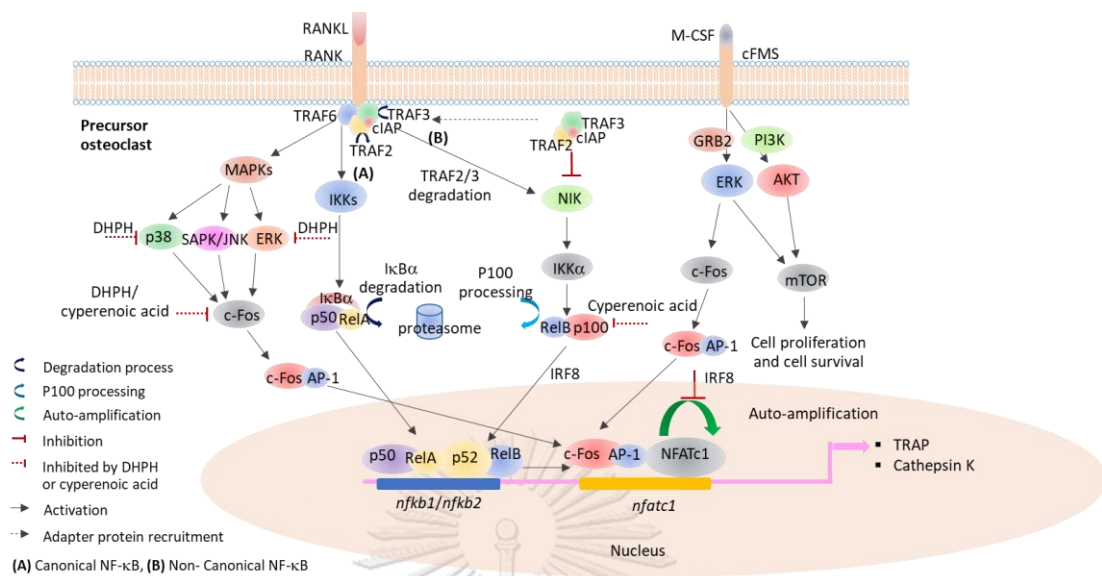


**Figure 24. Proposed model of anti-osteoclastogenic activity of DHPH or cyperenoic acid**

The black and red arrows indicate the activation or inhibition of RANK/RANKL signaling (Modified from Takayanagi (2007) (7), Boyce *et al.* (2015) (37) and, Aeschlimann and Evans, (2004) (38)).



## CHAPTER VI

### CONCLUSION

#### 6.1 Screening compounds from Thai medicinal plants with anti-osteoclastogenic activity

6.1.1 Diarylheptanoid (3*S*)-1-(3,4-dihydroxyphenyl)-3-hydroxy- 7-phenyl-(6*E*)-6-heptene (DHPH) and 1-(2-hydroxyphenyl)-7-(3-hydroxyphenyl)-(1*E*,4*E*,6*E*)-1,4,6-heptatrien-3-one) suppressed nitric oxide production with an  $IC_{50}$  of  $1.012 \pm 1.63 \mu\text{M}$  and  $10.32 \pm 1.46 \mu\text{M}$ , respectively.

6.1.2 DHPH from *C. comosa* and cyperenoic acid, cyperenol, cyperenyl 10-*O*-(4-acetoxy-trans-cinnamate) and cyperenol 10-*O*-(3,4-dihydroxy-trans-cinnamate) from *C. crassifolius* significantly inhibit osteoclast differentiation by suppressing the formation of TRAP<sup>+</sup> MNCs.

6.2 DHPH inhibited TRAP<sup>+</sup> MNCs at the  $IC_{50}$  of  $325 \pm 1.37 \text{ nM}$ . DHPH significantly decreased the expression of *nfatc1* and *ctsk* possibly by ERK inhibiting (p44/42) and p38 activation. Bone resorption by osteoclast was also abrogated by DHPH. In addition, DHPH increased both cell proliferation and cell differentiation in pre-osteoblast cell (MC3T3-E1).

6.3 Cyperenoic acid suppressed TRAP<sup>+</sup> MNCs at the  $IC_{50}$  of  $36.69 \pm 1.02 \mu\text{M}$ . Cyperenoic acid decreased the expression of *nfatc1* and *ctsk* and delayed the expression of *irf8*. Cyperenoic acid inhibited non-canonical NF- $\kappa$ B pathway at p100/52 activation. Cyperenoic acid partially reduced bone resorption. In addition, cyperenoic acid increased both bone area and trabecular area in SAMP6 mice with no systematic organ toxicity.

## REFERENCES

1. Hadjidakis DJ, Androulakis, II. Bone remodeling. *Ann N Y Acad Sci.* 2006;1092:385-96.
2. Bianco P, Riminucci M, Gronthos S, Robey PG. Bone marrow stromal stem cells: nature, biology, and potential applications. *Stem Cells.* 2001;19(3):180-92.
3. Herrmann M. Methods in bone biology in animals: biochemical markers. In: Duque G, Watanabe K, editors. *Osteoporosis research: Animal models.* London: Springer London; 2011. p. 57-82.
4. Kini U, Nandeesh BN. Physiology of bone formation, remodeling, and metabolism. In: Fogelman I, Gnanasegaran G, van der Wall H, editors. *Radionuclide and hybrid bone imaging.* Berlin, Heidelberg: Springer Berlin Heidelberg; 2012. p. 29-57.
5. Khosla S. Minireview: the OPG/RANKL/RANK system. *Endocrinology.* 2001;142(12):5050-5.
6. Komori T, Yagi H, Nomura S, Yamaguchi A, Sasaki K, Deguchi K, et al. Targeted disruption of *Cbfa1* results in a complete lack of bone formation owing to maturational arrest of osteoblasts. *Cell.* 1997;89(5):755-64.
7. Takayanagi H. Osteoimmunology: shared mechanisms and crosstalk between the immune and bone systems. *Nat Rev Immunol.* 2007;7(4):292-304.
8. Vaananen HK, Zhao H, Mulari M, Halleen JM. The cell biology of osteoclast function. *J Cell Sci.* 2000;113 ( Pt 3):377-81.
9. Choi Y, Aegean Conferences. *Osteoimmunology.* New York ; London: Springer; 2007. xvi, 156 p., 1 leaf of plates p.
10. Davies J, Warwick J, Totty N, Philp R, Helfrich M, Horton M. The osteoclast functional antigen, implicated in the regulation of bone resorption, is biochemically related to the vitronectin receptor. *J Cell Biol.* 1989;109(4 Pt 1):1817-26.
11. Teitelbaum SL, Ross FP. Genetic regulation of osteoclast development and function. *Nat Rev Genet.* 2003;4(8):638-49.
12. Edwards JR, Mundy GR. Advances in osteoclast biology: old findings and new insights from mouse models. *Nat Rev Rheumatol.* 2011;7(4):235-43.

13. Kessenich CR. The pathophysiology of osteoporotic vertebral fractures. *Rehabil Nurs.* 1997;22(4):192-5.
14. Kim CH, Takai E, Zhou H, von Stechow D, Muller R, Dempster DW, et al. Trabecular bone response to mechanical and parathyroid hormone stimulation: the role of mechanical microenvironment. *J Bone Miner Res.* 2003;18(12):2116-25.
15. Bellan M, Sainaghi PP, Pirisi M. Role of vitamin D in rheumatoid arthritis. *Adv Exp Med Biol.* 2017;996:155-68.
16. Sato T, Kawano H, Kato S. Study of androgen action in bone by analysis of androgen-receptor deficient mice. *J Bone Miner Metab.* 2002;20(6):326-30.
17. Hofbauer LC, Khosla S, Dunstan CR, Lacey DL, Spelsberg TC, Riggs BL. Estrogen stimulates gene expression and protein production of osteoprotegerin in human osteoblastic cells. *Endocrinology.* 1999;140(9):4367-70.
18. Arnett TR. Chapter 8 - osteoclast biology a2 - Marcus, Robert. In: Feldman D, Dempster DW, Luckey M, Cauley JA, editors. *Osteoporosis (Fourth Edition)*. San Diego: Academic Press; 2013. p. 149-60.
19. Hsu H, Lacey DL, Dunstan CR, Solovyev I, Colombero A, Timms E, et al. Tumor necrosis factor receptor family member RANK mediates osteoclast differentiation and activation induced by osteoprotegerin ligand. *Proc Natl Acad Sci of U S A.* 1999;96(7):3540-5.
20. Ross FP. M-CSF, c-Fms, and signaling in osteoclasts and their precursors. *Ann N Y Acad Sci.* 2006;1068:110-6.
21. Kobayashi K, Takahashi N, Jimi E, Udagawa N, Takami M, Kotake S, et al. Tumor necrosis factor alpha stimulates osteoclast differentiation by a mechanism independent of the ODF/RANKL-RANK interaction. *J Exp Med.* 2000;191(2):275-86.
22. De Benedetti F, Rucci N, Del Fattore A, Peruzzi B, Paro R, Longo M, et al. Impaired skeletal development in interleukin-6-transgenic mice: a model for the impact of chronic inflammation on the growing skeletal system. *Arthritis Rheum.* 2006;54(11):3551-63.
23. Walsh MC, Kim N, Kadono Y, Rho J, Lee SY, Lorenzo J, et al. Osteoimmunology: interplay between the immune system and bone metabolism. *Annu Rev Immunol.* 2006;24:33-63.

24. Bartell SM, Kim HN, Ambrogini E, Han L, Iyer S, Serra Ucer S, et al. FoxO proteins restrain osteoclastogenesis and bone resorption by attenuating H<sub>2</sub>O<sub>2</sub> accumulation. *Nat Commun.* 2014;5:3773.
25. Downing JR, Rettenmier CW, Sherr CJ. Ligand-induced tyrosine kinase activity of the colony-stimulating factor 1 receptor in a murine macrophage cell line. *Mol Cell Biol.* 1988;8(4):1795-9.
26. Wiktor-Jedrzejczak W, Bartocci A, Ferrante AW, Jr., Ahmed-Ansari A, Sell KW, Pollard JW, et al. Total absence of colony-stimulating factor 1 in the macrophage-deficient osteopetrotic (*op/op*) mouse. *Proc Natl Acad Sci U S A.* 1990;87(12):4828-32.
27. Naito A, Azuma S, Tanaka S, Miyazaki T, Takaki S, Takatsu K, et al. Severe osteopetrosis, defective interleukin-1 signalling and lymph node organogenesis in TRAF6-deficient mice. *Genes Cells.* 1999;4(6):353-62.
28. Lee ZH, Kim HH. Signal transduction by receptor activator of nuclear factor kappa B in osteoclasts. *Biochem Biophys Res Commun.* 2003;305(2):211-4.
29. Krens SF, Spaink HP, Snaar-Jagalska BE. Functions of the MAPK family in vertebrate-development. *FEBS Lett.* 2006;580(21):4984-90.
30. Bohm C, Hayer S, Kilian A, Zaiss MM, Finger S, Hess A, et al. The alpha-isoform of p38 MAPK specifically regulates arthritic bone loss. *J Immunol.* 2009;183(9):5938-47.
31. Huang H, Chang EJ, Ryu J, Lee ZH, Lee Y, Kim HH. Induction of c-Fos and NFATc1 during RANKL-stimulated osteoclast differentiation is mediated by the p38 signaling pathway. *Biochem Biophys Res Commun.* 2006;351(1):99-105.
32. Boyle WJ, Simonet WS, Lacey DL. Osteoclast differentiation and activation. *Nature.* 2003;423(6937):337-42.
33. Park MH, Hong JT. Roles of NF-kappaB in cancer and inflammatory diseases and their therapeutic approaches. *Cells.* 2016;5(2):15.
34. Sun S-C. Non-canonical NF-kappaB signaling pathway. *Cell Res.* 2011;21(1):71-85.
35. Baldwin AS, Jr. The NF-kappaB and I kappaB proteins: new discoveries and insights. *Annu Rev Immunol.* 1996;14:649-83.

36. Gilmore TD. Introduction to NF-kappaB: players, pathways, perspectives. *Oncogene*. 2006;25(51):6680-4.
37. Boyce BF, Xiu Y, Li J, Xing L, Yao Z. NF-kappaB-Mediated Regulation of Osteoclastogenesis. *Endocrinol Metab (Seoul)*. 2015;30(1):35-44.
38. Aeschlimann D, Evans BA. The vital osteoclast: how is it regulated? *Cell Death Differ*. 2004;11 Suppl 1:S5-7.
39. Novack DV, Yin L, Hagen-Stapleton A, Schreiber RD, Goeddel DV, Ross FP, et al. The IkappaB function of NF-kappaB2 p100 controls stimulated osteoclastogenesis. *J Exp Med*. 2003;198(5):771-81.
40. Vallabhapurapu S, Matsuzawa A, Zhang W, Tseng PH, Keats JJ, Wang H, et al. Nonredundant and complementary functions of TRAF2 and TRAF3 in a ubiquitination cascade that activates NIK-dependent alternative NF-kappaB signaling. *Nat Immunol*. 2008;9(12):1364-70.
41. He JQ, Zarnegar B, Oganessian G, Saha SK, Yamazaki S, Doyle SE, et al. Rescue of TRAF3-null mice by p100 NF-kappaB deficiency. *J Exp Med*. 2006;203(11):2413-8.
42. Xiao G, Fong A, Sun SC. Induction of p100 processing by NF-kappaB-inducing kinase involves docking IkappaB kinase alpha (IKKalpha) to p100 and IKKalpha-mediated phosphorylation. *J Biol Chem*. 2004;279(29):30099-105.
43. Xiao G, Harhaj EW, Sun SC. NF-kappaB-inducing kinase regulates the processing of NF-kappaB2 p100. *Mol Cell*. 2001;7(2):401-9.
44. Armstrong AP, Tometsko ME, Glaccum M, Sutherland CL, Cosman D, Dougall WC. A RANK/TRAF6-dependent signal transduction pathway is essential for osteoclast cytoskeletal organization and resorptive function. *J Biol Chem*. 2002;277(46):44347-56.
45. Takayanagi H, Kim S, Koga T, Nishina H, Isshiki M, Yoshida H, et al. Induction and activation of the transcription factor NFATc1 (NFAT2) integrate RANKL signaling in terminal differentiation of osteoclasts. *Dev Cell*. 2002;3(6):889-901.
46. Aliprantis AO, Ueki Y, Sulyanto R, Park A, Sigrist KS, Sharma SM, et al. NFATc1 in mice represses osteoprotegerin during osteoclastogenesis and dissociates systemic osteopenia from inflammation in cherubism. *J Clin Invest*. 2008;118(11):3775-89.

47. Grigoriadis AE, Wang ZQ, Cecchini MG, Hofstetter W, Felix R, Fleisch HA, et al. c-Fos: a key regulator of osteoclast-macrophage lineage determination and bone remodeling. *Science*. 1994;266(5184):443-8.
48. Kim JH, Kim N. Regulation of NFATc1 in osteoclast differentiation. *J Bone Metab*. 2014;21(4):233-41.
49. Blumer MJF, Hausott B, Schwarzer C, Hayman AR, Stempel J, Fritsch H. Role of tartrate-resistant acid phosphatase (TRAP) in long bone development. *Mech Dev*. 2012;129(5-8):162-76.
50. Lotinun S, Kiviranta R, Matsubara T, Alzate JA, Neff L, Luth A, et al. Osteoclast-specific cathepsin K deletion stimulates S1P-dependent bone formation. *J Clin Invest*. 2013;123(2):666-81.
51. Zhao B, Takami M, Yamada A, Wang X, Koga T, Hu X, et al. Interferon regulatory factor-8 regulates bone metabolism by suppressing osteoclastogenesis. *Nat Med*. 2009;15(9):1066-71.
52. Malaval L, Wade-Gueye NM, Boudiffa M, Fei J, Zirngibl R, Chen F, et al. Bone sialoprotein plays a functional role in bone formation and osteoclastogenesis. *J Exp Med*. 2008;205(5):1145-53.
53. Fohr B, Dunstan CR, Seibel MJ. Clinical review 165: Markers of bone remodeling in metastatic bone disease. *J Clin Endocrinol Metab*. 2003;88(11):5059-75.
54. Tsao Y-T, Huang Y-J, Wu H-H, Liu Y-A, Liu Y-S, Lee OK. Osteocalcin mediates biomineralization during osteogenic maturation in human mesenchymal stromal cells. *Int J Mol Sci*. 2017;18(1):159.
55. Horowitz MC, Xi Y, Pflugh DL, Hesslein DG, Schatz DG, Lorenzo JA, et al. Pax5-deficient mice exhibit early onset osteopenia with increased osteoclast progenitors. *J Immunol*. 2004;173(11):6583-91.
56. Takeda T, Hosokawa M, Takeshita S, Irino M, Higuchi K, Matsushita T, et al. A new murine model of accelerated senescence. *Mech Ageing Dev*. 1981;17(2):183-94.
57. Takeda T. Senescence-accelerated mouse (SAM): a biogerontological resource in aging research. *Neurobiol Aging*. 1999;20(2):105-10.
58. Matsushita M, Tsuboyama T, Kasai R, Okumura H, Yamamuro T, Higuchi K, et al. Age-related changes in bone mass in the senescence-accelerated mouse (SAM):

SAM-R/3 and SAM-P/6 as new murine models for senile osteoporosis. *Am J Pathol.* 1986;125(2):276-83.

59. Jilka RL, Weinstein RS, Takahashi K, Parfitt AM, Manolagas SC. Linkage of decreased bone mass with impaired osteoblastogenesis in a murine model of accelerated senescence. *J Clin Invest.* 1996;97(7):1732-40.

60. Okamoto M, Murai J, Yoshikawa H, Tsumaki N. Bone morphogenetic proteins in bone stimulate osteoclasts and osteoblasts during bone development. *J Bone Miner Res.* 2006;21(7):1022-33.

61. Shimizu M, Higuchi K, Kasai S, Tsuboyama T, Matsushita M, Mori M, et al. Chromosome 13 locus, *Pbd2*, regulates bone density in mice. *J Bone Miner Res.* 2001;16(11):1972-82.

62. Nakanishi R, Shimizu M, Mori M, Akiyama H, Okudaira S, Otsuki B, et al. Secreted frizzled-related protein 4 is a negative regulator of peak BMD in SAMP6 mice. *J Bone Miner Res.* 2006;21(11):1713-21.

63. Soontornchainaksaeng P, Jenjittikul T. Chromosome number variation of phytoestrogen-producing *Curcuma* (Zingiberaceae) from Thailand. *J Nat Med.* 2010;64(3):370-7.

64. Weerachayaphorn J, Chuncharunee A, Mahagita C, Lewchalermwongse B, Suksamrarn A, Piyachaturawat P. A protective effect of *Curcuma comosa* Roxb. on bone loss in estrogen deficient mice. *J Ethnopharmacol.* 2011;137(2):956-62.

65. Tantikanlayaporn D, Robinson LJ, Suksamrarn A, Piyachaturawat P, Blair HC. A diarylheptanoid phytoestrogen from *Curcuma comosa*, 1,7-diphenyl-4,6-heptadien-3-ol, accelerates human osteoblast proliferation and differentiation. *Phytomedicine.* 2013;20(8-9):676-82.

66. Tantikanlayaporn D, Wichit P, Weerachayaphorn J, Chairoungdua A, Chuncharunee A, Suksamrarn A, et al. Bone sparing effect of a novel phytoestrogen diarylheptanoid from *Curcuma comosa* Roxb. in ovariectomized rats. *PLoS One.* 2013;8(11):e78739.

67. Sornkaewa N, Lin Y, Wang F, Zhang G, Chokchaisiri R, Zhang A, et al. Diarylheptanoids of *Curcuma comosa* with inhibitory effects on nitric oxide production in macrophage RAW 264.7 cells. *Nat Prod Commun.* 2015;10(1):89-93.

68. Singthong J, Oonsivilai R, Oonmetta-aree J, Ningsanond S. Bioactive compounds and encapsulation of yanang (*Tiliacora Triandra*) leaves. *Afr J Tradit Complement Altern Med*. 2014;11(3):76-84.
69. Phunchago N, Wattanathorn J, Chaisiwamongkol K. *Tiliacora triandra*, an anti-intoxication plant, improves memory impairment, neurodegeneration, cholinergic function, and oxidative stress in hippocampus of ethanol dependence rats. *Oxid Med Cell Longev*. 2015;2015:918426.
70. Janeklang S, Nakaew A, Vaeteewoottacharn K, Seubwai W, Boonsiri P, Kismali G, et al. *In vitro* and *in vivo* antitumor activity of tiliacorinine in human cholangiocarcinoma. *Asian Pac J Cancer Prev*. 2014;15(17):7473-8.
71. Liju VB, Jeena K, Kuttan R. An evaluation of antioxidant, anti-inflammatory, and antinociceptive activities of essential oil from *Curcuma longa*. *L. Indian J Pharmacol*. 2011;43(5):526-31.
72. Prucksunand C, Indrasukhsri B, Leethochawalit M, Hungspreugs K. Phase II clinical trial on effect of the long turmeric (*Curcuma longa* Linn) on healing of peptic ulcer. *Southeast Asian J Trop Med Public Health*. 2001;32(1):208-15.
73. Hu Y, Zhang J, Kong W, Zhao G, Yang M. Mechanisms of antifungal and anti-aflatoxigenic properties of essential oil derived from turmeric (*Curcuma longa* L.) on *Aspergillus flavus*. *Food Chem*. 2017;220:1-8.
74. Zhao J, Fang F, Yu L, Wang G, Yang L. Anti-nociceptive and anti-inflammatory effects of *Croton crassifolius* ethanol extract. *J Ethnopharmacol*. 2012;142(2):367-73.
75. Wang GC, Li JG, Li GQ, Xu JJ, Wu X, Ye WC, et al. Clerodane diterpenoids from *Croton crassifolius*. *J Nat Prod*. 2012;75(12):2188-92.
76. Boonyarathanakornkit L, Che C-t, Fong HHS, Farnsworth NR. Constituents of *Croton crassifolius* roots. *Planta Med*. 1988;54(01):61-3.
77. Huang W, Wang J, Liang Y, Ge W, Wang G, Li Y, et al. Potent anti-angiogenic component in *Croton crassifolius* and its mechanism of action. *J Ethnopharmacol*. 2015;175:185-91.
78. Chen Y, Tian JL, Wu JS, Sun TM, Zhou LN, Song SJ, et al. Biotransformation of cyperenoic acid by *Cunninghamella elegans* AS 3.2028 and the potent anti-angiogenic activities of its metabolites. *Fitoterapia*. 2017;118:32-7.



79. Lee SY, Lee KS, Yi SH, Kook SH, Lee JC. Acteoside suppresses RANKL-mediated osteoclastogenesis by inhibiting c-Fos induction and NF-kappaB pathway and attenuating ROS production. *PLoS One*. 2013;8(12):e80873.
80. Wisutthiwong C, Buranaruk C, Pudhom K, Palaga T. The plant limonoid 7-oxo-deacetoxygedunin inhibits RANKL-induced osteoclastogenesis by suppressing activation of the NF-kappaB and MAPK pathways. *Biochem Biophys Res Commun*. 2011;415(2):361-6.
81. Kim JY, Cheon YH, Oh HM, Rho MC, Erkhembaatar M, Kim MS, et al. Oleanolic acid acetate inhibits osteoclast differentiation by downregulating PLCgamma2-Ca(2+)-NFATc1 signaling, and suppresses bone loss in mice. *Bone*. 2014;60:104-11.
82. Li X, He L, Hu Y, Duan H, Li X, Tan S, et al. Sinomenine suppresses osteoclast formation and *Mycobacterium tuberculosis* H37Ra-induced bone loss by modulating RANKL signaling pathways. *PLoS One*. 2013;8(9):e74274.
83. Yu M, Chen X, Lv C, Yi X, Zhang Y, Xue M, et al. Curcumol suppresses RANKL-induced osteoclast formation by attenuating the JNK signaling pathway. *Biochem Biophys Res Commun*. 2014;447(2):364-70.
84. Lee HW, Suh JH, Kim HN, Kim AY, Park SY, Shin CS, et al. Berberine promotes osteoblast differentiation by Runx2 activation with p38 MAPK. *J Bone Miner Res*. 2008;23(8):1227-37.
85. Li H, Miyahara T, Tezuka Y, Tran QL, Seto H, Kadota S. Effect of berberine on bone mineral density in SAMP6 as a senile osteoporosis model. *Biol Pharm Bull*. 2003;26(1):110-1.
86. Kwak SC, Lee C, Kim JY, Oh HM, So HS, Lee MS, et al. Chlorogenic acid inhibits osteoclast differentiation and bone resorption by down-regulation of receptor activator of nuclear factor kappaB ligand-induced nuclear factor of activated T cells c1 expression. *Biol Pharm Bull*. 2013;36(11):1779-86.
87. Choi EM, Hwang JK. Effects of (+)-catechin on the function of osteoblastic cells. *Biol Pharm Bull*. 2003;26(4):523-6.
88. Jeong HM, Han EH, Jin YH, Choi YH, Lee KY, Jeong HG. Xanthohumol from the hop plant stimulates osteoblast differentiation by RUNX2 activation. *Biochem Biophys Res Commun*. 2011;409(1):82-9.

89. Jeong HM, Han EH, Jin YH, Hwang YP, Kim HG, Park BH, et al. Saponins from the roots of *Platycodon grandiflorum* stimulate osteoblast differentiation via p38 MAPK- and ERK-dependent RUNX2 activation. *Food Chem Toxicol.* 2010;48(12):3362-8.
90. Huang Q, Gao B, Jie Q, Wei BY, Fan J, Zhang HY, et al. Ginsenoside-Rb2 displays anti-osteoporosis effects through reducing oxidative damage and bone-resorbing cytokines during osteogenesis. *Bone.* 2014;66:306-14.
91. Reszka AA, Rodan GA. Mechanism of action of bisphosphonates. *Curr Osteoporos Rep.* 2003;1(2):45-52.
92. Pazianas M, Cooper C, Ebetino FH, Russell RG. Long-term treatment with bisphosphonates and their safety in postmenopausal osteoporosis. *Ther Clin Risk Manag.* 2010;6:325-43.
93. Odvina CV, Zerwekh JE, Rao DS, Maalouf N, Gottschalk FA, Pak CY. Severely suppressed bone turnover: a potential complication of alendronate therapy. *J Clin Endocrinol Metab.* 2005;90(3):1294-301.
94. Baron R, Ferrari S, Russell RG. Denosumab and bisphosphonates: different mechanisms of action and effects. *Bone.* 2011;48(4):677-92.
95. Cummings SR, San Martin J, McClung MR, Siris ES, Eastell R, Reid IR, et al. Denosumab for prevention of fractures in postmenopausal women with osteoporosis. *N Engl J Med.* 2009;361(8):756-65.
96. Hanley DA, Adachi JD, Bell A, Brown V. Denosumab: mechanism of action and clinical outcomes. *Int J Clin Pract.* 2012;66(12):1139-46.
97. Lewiecki EM. Safety and tolerability of denosumab for the treatment of postmenopausal osteoporosis. *Drug Healthc Patient Saf.* 2011;3:79-91.
98. Drake MT, Clarke BL, Oursler MJ, Khosla S. Cathepsin K Inhibitors for Osteoporosis: Biology, Potential Clinical Utility, and Lessons Learned. *Endocr Rev.* 2017;38(4):325-50.
99. Gowen M, Lazner F, Dodds R, Kapadia R, Feild J, Tavarria M, et al. Cathepsin K knockout mice develop osteopetrosis due to a deficit in matrix degradation but not demineralization. *J Bone Miner Res.* 1999;14(10):1654-63.
100. Ng KW. Potential role of odanacatib in the treatment of osteoporosis. *Clin Interv Aging.* 2012;7:235-47.

101. Chuprajob T, Changtam C, Chokchaisiri R, Chunglok W, Sornkaew N, Suksamrarn A. Synthesis, cytotoxicity against human oral cancer KB cells and structure-activity relationship studies of trienone analogues of curcuminoids. *Bioorg Med Chem Lett*. 2014;24(13):2839-44.
102. Schmolz L, Wallert M, Lorkowski S. Optimized incubation regime for nitric oxide measurements in murine macrophages using the Griess assay. *J Immunol Methods*. 2017;449:68-70.
103. Bradley EW, Oursler MJ. Osteoclast culture and resorption assays. *Methods Mol Biol*. 2008;455:19-35.
104. Livak KJ, Schmittgen TD. Analysis of relative gene expression data using real-time quantitative PCR and the  $2^{-\Delta\Delta C(T)}$  method. *Methods*. 2001;25(4):402-8.
105. Yazid MD, Ariffin SHZ, Senafi S, Razak MA, Wahab RMA. Determination of the differentiation capacities of murines' primary mononucleated cells and MC3T3-E1 cells. *Cancer Cell Int*. 2010;10:42.
106. Katayama S, Sugiyama H, Kushimoto S, Uchiyama Y, Hirano M, Nakamura S. Effects of sesaminol feeding on brain abeta accumulation in a senescence-accelerated mouse-prone 8. *J Agric Food Chem*. 2016;64(24):4908-13.
107. Orriss IR, Arnett TR. Rodent osteoclast cultures. *Methods Mol Biol*. 2012;816:103-17.
108. Vidal B, Pinto A, Galvao MJ, Santos AR, Rodrigues A, Cascao R, et al. Bone histomorphometry revisited. *Acta Reumatol Port*. 2012;37(4):294-300.
109. Qiu M, Jin J, Zhou L, Zhou W, Liu Y, Tan Q, et al. Diterpenoids from *Croton crassifolius* include a novel skeleton possibly generated via an intramolecular [2+2]-photocycloaddition reaction. *Phytochemistry*. 2017;145:103-10.
110. Boyce BF, Xing L. Functions of RANKL/RANK/OPG in bone modeling and remodeling. *Arch Biochem Biophys*. 2008;473(2):139-46.
111. Schett G, Gravallese E. Bone erosion in rheumatoid arthritis: mechanisms, diagnosis and treatment. *Nat Rev Rheumatol*. 2012;8(11):656-64.
112. Kim JH, Kim K, Youn BU, Jin HM, Kim JY, Moon JB, et al. RANKL induces NFATc1 acetylation and stability via histone acetyltransferases during osteoclast differentiation. *Biochem J*. 2011;436(2):253-62.

113. Mao D, Epple H, Uthgenannt B, Novack DV, Faccio R. PLCgamma2 regulates osteoclastogenesis via its interaction with ITAM proteins and GAB2. *J Clin Invest.* 2006;116(11):2869-79.
114. Valdor R, Schreiber V, Saenz L, Martinez T, Munoz-Suano A, Dominguez-Villar M, et al. Regulation of NFAT by poly(ADP-ribose) polymerase activity in T cells. *Mol Immunol.* 2008;45(7):1863-71.
115. Matsuo K, Galson DL, Zhao C, Peng L, Laplace C, Wang KZ, et al. Nuclear factor of activated T-cells (NFAT) rescues osteoclastogenesis in precursors lacking c-Fos. *J Biol Chem.* 2004;279(25):26475-80.
116. Fong A, Sun SC. Genetic evidence for the essential role of beta-transducin repeat-containing protein in the inducible processing of NF-kappaB2/p100. *J Biol Chem.* 2002;277(25):22111-4.
117. Iotsova V, Caamano J, Loy J, Yang Y, Lewin A, Bravo R. Osteopetrosis in mice lacking NF-kappaB1 and NF-kappaB2. *Nat Med.* 1997;3(11):1285-9.
118. Kim YM, Kim YM, Lee YM, Kim HS, Kim JD, Choi Y, et al. TNF-related activation-induced cytokine (TRANCE) induces angiogenesis through the activation of Src and phospholipase C (PLC) in human endothelial cells. *J Biol Chem.* 2002;277(9):6799-805.
119. Thongon N, Boonmuen N, Suksen K, Wichit P, Chairoungdua A, Tuchinda P, et al. Selective estrogen receptor modulator (SERM)-like activities of diarylheptanoid, a phytoestrogen from *Curcuma comosa*, in breast cancer cells, pre-osteoblast cells, and rat uterine tissues. *J Agric Food Chem.* 2017;65(17):3490-6.
120. Pardhe BD, Pathak S, Bhetwal A, Ghimire S, Shakya S, Khanal PR, et al. Effect of age and estrogen on biochemical markers of bone turnover in postmenopausal women: a population-based study from Nepal. *Int J Womens Health.* 2017;9:781-8.
121. Brejc K, van Dijk WJ, Klaassen RV, Schuurmans M, van Der Oost J, Smit AB, et al. Crystal structure of an ACh-binding protein reveals the ligand-binding domain of nicotinic receptors. *Nature.* 2001;411(6835):269-76.
122. Guo HF, Shao HY, Yang ZY, Xue ST, Li X, Liu ZY, et al. Substituted benzothiophene or benzofuran derivatives as a novel class of bone morphogenetic protein-2 up-regulators: synthesis, structure-activity relationships, and preventive bone

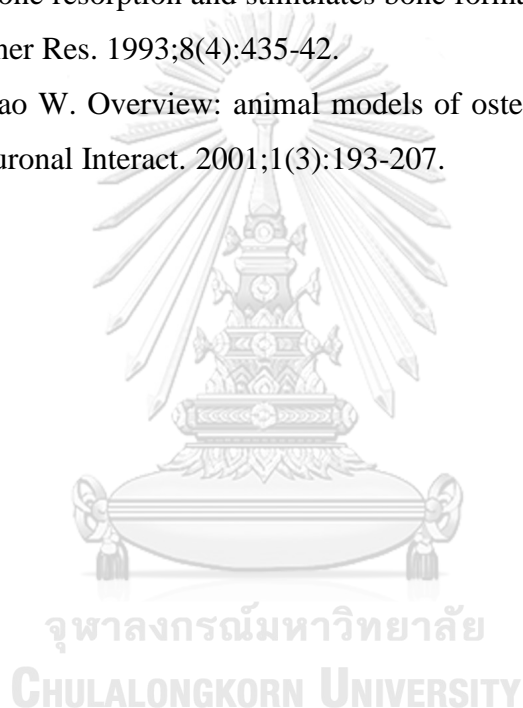
loss efficacies in senescence accelerated mice (SAMP6) and ovariectomized rats. *J Med Chem.* 2010;53(4):1819-29.

123. Watanabe K. Classical models of senile osteoporosis. In: Duque G, Watanabe K, editors. *Osteoporosis Research: Animal Models.* London: Springer London; 2011. p. 115-21.

124. Redlich K, Smolen JS. Inflammatory bone loss: pathogenesis and therapeutic intervention. *Nat Rev Drug Discov.* 2012;11(3):234-50.

125. Bain SD, Bailey MC, Celino DL, Lantry MM, Edwards MW. High-dose estrogen inhibits bone resorption and stimulates bone formation in the ovariectomized mouse. *J Bone Miner Res.* 1993;8(4):435-42.

126. Jee WS, Yao W. Overview: animal models of osteopenia and osteoporosis. *J Musculoskelet Neuronal Interact.* 2001;1(3):193-207.



**APPENDIX**



จุฬาลงกรณ์มหาวิทยาลัย  
**CHULALONGKORN UNIVERSITY**

### List of preparing reagents

#### 1) DMEM complete media (total 100 ml)

|                              |    |    |
|------------------------------|----|----|
| DMEM                         | 87 | ml |
| FBS                          | 10 | ml |
| 1M HEPES free acid           | 1  | ml |
| 100 Mm Sodium pyruvate       | 1  | ml |
| 100x Penicillin-streptomycin | 1  | ml |

#### 2) MEM complete media (total 100 ml)

|                              |    |    |
|------------------------------|----|----|
| MEM without ascorbic acid    | 87 | ml |
| FBS                          | 10 | ml |
| 1M HEPES free acid           | 1  | ml |
| 100 Mm Sodium pyruvate       | 1  | ml |
| 100x Penicillin-streptomycin | 1  | ml |

#### 3) Freezing media (total 1000 $\mu$ l)

##### 3.1) BMMs cell

|      |     |         |
|------|-----|---------|
| FBS  | 900 | $\mu$ l |
| DMSO | 100 | $\mu$ l |

##### 3.2) RAW264.7 cell

|                     |     |         |
|---------------------|-----|---------|
| DMEM complete media | 900 | $\mu$ l |
| DMSO                | 100 | $\mu$ l |

##### 3.3) MC3T3-E1 cell

|                    |     |         |
|--------------------|-----|---------|
| MEM complete media | 900 | $\mu$ l |
| DMSO               | 100 | $\mu$ l |

**4) PBS (total 1000 ml)**

|                                  |      |   |
|----------------------------------|------|---|
| NaCl                             | 8    | g |
| KCl                              | 0.2  | g |
| Na <sub>2</sub> HPO <sub>4</sub> | 3.63 | g |
| KH <sub>2</sub> PO <sub>4</sub>  | 0.24 | g |
| DDW                              | 1    | L |

Adjusted pH to 7.4 and autoclaved at 121 °C

**5) MTT solution (5 mg/ml) (total 40 ml)**

|                |     |    |
|----------------|-----|----|
| MTT            | 200 | mg |
| Sterile 1x PBS | 40  | ml |

**6) Sulfanilamide solution (1% w/v in 5% phosphoric acid)**

|                     |       |    |
|---------------------|-------|----|
| Sulfanilamide       | 1     | g  |
| 85% Phosphoric acid | 5.88  | ml |
| DDW                 | 94.12 | ml |

**7) N-(1-naphthyl)-Ethylenediamine Dihydrochloride (NED) solution (0.1% w/v)**

|     |     |    |
|-----|-----|----|
| NED | 0.1 | g  |
| DDW | 100 | ml |

**8) TRAP solution for TRAP staining assay (total 1000 ml)**

50 mM sodium acetate with 50 mM sodium tartrate

|                           |        |    |
|---------------------------|--------|----|
| Glacial acetic acid       | 11.025 | μl |
| Sodium acetate trihydrate | 6.8    | g  |
| Sodium tartrate dihydrate | 11.5   | g  |
| DDW                       | 1000   | ml |

Adjusted pH to 5.0 and autoclaved at 121 °C

**9) TRAP solution for TRAP activity assay (total 1000 ml)**

50 mM citrate buffer with 10 mM solution

|                          |       |   |
|--------------------------|-------|---|
| Citric acid              | 10.51 | g |
| Sodium citrate dihydrate | 14.71 | g |



|  |        |    |
|--|--------|----|
| Sodium tartrate dihydrate  | 2.3    | g  |
| DDW  | 1000   | ml |
| Adjusted pH to 4.6 and autoclaved at 121 °C                              |        |    |
| <b>10) TRAP activity for working solution (total 5 ml)</b>               |        |    |
| 50 mM citrate buffer with 10 mM solution                                 | 5      | ml |
| p-nitrophenylphosphate   | 18.375 | mg |
| <b>11) Naphtol AS-MX phosphate (10 mg/ml)</b>                            |        |    |
| Naphtol AS-MX phosphate  | 10     | mg |
| N, N-dimethylformamide (DMF)   | 1      | ml |
| <b>12) TRAP staining for working solution (total 5 ml)</b>               |        |    |
| 50 mM sodium acetate with 50 mM sodium tartrate                          | 5      | ml |
| 10mg/ml Naphtol AS-MX phosphate  | 50     | µl |
| Fast red violet LB salt  | 0.6    | mg |
| <b>13) 10% formaldehyde (total 100 ml)</b>                               |        |    |
| 37% formalin   | 27     | ml |
| DDW  | 73     | ml |
| <b>14) 95% Ethanol (total 100 ml)</b>                                    |        |    |
| Absolute ethanol   | 95     | ml |
| DDW  | 5      | ml |
| <b>15) DEPC water (total 100 ml)</b>                                     |        |    |
| DEPC (0.01% v/v)   | 10     | µl |
| DDW (Autoclaved)   | 100    | ml |
| The DEPC water was incubated at 25 °C overnight and autoclaved at 121 °C |        |    |
| <b>16) RIPA buffer</b>   |        |    |
| 1 M Tris-HCl pH 7.4  | 0.35   | ml |
| 0.5 M NaCl   | 2.1    | ml |
| 100% Nonidet P-40  | 0.7    | ml |
| 10% Sodium deoxycholate  | 0.35   | ml |
| 20% SDS  | 0.035  | ml |
| DWW  | 3.095  | ml |

|  |        |    |
|--|--------|----|
| Protease inhibitor (1tablet/1.5 ml)                | 1      | ml |
| Phosphatase inhibitor 100x                         |        |    |
| <b>17) 2x SDS-dye (total 10 ml)</b>                |        |    |
| 1 M Tris-HCl pH 6.8                                | 1      | ml |
| 10 % SDS   | 4      | ml |
| 99.5% Glycerol                                     | 2.01   | ml |
| Bromphenol blue                                    | 0.001  | g  |
| DDW  | 2.989  | ml |
| <b>18) 1.5 M Tris buffer pH 8.8 (total 500 ml)</b> |        |    |
| Trisma base  | 90.855 | g  |
| DDW  | 500    | ml |
| Adjusted pH to 8.8 and autoclaved at 121 °C        |        |    |
| <b>19) 1 M Tris buffer pH 6.8 (total 500 ml)</b>   |        |    |
| Trisma base  | 60.57  | g  |
| DDW  | 500    | ml |
| Adjusted pH to 6.8 and autoclaved at 121 °C        |        |    |
| <b>20) PBST solution (total 1000 ml)</b>           |        |    |
| 1x PBS   | 1000   | ml |
| Tween20  | 500    | µl |
| <b>21) 10x PBS (total 1000 ml)</b>                 |        |    |
| NaCl   | 80     | g  |
| KCl  | 2      | g  |
| Na <sub>2</sub> HPO <sub>4</sub>                   | 36.3   | g  |
| KH <sub>2</sub> PO <sub>4</sub>                    | 2.4    | g  |
| DDW  | 1      | L  |
| Adjusted pH to 7.4 and autoclaved at 121 °C        |        |    |
| <b>22) SDS-polyacrylamide gel preparation</b>      |        |    |
| 22.1) 8% Separating gel (total 8 ml)               |        |    |
| DDW  | 4.236  | ml |
| 40% Acrylamide and Bis-acrylamide solution         | 1.6    | ml |
| 1.5 M Tris-HCl pH 8.8                              | 2      | ml |

|  |       |    |
|--|-------|----|
| 10% SDS                                      | 80    | μl |
| 10% APS                                      | 80    | μl |
| TEMED  | 4     | μl |
| <b>22.2) 12% Separating gel (total 8 ml)</b> |       |    |
| DDW  | 3.436 | ml |
| 40% Acrylamide and Bis-acrylamide solution   | 2.4   | ml |
| 1.5 M Tris-HCl pH 8.8                        | 2     | ml |
| 10% SDS                                      | 80    | μl |
| 10% APS                                      | 80    | μl |
| TEMED  | 4     | μl |
| <b>22.3) 5% Stacking gel (total 2 ml)</b>    |       |    |
| DDW  | 1.204 | ml |
| 40% Acrylamide and Bis-acrylamide solution   | 0.25  | ml |
| 1 M Tris-HCl pH 6.8                          | 0.504 | ml |
| 10% SDS                                      | 20    | μl |
| 10% APS                                      | 20    | μl |
| TEMED  | 2     | μl |
| <b>23) 5x Running buffer (total 1000 ml)</b> |       |    |
| Trisma base                                  | 15.1  | g  |
| Glycine                                      | 94    | g  |
| SDS  | 5     | g  |
| DDW  | 1000  | ml |
| <b>24) Transfer buffer (total 1000 ml)</b>   |       |    |
| Trisma base                                  | 5.08  | g  |
| Glycine                                      | 2.9   | g  |
| SDS  | 0.37  | g  |
| DDW  | 800   | ml |
| Absolute Methanol                            | 200   | ml |
| <b>25) 100 mM Tris buffer pH 8.5</b>         |       |    |
| Trisma base                                  | 6.057 | g  |
| DDW  | 500   | ml |

Adjusted pH to 8.5 and autoclaved at 121 °C

## 26) ECL substrate

### 26.1) 90 mM Coumaric acid

|               |      |    |
|---------------|------|----|
| Coumaric acid | 14.8 | mg |
| DMSO          | 1    | ml |

### 26.2) 250 mM Luminol

|         |      |    |
|---------|------|----|
| Luminol | 44.3 | mg |
| DMSO    | 1    | ml |

### 26.3) Solution A

|                           |     |    |
|---------------------------|-----|----|
| 100 mM Tris buffer pH 8.5 | 2.5 | ml |
| 90 mM Coumaric acid       | 11  | μl |
| 250 mM Luminol            | 25  | μl |

### 26.4) Solution B

|                                   |     |    |
|-----------------------------------|-----|----|
| 100 mM Tris buffer pH 8.5         | 2.5 | ml |
| 30% H <sub>2</sub> O <sub>2</sub> | 1.5 | μl |

## 27) Film developer and fixer

The working solution was prepared and diluted with tap water (1:4)

## 28) Alkaline phosphatase assay (total 10 ml)

|   |      |    |
|---|------|----|
| 0.1 M sodium bicarbonate-carbonate buffer pH 10 | 10   | ml |
| 2 mM MgSO <sub>4</sub> (0.24 mg/ml)             | 2.4  | mg |
| 6 mM p-nitrophenyl phosphate (2.22 mg/ml)       | 22.2 | mg |

## 29) 0.1% Triton-X 100 (total 40 ml)

|              |    |    |
|--------------|----|----|
| Triton-X 100 | 40 | μl |
| DDW          | 40 | ml |

## 30) The staining step for bone histomorphometry

|                                 |      |    |
|---------------------------------|------|----|
| 0.1% Fast green (FCF) in 100 ml | 0.1  | g  |
| 0.1% Safranin O in 100 ml       | 0.01 | g  |
| 1% Acetic acid in 100 ml        | 1    | ml |

**Table 1. The SAMP6 mice separation by using body weight**

| No | Control group | Weight (g) | Cyperenoic acid<br>Treated with | Weight (g) |
|----|---------------|------------|---------------------------------|------------|
| 1  | M1            | 22.0       | M15                             | 22.4       |
| 2  | M2            | 21.7       | M16                             | 22.1       |
| 3  | M3            | 21.4       | M17                             | 22         |
| 4  | M4            | 20.3       | M18                             | 19.9       |
| 5  | M5            | 18.8       | M19                             | 20         |
| 6  | M6            | 20.2       | M20                             | 20.9       |
|    | Average       | 20.8       | Average                         | 21.21      |
|    | SD            | 1.1        | SD                              | 1.08       |

M\* Mice code number

**Table 2. The dehydration process for bone histomorphometry**

| Reagents          | Time (h) | Temperature (°C) |
|-------------------|----------|------------------|
| 4.5% formaldehyde | 1        | RT               |
| 70% ethanol       | 1        | RT               |
| 80% ethanol       | 1        | RT               |
| 96% ethanol       | 1        | RT               |
| 96% ethanol       | 1        | RT               |
| 100% ethanol      | 1        | RT               |
| 100% ethanol      | 1        | RT               |
| 100% ethanol      | 1        | RT               |

**Table 3. The staining process for bone histomorphometry**

| Solutions        | Reagents                             | preparing  |
|------------------|--------------------------------------|--|
| Hematoxylin      | Carrazzi's Hematoxylin Solution (x2) | -  |
| Fast green (FCF) | 0.1% Fast green (FCF)                | Fast green: 0.1 g<br>Distilled water: 100 ml         |
| Safranin O       | 0.1% Safranin O                      | Safranin O: 0.1 g<br>Distilled water: 100 ml         |
| Acetic acid      | 1% Acetic acid                       | Acetic acid, glacial: 1 ml<br>Distilled water: 99 ml |

| Staining Procedure | Solution                           | Times (min) |
|--------------------|------------------------------------|-------------|
|                    | 1) Xylene                          | 4           |
|                    | 2) Xylene                          | 4           |
|                    | 3) Xylene                          | 4           |
|                    | 4) 96% Alcohol                     | 1           |
|                    | 5) 96% Alcohol                     | 1           |
|                    | 6) 70% Alcohol                     | 1           |
|                    | 7) Tap water rinse                 | 1           |
|                    | 8) Carrazzi's Hematoxylin Solution | 10          |
|                    | 9) Running tap water               | 5           |
|                    | 10) 0.1% Fast green (FCF) solution | 10          |
|                    | 11) 1% Acetic acid                 | 10          |
|                    | 12) 0.1% Safranin O solution       | 5           |
|                    | 13) 100% Alcohol                   | 5           |
|                    | 14) 100% Alcohol                   | 5           |
|                    | 15) 100% Alcohol                   | Overnight   |
|                    | 16) Xylene                         |             |
|                    | 17) Mount with softmount (wako)    |             |

---

|                  |                  |               |
|------------------|------------------|---------------|
| Expected results | Cartilage matrix | Orange to red |
|                  | Underlying bone  | Green         |
|                  | Nuclei           | Black         |
|                  | Cytoplasm        | Grey green    |

---



## VITA

I was born on 5th August 1986 in Nakhon-Sawan province, Thailand. I earned my undergraduate degree in Science from Department of Zoology, Faculty of Science, Chiang Mai University (Thailand) in 2008. During my undergraduate study, I received a "Phet-Thong-Kwang scholarship", an academic award for undergraduate student, between 2005 to 2009 from Chiang Mai University. My research project focused on the anti-lung cancer activities of Thai medicinal plants.

After my bachelor degree, I received a prestigious scholarship from the Thailand Government "Science Achievement Thailand" to support my post-graduate studies for Master's and Ph.D. degree. Under this support, I enrolled in the Graduate Program in the Department of Zoology for my Master's degree and the Graduate Program in Biotechnology, Faculty of Science, Chulalongkorn University (Thailand) for my Ph.D.

In 2012, I graduated with a Master's degree working with breast cancer cell line and Thai medicinal herb with female hormone-like compounds. In addition, during this period, I presented my research in two conferences, (1) Proceeding the 50th Kasetsart University Annual Conference (Thailand) and (2) Abstract the 16th Biological Science Graduate Congress (Singapore).

In 2013, I enrolled in a Ph.D. program in Biotechnology, Faculty of Science, Chulalongkorn University. My research investigates Thai medicinal plants for its effect on differentiation of osteoclasts. Part of my work was presented at the 27th Annual Meeting of the Thai Society for Biotechnology and International Conference "Innovative Biotechnology" and received the first prize for the best poster award.

In 2016, my work was published in European Journal of Pharmacology with the title "Diarylheptanoid from Curcuma comosa Rox. suppresses RANKL-induced osteoclast differentiation by decreasing NFATc1 and c-Fos expression via MAPK pathway". Furthermore, I had an opportunity to perform an in vivo experiment at Shinshu University, Nagano, Japan (Nov 2016 - Jun 2017) under the supervision of Professor Soichiro Nakamura and Associate Professor Shigeru Katayama. During this time, I had attended two conferences which are the 71st Japanese Society of Nutrition and Food Science, Okinawa, Japan and the 23rd General Meeting of the Japan Food Chemistry Association.